



UvA-DARE (Digital Academic Repository)

Radiotherapy for lung cancer

Borst, G.R.

Publication date

2009

Document Version

Final published version

[Link to publication](#)

Citation for published version (APA):

Borst, G. R. (2009). *Radiotherapy for lung cancer*. [Thesis, fully internal, Universiteit van Amsterdam].

General rights

It is not permitted to download or to forward/distribute the text or part of it without the consent of the author(s) and/or copyright holder(s), other than for strictly personal, individual use, unless the work is under an open content license (like Creative Commons).

Disclaimer/Complaints regulations

If you believe that digital publication of certain material infringes any of your rights or (privacy) interests, please let the Library know, stating your reasons. In case of a legitimate complaint, the Library will make the material inaccessible and/or remove it from the website. Please Ask the Library: <https://uba.uva.nl/en/contact>, or a letter to: Library of the University of Amsterdam, Secretariat, P.O. Box 19185, 1000 GD Amsterdam, The Netherlands. You will be contacted as soon as possible.

Radiotherapy for Lung Cancer

Amelioration by controlling the flames

Radiotherapy for Lung Cancer

Gerben Borst

Gerben Borst

Radiotherapy for Lung Cancer

Gerben R. Borst

Radiotherapy for Lung Cancer

© Gerben Borst, Amsterdam 2009

ISBN/EAN: 978-90-9024742-7

printed by: Ipskamp Drukkers, The Netherlands

Cover design: Gysbert S. Zijlstra www.ehgz.nl

The research described in this thesis was performed at the division of Radiation Oncology of the Netherlands Cancer Institute - Antoni van Leeuwenhoek Hospital (NKI-AvL), Amsterdam, the Netherlands.

Printing of this thesis was financially supported by the division of Radiation Oncology of the Netherlands Cancer Institute - Antoni van Leeuwenhoek Hospital (NKI-AvL) and the Netherlands Cancer Institute (NKI).

Radiotherapy for Lung Cancer

ACADEMISCH PROEFSCHRIFT

Ter verkrijging van de graad van doctor
aan de Universiteit van Amsterdam
op gezag van de Rector Magnificus
prof. dr. D.C. van den Boom
ten overstaan van een door het college voor promoties
ingestelde commissie,
in het openbaar te verdedigen in de Agnietenkapel
op vrijdag 13 november 2009, te 12:00 uur

door

Gerben Roelof Borst
geboren te Ermelo

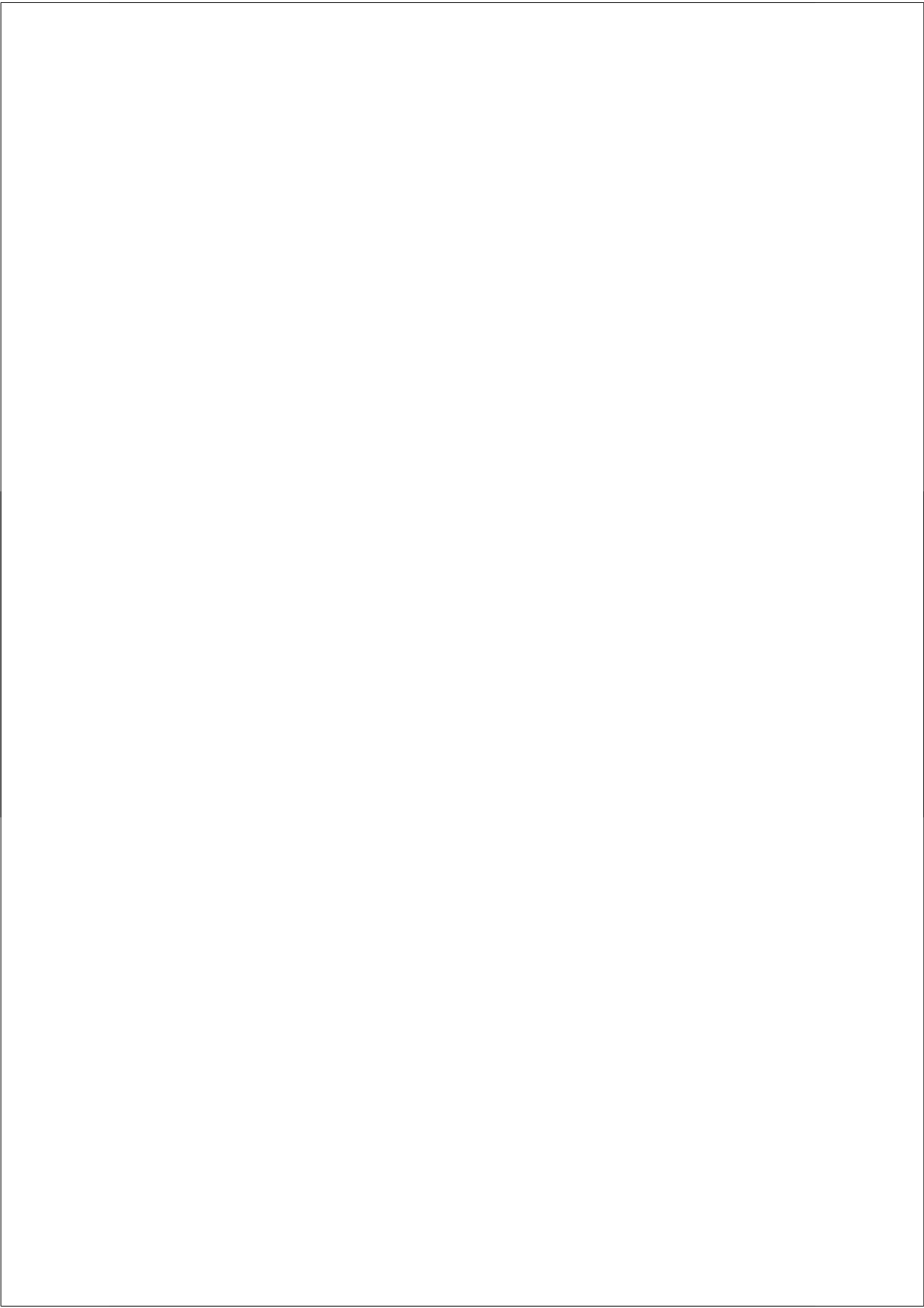
Promotiecommissie

Promotor: Prof. dr. G.M.M. Bartelink

Co-promotores: Dr. J.V. Lebesque
Dr. ir. J.J. Sonke

Overige leden: Prof. dr. E.H.D. Bel
Prof. dr. A.C. Begg
Prof. dr. ir. C.A. Grimbergen
Prof. dr. L.B. Marks
Prof. dr. M.B. van Herk
Prof. dr. M. Verheij

Faculteit der Geneeskunde



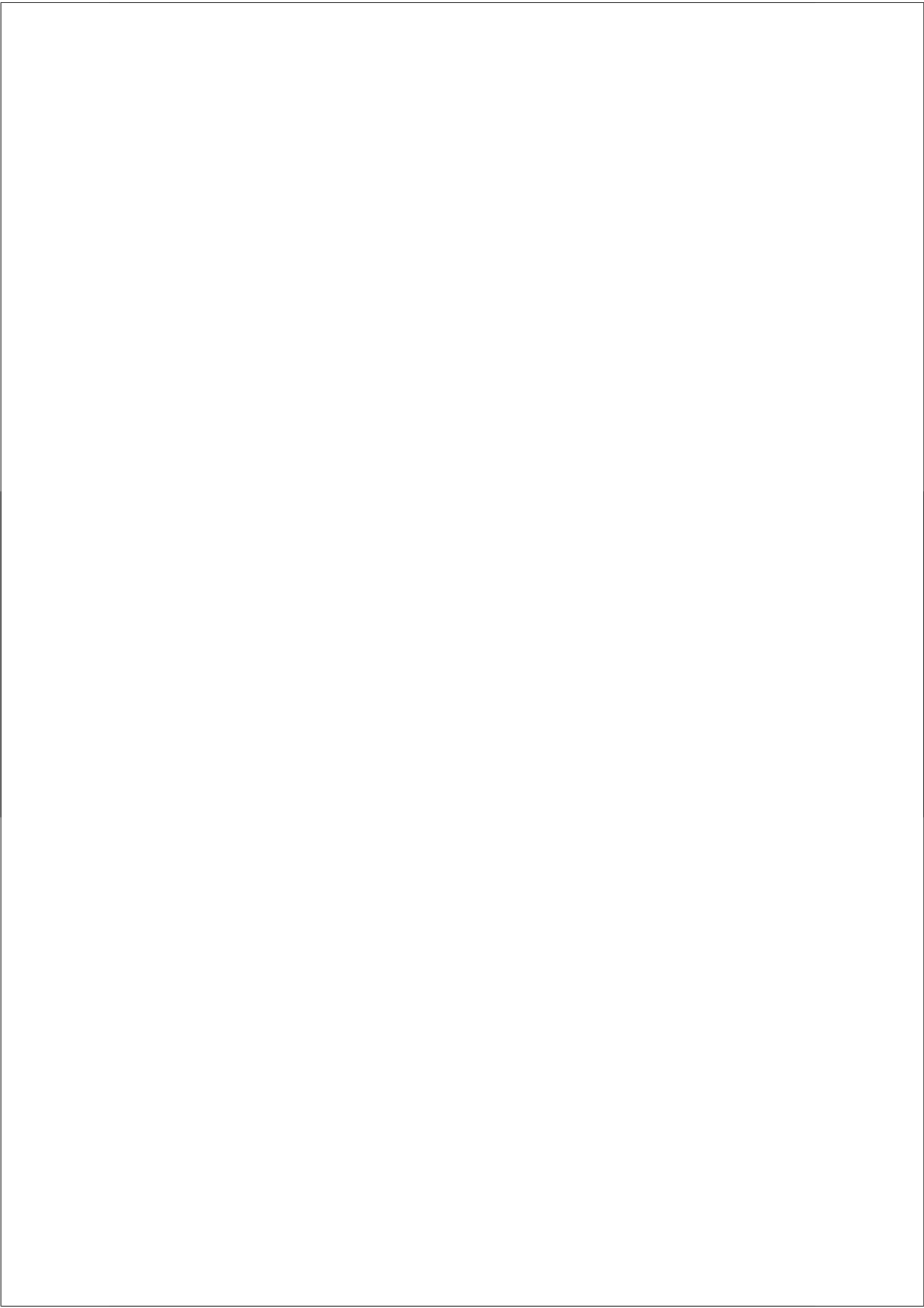
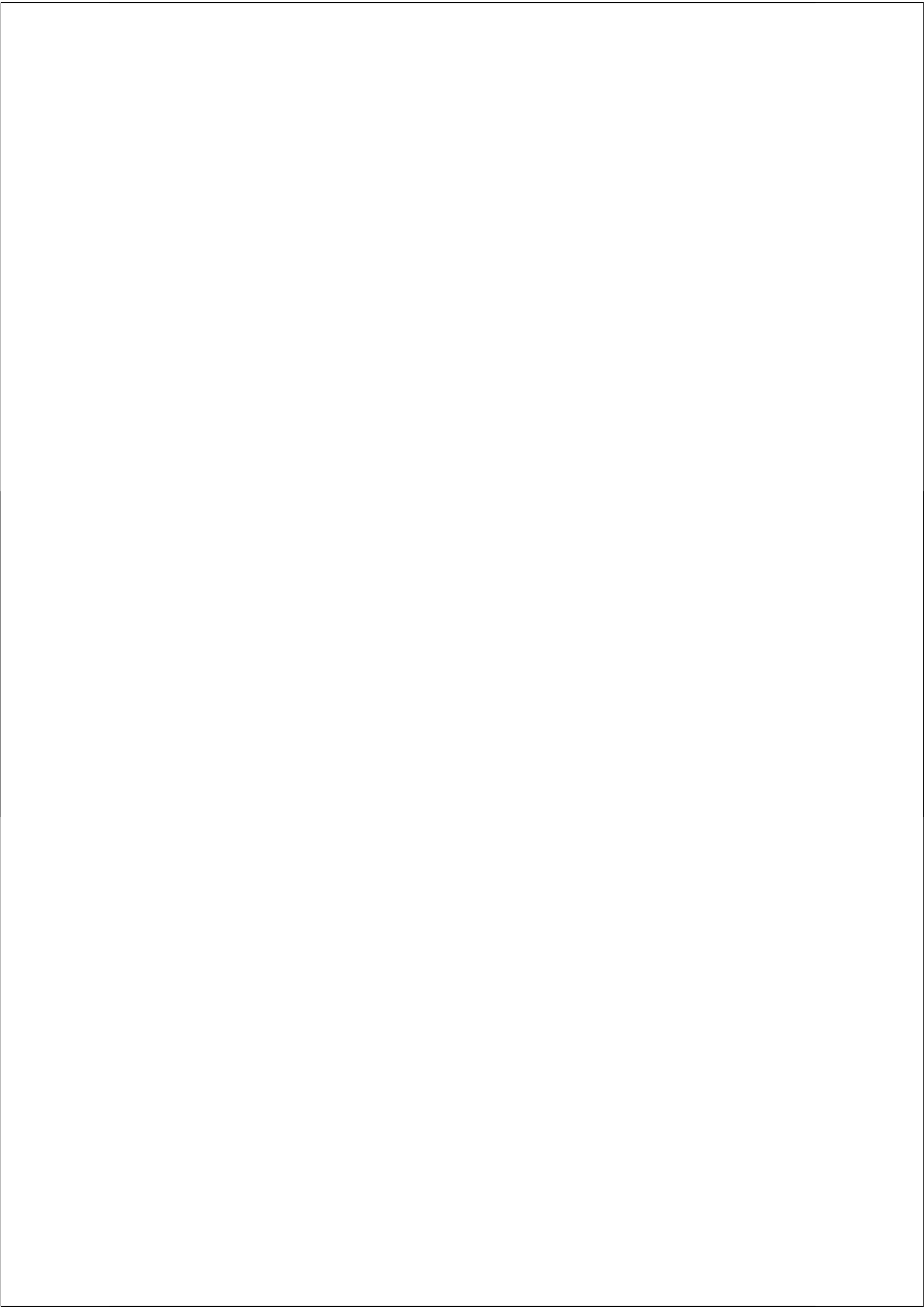


Table of contents

Chapter 1.	Introduction	9
Chapter 2.	FDG standardized uptake value as prognostic factor for inoperable non-small cell lung cancer.	21
Chapter 3.	Prospective assessment of dosimetric/physiologic-based models for predicting radiation pneumonitis.	39
Chapter 4.	Radiation pneumonitis for patients treated for malignant pulmonary lesions with stereotactic body radiation therapy.	59
Chapter 5.	Pulmonary function changes after radiotherapy in non-small cell lung cancer patients with a long-term disease free survival	77
Chapter 6.	Radiation Pneumonitis after Hypofractionated Radiotherapy: Evaluation of the LQ(L) model and different dose parameters	91
Chapter 7.	Kilo-voltage cone beam CT setup measurements for lung cancer patients; first clinical results and comparison with electronic portal-imaging device	109
Chapter 8.	General Discussion	125
Appendices	Summary Samenvatting LQ-model modification of chapter 6 List of publications Curriculum Vitae Acknowledgements Abbreviations	149



1

Introduction

1. Lung Cancer

Lung cancer is the most common cause of cancer mortality for both men and women, causing approximately 1.2 million deaths per year worldwide [1]. More than 90 percent of all lung cancers is caused by cigarette smoking [2]. A decreasing prevalence of lung cancer is observed in men caused by a reduction of smoking [2]. Unfortunately, the incidence of lung cancer and lung cancer related death is still increasing for women, and currently almost one half of all lung cancer related death occurs in women. About 80 % of the lung cancers are diagnosed as non-small cell lung cancer (NSCLC). The distinction between NSCLC and small cell lung cancer (SCLC) is important for the treatment of choice. The studies included in this thesis are focussed on the treatment of NSCLC.

Lung cancer is mostly diagnosed after presentation of clinical symptoms of the patient. Complaints of the patients are caused by the primary tumour or its spread (metastasis) and are presented by one or more symptoms like coughing, chest pain, haemoptysis and dyspnoea [3]. To date, no screening test (e.g. chest X-ray, CT thorax, sputum test) in smokers has been found to reduce the mortality in lung cancer patients, but randomized screening trials are ongoing to evaluate the beneficial effect of screening techniques [4,5].

Radiotherapy is the cornerstone of the treatment of the majority of NSCLC patients. The first reason is that lung cancer is an aggressive disease whereby most patients are diagnosed in an locally advanced stage of the disease. For these patients definitive (chemo)radiation (i.e. technically inoperable) or neoadjuvant chemoradiation (i.e. potentially technically operable) is indicated. Secondly, because lung cancer is so strongly related with smoking, patients are often suffering from smoking induced pulmonary and cardiovascular co-morbidities [6] resulting in a physical performance that is insufficient for a major surgical procedure and/or removal of lung tissue (i.e. medically inoperable) and also these patients are candidates for irradiation. Thirdly, sometimes (older) patients refuse surgery and prefer radiotherapy (RT). This third group of patients is increasing after the introduction of hypofractionated RT (see later) for early stage NSCLC. A fourth group of lung cancer patients who are often referred for RT are non-curable lung cancer patients (i.e. metastasized disease) whereby symptoms caused by the tumour spread or metastasis can often be (temporarily) relieved by irradiation.

2. Staging and Prognosis of NSCLC

The prognosis of lung cancer patients is dependent of tumour, patient and treatment related characteristics. Higher tumour stages and larger tumour volumes are related with worse outcome. Stage I patients have a five year survival of 73 percent. Five-year survival of stages II and III are 36 to 46 percent and 9 to 24 percent, respectively. For patients with clinical stage IV disease the five-year survival rate is 2 percent, with a

median survival of 6 months [7].

The histopathology of the tumour also is of prognostic value and important for the decision on treatment strategy [8]. Consequently, pathological verification (and specification) of the tumour is aimed for all lung cancer patients. Unfortunately, tumour material cannot always be obtained (biopsy failed or the biopsy is a too invasive procedure). For patients who are candidates for radiotherapy (whereby tumour material is not available in contrast to surgery), evaluation of the clinical setting is important before a decision for treatment is made (e.g. tumour growing on CT images and Positron Emission Tomography (PET) positive lesions) [9]. Patient related factors (e.g. age, performance status, weight loss and co-morbidity) are also influencing both the prognosis and treatment choice.

After appropriate tumour staging and assessment of the patient characteristics, a multidisciplinary team (i.e. pulmonologist, surgeon, radiation oncologist, nuclear medicine physician, pathologist, radiologist) should determine the most suitable individually adapted treatment strategy because good patient selection for the often multi-modality treatment is crucial to maximize the survival rate and minimize toxicity.

3. Indication for Irradiation of NSCLC

3.1 Stage I and II

For medically inoperable stage I patients with a centrally located tumour and stage II patients, conventional fractionated (2-3 Gy / fraction) radiotherapy is the treatment of choice. The addition of chemotherapy for stage II is depending on the physical performance of the patient (which is deprived since the surgery could not be performed for this reason). For small peripherally located stage I tumours hypofractionated RT (i.e. >>2-3 Gy/fraction) is used in an increasing number of institutes. This is a technique whereby a high dose to the lung tumour is delivered with only a small number of fractions using high accuracy irradiation. This technique is first described by Blomgren et al. in 1995 [10] and is derived from stereotactic radiosurgery used for intracranial, orbital and base of skull malignancies or non-malignant anatomical malformations (e.g. arteriovenous malformations). Hypofractionated RT shows encouraging reports of good tumour control and little toxicity resulting in an increasing number of RT departments treating early stage lung cancer and lung metastases with hypofractionated RT [10-17]. Ongoing studies are evaluating the differences between operable stage I patients undergoing surgery or hypofractionated RT (ROSEL-study).

A meta-analysis evaluating postoperative radiotherapy (PORT) showed a detrimental effect for patients irradiated after surgery for stage I/II lung cancer patients [18].

Chapter 1

3.2 Stage III

The optimal treatment for stage III patients is a moving field subject to improvements in staging and therapy. For stage T3N1 and T4N0-N1 (stage IIIA in the IASLC proposals for the revision of the TNM staging [7]), surgery is recommended (with or without (neo)adjuvant chemotherapy). If pathology shows positive margins, nodal extra capsular extension or N2 disease, PORT can be considered [19-21]. Although surgery is also performed for N2 disease, concomitant chemoradiation is increasingly becoming the standard of care [22]. For operated N2 patients, PORT did not show an adverse effect as was observed in stage I and II patients but only a small reduction in local recurrence was observed [18]. This issue is currently prospectively studied in the LUNG-ART trial [23]. For stage IIIB a recent phase II study of Stupp et al. showed that chemoradiation followed by surgery is feasible with a favourable outcome compared to historical stage IIIA patients [24].

For inoperable stage IIIA or stage IIIB patients (who are physically capable to receive chemotherapy), concurrent radiation-chemotherapy (chemotherapy is given as a radio-sensitizer) followed or preceded by (neo)adjuvant chemotherapy is the treatment of choice [25]. Patients for whom the physical performance is insufficient for adding chemotherapy are treated by conventional fractionated radiotherapy alone. (Marginally) operable stage I and II patients are treated similar to possibly technical operable stage IIIA patients.

3.3 Stage IV

A large group of lung cancer patients are ineligible for a (irradiation) treatment regimen with a curative intent. These are patients presenting with metastasized disease or with a locoregional recurrence. Although these patients can be referred for systemic treatment the survival remains very poor [7]. Especially these patients with advanced tumour stage are often suffering from tumour induced complaints. These patients should be optimally supported in the terminal phase of their life. Individually adapted treatment regimen is often helpful for patients with haemoptysis, pain, neurological complaints and sometimes dyspnoea.

4. New treatment strategies

To date, targeted therapies are introduced which attack the tumour cells without affecting healthy tissue. Altered cell signalling and survival pathways are often overexpressed or mutated in tumour cells and are identified as potential therapeutic targets. Also tumour associated antigens are a potential target for immunotherapy. Consequently, small molecule inhibitors, immunotherapy and gene therapy are of great interest to improve outcome of lung cancer patients. The introduction of targeted therapies has shown favourable results in the treatment of lung cancer. One example is the administration of a recombinant humanized monoclonal antibody

(bevacizumab) that binds vascular endothelial growth factor (VEGF) and thereby preventing its interaction with the VEGF receptor [27]. Another example is the inhibition of the epidermal growth factor receptor (EGFR) pathway with small molecule tyrosine kinase (TK) inhibitors (gefitinib, erlotinib) [28]. These molecules have shown significant benefit in second line and are investigated in first line treatment. Also combinations of small molecules with conventional chemotherapy and radiotherapy are under clinical investigation.

5. Radiotherapy and Lung Cancer

5.1 Target Definition and Imaging

The definition of the target (tumour) and the position of the target is critical before and during the irradiation. Consequently, appropriate imaging is of great importance for RT. Computer tomography (CT) scans are often used to define and delineate the tumour and to design the treatment plan. However, because CT images are based on tissue density, discrimination of the tumour surrounded by other non-tumour tissue with similar density (e.g. atelectasis, vasculature, mediastinum) is difficult. Consequently, the probability of observer delineation variability and anatomical misses (e.g. too small or too large irradiation volumes) is increased. The introduction of the positron emission tomography (PET) scan, visualizing metabolic active tissue using a radioactive labelled glucose analogue ([¹⁸F]fluorodeoxyglucose, FDG), proved to have a major impact for staging and RT target defisecondition for lung cancer patients [29,30].

5.2 Irradiation Technique

Technical developments of irradiation equipment and treatment planning systems improved the possibility to irradiate lung tumours more precise. In the early eighties, CT-assisted 2-D treatment planning was introduced and proved to have significant impact on the treatment planning [31]. 2-D planning was followed by 3-D treatment planning later in the eighties. First, patients were treated with two (AP-PA) beam directions whereby an additional boost was given to the tumour by oblique fields. Subsequently, according to the 3-D planning system more advanced treatment plans could be made using multiple beams resulting in the possibility to increase the dose in the tumour [32].

Nowadays, Intensity Modulated Radiotherapy (IMRT) is used in an increasing number of institutes. This treatment is given by multiple segments (i.e. individually modified treatment fields created by multi leaf collimators) per beam whereby many different beam angles are used according to coplanar and non-coplanar (off-axis of the patient) gantry positions. Consequently, the high dose can be better given to the defined target whereby the dose in the vicinity of the target can be spread to surrounding tissue [33].

5.3 Dose Delivery and Setup Correction

Indispensable for good tumour dose coverage during irradiation is knowledge concerning the position of the tumour during the treatment, which is often based on surrogate markers on (or bony anatomy of) the patient and on imaging prior to the start of the irradiation. For decades, setup verification was performed using the 2-D images (electronic portal image device, EPID) made by the linear accelerator (linac). Nowadays, more advanced techniques are introduced improving the patient setup variability and knowledge of the tumour position. For example, fiducial markers inserted around the tumour can be imaged or ideally the tumour itself can be localised using fluoroscopy [34]. An increasing number of radiotherapy departments do have a linac equipped with a Cone Beam CT (CBCT) scan. A CBCT is an integrated kV-source and imager enabling acquisition of radiographs, fluoroscopy and CBCT scans (3-D/4-D images) [35-37]. Another technique is based on infra-red reflecting markers on the patient and a stereoscopic X-ray imaging device placed in the floor and two detectors mounted at the treatment room ceiling [38]. Other techniques are the cyberknife [39] (whereby the accelerator is mounted on a robotic arm and X-ray imaging cameras are located around the patient) and tomography [40] whereby a small megavoltage X-ray source is mounted in a similar way to a CT X-ray source.

6. Normal Tissue Complications after Radiotherapy

6.1 Normal Tissue Complication Probability

In the decision whether to treat a patient, with what intent, and which treatment would be feasible, the (possible) benefits are weighted against the (possible) negative side effects. Therefore, a reliable estimation of the probability that a specific toxicity occurs is important. Normal tissue complication probability (NTCP) models are helpful in the daily clinic but also in the design of new treatment strategies to formulate dose constraints. From clinical data, NTCP curves are fitted as a function of the dose and/or volume. To develop robust NTCP models, objective well defined endpoints, sufficient number of patients and events and coverage of a wide dose range are needed.

6.2 Radiation Induced Lung Toxicity

Radiation pneumonitis (RP) is a serious side effect which might be life threatening. For lung cancer patients treated with conventional fractionated RT (CFRT) the relation between the lung dose and the incidence of radiation pneumonitis (RP) is known [41,42], however, for patients treated with hypofractionated schemes this relation is unknown.

Because lung cancer patients are often suffering from pulmonary co-morbidities it is a challenge to discriminate whether an increase of pulmonary complaints is due to the

irradiation or is due to an exacerbation of a pre-existing pulmonary disease. Therefore, comprehensive collaboration with the pulmonologist is needed. Moreover, long term follow up, pulmonary function tests, and comprehensively described clinical and dosimetric characteristics might help to reveal the predictive and prognostic factors to identify the patients at high risk for severe radiation induced lung toxicity.

6.3 Radiation Dose

From cell survival data it is known that the relation between dose and cell kill is not linear and dependent on multiple factors. Cellular recovery (repair), cell-cycle progression (redistribution), proliferation (repopulation), hypoxia (reoxygenation) influences the response (i.e. radiosensitivity) of normal tissue and tumour after irradiation. Clinically, the physical irradiation dose is converted into a biological equivalent dose according to a mathematical model (i.e. the linear quadratic (LQ) model) derived from the log cell survival as function of the dose. This model uses a linear (α) and a quadratic (β) component to describe the radiosensitivity as function of the dose. Thames et al. [43] published a survey of iso-effect curves for various normal tissues in animals; the response of various normal tissues was plotted for a range of doses per fraction. They showed that the LQ model can be used to describe the relationship between the total iso-effective dose and the total physical dose, the dose per fraction and the tissue specific radiosensitivity parameter (α/β ratio). However, the bending curve of log cell survival as function of the dose as described by the LQ-model becomes a linear line for higher dose levels [44]. Consequently, it should be questioned whether the LQ-model can be applied for RT schedules using a high dose per fraction. The consequences of these hypofractionated dose schedules for the toxicity are still uncertain.

7. The purpose of this thesis

As described above, RT is an important treatment modality for lung cancer patients but the prognosis of irradiated patients remains poor. To improve the prognosis better patient selection, development of high accuracy irradiation techniques and the optimization of predictive toxicity models are needed. These topics are subject of studies included in this thesis.

I. Pre-RT PET scans are obtained primarily for tumour staging and can be helpful for target delineation. The amount of FDG uptake in the primary tumour is correlated with the metabolism of the tumour cells. If higher uptake of FDG is correlated with worse outcome, the quantification of the FDG can be of great interest for patient selection and future treatment strategies. We evaluated the prognostic value of FDG in pre-RT scan for inoperable lung cancer patients (Chapter 2).

Chapter 1

II. The use of NTCP models is an important but complicated subject in the treatment of lung cancer patients. Previous (validated) studies found a dose-response analysis for RP after conventional fractionated RT. However, the variability within the prediction of RP is substantial. We evaluated whether the prediction of RP can be improved by the addition of pulmonary function test parameters (Chapter 3).

III. In contrast to conventional fractionated RT, for hypofractionated RT the relation between dose and RP is still unknown. Moreover, the incidence and period of risk of RP after hypofractionated RT is uncertain and are also evaluated (Chapter 4).

IV. Long term consequences of irradiation of large lung volumes is poorly studied since clinical data is scarce because of the bad prognosis. The pulmonary function of a group of lung cancer patients fortunate with a long term disease free survival is indicative of what can be expected if the prognosis of lung cancer patients is improving (Chapter 5).

V. The LQ model and NTCP calculations are important in the daily clinic to estimate the complication probabilities after conventional fractionated RT. The relation between the physical and biological lung dose (and the applicability of the LQ and the NTCP model) after hypofractionated RT is evaluated in Chapters 4 and 6.

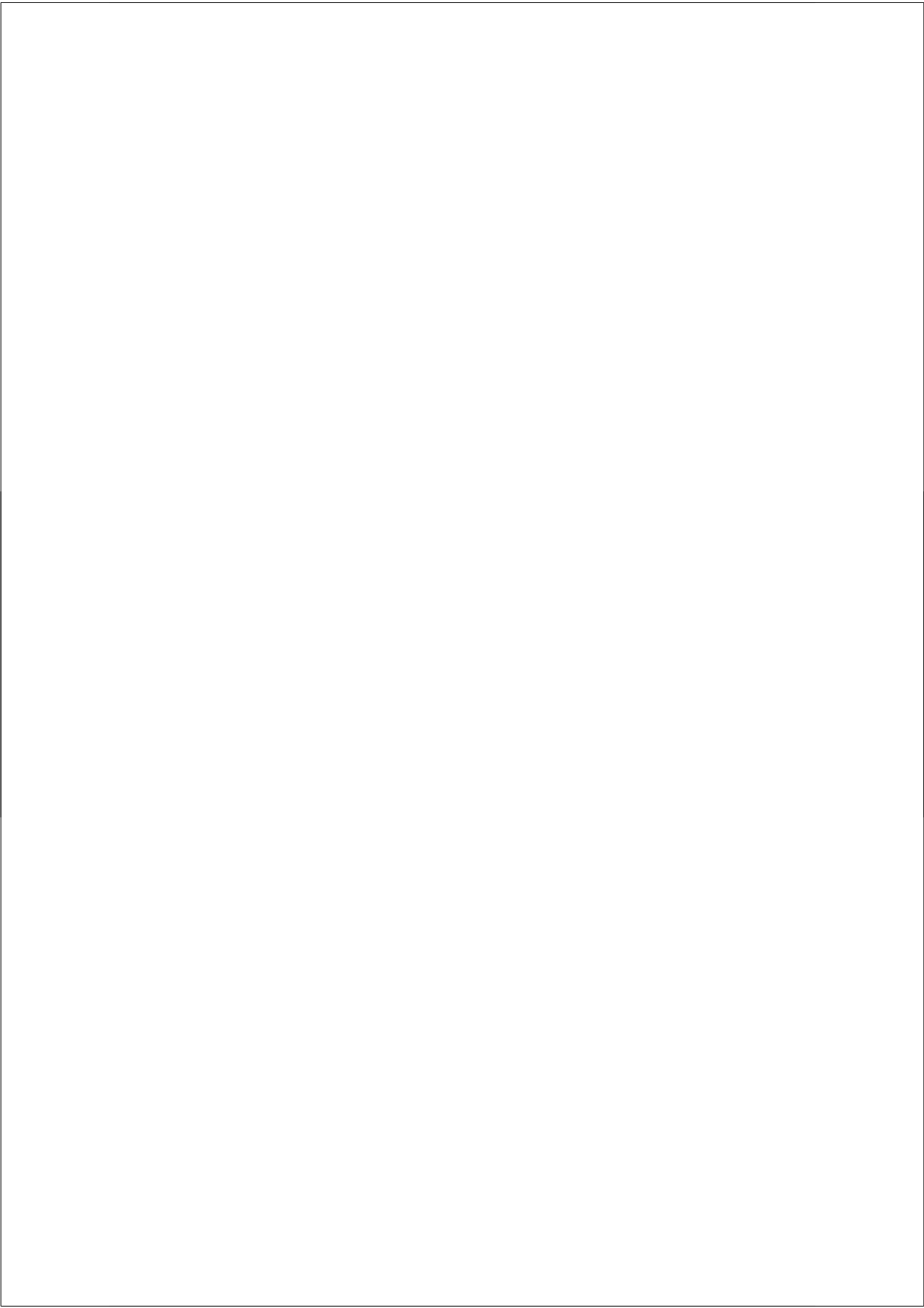
VI. More sophisticated irradiation techniques delivering higher doses to the tumour are dependent of better imaging techniques to visualize the regions of interest. The introduction of linear accelerators equipped with a CBCT was a major improvement for safe and accurate RT treatment. Nevertheless, older verification techniques are still in widespread use. Consequently, differences between the patient setup verification using the CBCT and the EPID are of great interest (Chapter 7).

References

1. Parkin DM, Bray F, Ferlay J et al. Global cancer statistics, 2002. *CA Cancer J Clin* 2005;55:74-108.
2. Alberg AJ, Ford JG, Samet JM. Epidemiology of lung cancer: ACCP evidence-based clinical practice guidelines (2nd edition). *Chest* 2007;132:29S-55S.
3. Clark OH, Hall AD, Schambelan M. Clinical manifestations of adrenal hemorrhage. *Am J Surg* 1974;128:219-224.
4. Bach PB, Jett JR, Pastorino U et al. Computed tomography screening and lung cancer outcomes. *JAMA* 2007;297:953-961.
5. Hillman BJ. Economic, legal, and ethical rationales for the ACRIN national lung screening trial of CT screening for lung cancer. *Acad Radiol* 2003;10:349-350.
6. Brody JS, Spira A. State of the art. Chronic obstructive pulmonary disease, inflammation, and lung cancer. *Proc Am Thorac Soc* 2006;3:535-537.
7. Goldstraw P, Crowley J, Chansky K et al. The IASLC Lung Cancer Staging Project: proposals for the revision of the TNM stage groupings in the forthcoming (seventh) edition of the TNM Classification of malignant tumours. *J Thorac Oncol* 2007;2:706-714.
8. Brundage MD, Davies D, Mackillop WJ. Prognostic factors in non-small cell lung cancer: a decade of progress. *Chest* 2002;122:1037-1057.
9. Vansteenkiste JF, Stroobants SG. The role of positron emission tomography with 18F-fluoro-2-deoxy-D-glucose in respiratory oncology. *Eur Respir J* 2001;17:802-820.
10. Blomgren H, Lax I, Naslund I et al. Stereotactic high dose fraction radiation therapy of extracranial tumors using an accelerator. Clinical experience of the first thirty-one patients. *Acta Oncol* 1995;34:861-870.
11. Nagata Y, Takayama K, Matsuo Y et al. Clinical outcomes of a phase I/II study of 48 Gy of stereotactic body radiotherapy in 4 fractions for primary lung cancer using a stereotactic body frame. *Int J Radiat Oncol Biol Phys* 2005;63:1427-1431.
12. Nyman J, Johansson KA, Hulten U. Stereotactic hypofractionated radiotherapy for stage I non-small cell lung cancer--mature results for medically inoperable patients. *Lung Cancer* 2006;51:97-103.
13. Onimaru R, Fujino M, Yamazaki K et al. Steep dose-response relationship for stage I non-small-cell lung cancer using hypofractionated high-dose irradiation by real-time tumor-tracking radiotherapy. *Int J Radiat Oncol Biol Phys* 2008;70:374-381.
14. Onishi H, Araki T, Shirato H et al. Stereotactic hypofractionated high-dose irradiation for stage I nonsmall cell lung carcinoma: clinical outcomes in 245 subjects in a Japanese multiinstitutional study. *Cancer* 2004;101:1623-1631.
15. Timmerman R, Papiez L, McGarry R et al. Extracranial stereotactic radioablation: results of a phase I study in medically inoperable stage I non-small cell lung cancer. *Chest* 2003;124:1946-1955.
16. Wulf J, Haedinger U, Oppitz U et al. Stereotactic radiotherapy for primary lung cancer and pulmonary metastases: a noninvasive treatment approach in medically inoperable patients. *Int J Radiat Oncol Biol Phys* 2004;60:186-196.
17. Zimmermann FB, Geinitz H, Schill S et al. Stereotactic hypofractionated radiotherapy in stage I (T1-2 N0 M0) non-small-cell lung cancer (NSCLC). *Acta Oncol*

- 2006;45:796-801.
18. Postoperative radiotherapy for non-small cell lung cancer. *Cochrane Database Syst Rev* 2005;CD002142
 19. Depierre A, Milleron B, Moro-Sibilot D et al. Preoperative chemotherapy followed by surgery compared with primary surgery in resectable stage I (except T1N0), II, and IIIa non-small-cell lung cancer. *J Clin Oncol* 2002;20:247-253.
 20. Rosell R, Gomez-Codina J, Camps C et al. A randomized trial comparing preoperative chemotherapy plus surgery with surgery alone in patients with non-small-cell lung cancer. *N Engl J Med* 1994;330:153-158.
 21. Roth JA, Fossella F, Komaki R et al. A randomized trial comparing perioperative chemotherapy and surgery with surgery alone in resectable stage IIIA non-small-cell lung cancer. *J Natl Cancer Inst* 1994;86:673-680.
 22. van Meerbeeck JP, Surmont VF. Stage IIIA-N2 NSCLC: a review of its treatment approaches and future developments. *Lung Cancer* 2009;65:257-267.
 23. Phase III Study Comparing Post-Operative Conformal Radiotherapy to No Post-Operative Radiotherapy in Patients With Completely Resected Non-Small Cell Lung Cancer and Mediastinal N2 Involvement [Lung ART]. www.clinicaltrials.gov/NCT00410683 . 2009.
 24. Stupp R, Mayer M, Kann R et al. Neoadjuvant chemotherapy and radiotherapy followed by surgery in selected patients with stage IIIB non-small-cell lung cancer: a multicentre phase II trial. *Lancet Oncol* 2009;10:785-793.
 25. Belani CP, Wang W, Johnson DH et al. Phase III study of the Eastern Cooperative Oncology Group (ECOG 2597): induction chemotherapy followed by either standard thoracic radiotherapy or hyperfractionated accelerated radiotherapy for patients with unresectable stage IIIA and B non-small-cell lung cancer. *J Clin Oncol* 2005;23:3760-3767.
 26. Ozturk B, Egehan I, Atavci S et al. Pentoxifylline in prevention of radiation-induced lung toxicity in patients with breast and lung cancer: a double-blind randomized trial. *Int J Radiat Oncol Biol Phys* 2004;58:213-219.
 27. Sandler A, Gray R, Perry MC et al. Paclitaxel-carboplatin alone or with bevacizumab for non-small-cell lung cancer. *N Engl J Med* 2006;355:2542-2550.
 28. Butts CA, Bodkin D, Middleman EL et al. Randomized phase II study of gemcitabine plus cisplatin or carboplatin [corrected], with or without cetuximab, as first-line therapy for patients with advanced or metastatic non small-cell lung cancer. *J Clin Oncol* 2007;25:5777-5784.
 29. Steenbakkers R, Duppen J, Fitton I et al. A 3D Analysis and Reduction of Observer Variation in Delineation of Lung Cancer for Radiotherapy. *ASTRO 2004 Abstract 2327* 2004.
 30. Vanuytsel LJ, Vansteenkiste JF, Stroobants SG et al. The impact of (18)F-fluoro-2-deoxy-D-glucose positron emission tomography (FDG-PET) lymph node staging on the radiation treatment volumes in patients with non-small cell lung cancer. *Radiother Oncol* 2000;55:317-324.
 31. Ragan DP, Perez CA. Efficacy of CT-assisted two dimensional treatment planning: analysis of 45 patients. *AJR Am J Roentgenol* 1978;131:75-79.

32. Belderbos JS, De Jaeger K, Heemsbergen WD et al. First results of a phase I/II dose escalation trial in non-small cell lung cancer using three-dimensional conformal radiotherapy. *Radiother Oncol* 2003;66:119-126.
33. Schwarz M, Alber M, Lebesque JV et al. Dose heterogeneity in the target volume and intensity-modulated radiotherapy to escalate the dose in the treatment of non-small-cell lung cancer. *Int J Radiat Oncol Biol Phys* 2005;62:561-570.
34. Shirato H, Harada T, Harabayashi T et al. Feasibility of insertion/implantation of 2.0-mm-diameter gold internal fiducial markers for precise setup and real-time tumor tracking in radiotherapy. *Int J Radiat Oncol Biol Phys* 2003;56:240-247.
35. Inoue A, Kunitoh H, Sekine I et al. Radiation pneumonitis in lung cancer patients: a retrospective study of risk factors and the long-term prognosis. *Int J Radiat Oncol Biol Phys* 2001;49:649-655.
36. Sonke JJ, Zijp L, Remeijer P et al. Respiratory correlated cone beam CT. *Med Phys* 2005;32:1176-1186.
37. Jaffray DA, Siewerdsen JH, Wong JW et al. Flat-panel cone-beam computed tomography for image-guided radiation therapy. *Int J Radiat Oncol Biol Phys* 2002;53:1337-1349.
38. Yan H, Yin FF, Kim JH. A phantom study on the positioning accuracy of the Novalis Body system. *Med Phys* 2003;30:3052-3060.
39. Adler JR, Jr., Chang SD, Murphy MJ et al. The Cyberknife: a frameless robotic system for radiosurgery. *Stereotact Funct Neurosurg* 1997;69:124-128.
40. Mackie TR, Balog J, Ruchala K et al. Tomotherapy. *Semin Radiat Oncol* 1999;9:108-117.
41. Kwa SL, Lebesque JV, Theuws JC et al. Radiation pneumonitis as a function of mean lung dose: an analysis of pooled data of 540 patients. *Int J Radiat Oncol Biol Phys* 1998;42:1-9.
42. Seppenwoolde Y, Lebesque JV, De Jaeger K et al. Comparing different NTCP models that predict the incidence of radiation pneumonitis. Normal tissue complication probability. *Int J Radiat Oncol Biol Phys* 2003;55:724-735.
43. Thames HD, Ang KK, Stewart FA et al. Does incomplete repair explain the apparent failure of the basic LQ model to predict spinal cord and kidney responses to low doses per fraction? *Int J Radiat Biol* 1988;54:13-19.
44. Puck T, Marcus P. Action of x-rays on mammalian cells. *J Exp Med* 1956;103:653-666.



FDG standardized uptake value as prognostic factor for inoperable non-small cell lung cancer

Gerben R. Borst¹, José S.A. Belderbos¹, Ronald Boellaard², Emile F.I. Comans², Katrien De Jaeger¹, Adriaan A. Lammertsma², Joos V. Lebesque¹

¹*Department of Radiation Oncology, The Netherlands Cancer Institute-Antoni van Leeuwenhoek Hospital, Amsterdam, The Netherlands.*

²*Clinical PET Centre, VU University Medical Centre, Amsterdam, The Netherlands*

European Journal of Cancer
Volume 41, Issue 11, July 2005, Pages 1533-1541

Abstract

The aim of this study was to investigate the relationship between standardized uptake value (SUV), obtained from [¹⁸F]fluorodeoxyglucose positron emission tomography (FDG PET), and treatment response and survival of inoperable NSCLC patients treated with high dose radiotherapy. Fifty-one patients were included, recording stage, performance, weight loss, tumour volume, histology, lymph node involvement, SUV, and delivered radiation dose. The maximum SUV (SUV_{max}) within the primary tumour was a sensitive and specific factor for predicting treatment response. Apart from SUV_{max}, stage and performance were also independent predictive factors for treatment response. In a multivariate disease-specific survival (DSS) analysis, SUV_{max} (p = 0.01), performances status (p = 0.008) and stage (p = 0.04) were prognostic factors. For overall survival (OS), SUV_{max} (p = 0.001) and performance (p = 0.06) were important prognostic factors. SUV_{max} was an important prognostic factor for survival of inoperable NSCLC patients and a predictive factor for treatment response. Although the number of patients was small, the treatment was inhomogeneous and the use of FDG SUV may have constraints, we still conclude that the FDG SUV is potentially a good indicator for selecting patients for different treatment strategies.

Introduction

TNM stage, performance status and weight loss are important prognostic factors used to stratify NSCLC patients for the most optimal treatment regimen [1]. These factors, however, do not always provide a satisfactory explanation for differences in outcome between patients. Molecular markers and other features, such as tumour doubling time, are also closely related to prognosis [2], although these factors are not always available in case of inoperable NSCLC patients (e.g. no pathology). A non-invasive prognostic classifier may improve selection of those inoperable NSCLC patients, who are appropriate candidates for individually adapted therapy (dose escalation, chemoradiation), potentially improving the poor prognosis of these NSCLC patients.

Neoplastic cells demonstrate up-regulation of glucose metabolism in order to obtain energy needed for proliferation [3]. Consequently, uptake of glucose or glucose analogues like deoxy-glucose is increased. Labelling deoxy-glucose with the positron emitting radionuclide ^{18}F to form [^{18}F]fluorodeoxyglucose (FDG) renders these cells detectable using positron emitting tomography (PET) because, in contrast to glucose, FDG is no substrate for hexokinase and is therefore trapped in the cells.

The standardized uptake value (SUV) is a semi-quantitative method for assessing glucose metabolism, which is often used in clinical studies. Higher SUV values were observed in NSCLC with higher proliferation rates [4-6]. Moreover, it was demonstrated that SUV was a significant prognostic factor in the survival analysis of NSCLC patients [7-12].

The purpose of the present study was to investigate whether SUV could be used as a classifier for predicting which patients will have favorable treatment response, and to assess the significance of SUV as a prognostic factor in survival analysis of inoperable NSCLC patients treated with high dose radiotherapy.

Patients and Methods

Patients

Patients included in this study were diagnosed and treated at the Department of Radiation Oncology in The Netherlands Cancer Institute - Antoni van Leeuwenhoek Hospital. The FDG scan was performed at the Department of Nuclear Medicine and PET research of the VU University Medical Centre, Amsterdam. PET imaging was requested for the evaluation of mediastinal lymph node involvement and as a screening method for the presence of clinically unsuspected distant metastasis in patients diagnosed with NSCLC. For patients with small progressive peripheral lesions on computed tomography (where histology or cytology was not feasible) increased FDG uptake was used as a criterion to confirm diagnosis.

From January 1999 and November 2001, data of 60 consecutive patients meeting

Chapter 2

the following eligibility criteria could be evaluated in the present analysis. Patients had to have histologically proven NSCLC, or a progressive lesion on computed tomography with increased FDG uptake on the PET image. Both transmission and emission scan were required to analyze the SUV retrospectively. Nine of the 60 patients were suspected to have distant metastases on the PET images and were excluded from this study because curative therapy was not feasible. Follow up of patients was closed on 31 July 2004.

Recorded characteristics were age, gender, performance status, histology, tumour volume, weight loss, treatment response, and tumour and- lymph node stage. Weight loss was scored into 3 groups defined as 0 – 5 %, 5 % - 10 % or > 10 % loss of the original weight during 3 months prior to therapy. Treatment response was scored 3 months after treatment and defined according to the Response Evaluation Criteria in Solid Tumours (RECIST) criteria [13]. The performance status of the patient was defined according to the World Health Organization (WHO) criteria.

The mean age of the 51 patients (34 men and 17 women) was 69 years. Fifteen patients had WHO performance status 0, 33 performance status 1, and only 3 patients performance status 2, respectively. Stage I disease was diagnosed in 21 patients and 11 patients had stage II disease. These patients were medically inoperable or refused surgery. Nineteen patients had stage III disease and were technically inoperable. Concerning the lymph nodes, 23 patients had N0 disease, 10 patients N1 and 18 patients proved to have N2-3 disease based on CT and PET (Table 1). Tumour volume was computed as the volume of the primary tumour delineated by the

Table 1. Patient Characteristics

<i>Characteristic</i>	<i>Number of patients Mean (Range)</i>	<i>Characteristic</i>	<i>Number of patients Mean (Range)</i>
Total	51	Tumour volume (cm ³)	80.0 (4.2 – 455.6)
Age	69 (32 – 88)	Histology	
Gender		Squamous cell	17
Male	34	Adenocarcinoma	13
Female	17	Large Cell	10
		Unknown	11
WHO performance status		SUV _{max} *	17.0 (3.4 – 40.8)
0	15		
1	33	Chemotherapy	
2	3	Sequential	6
		Concurrent	4
Stage		Radiotherapy dose (Gy)	77 (60 - 94.5)
I	21		
II	11		
III	19		
Lymph node			
N0	23		
N1	10		
N2-3	18		

*SUV_{max} is the maximum standardized uptake value within the primary tumour.

FDG SUV as prognostic factor for inoperable NSCLC

radiation oncologist on the pre-radiotherapy CT scan. The mean tumour volume was 80 cm³ (range: 4.2 - 455.6 cm³). The smallest and largest tumour had a maximum diameter of 1.5 and 12.3 cm, respectively. Pathology was not available for 11 patients with a small peripheral tumour, which was progressive on CT and positive on PET. Seventeen patients had squamous cell carcinoma, 13 patients adenocarcinoma and 10 patients large cell carcinoma (Table 1).

Thirty-four patients were included in a Phase I/II dose escalation study [14] and were treated with doses between 60.8 and 94.5 Gy (2.25 Gy per fraction, fixed overall treatment time of 6 weeks). Six of these dose escalation patients had stage IIIA or IIIB NSCLC and received induction chemotherapy (gemcitabin with either carboplatin or cisplatin). Four patients received 66 Gy (2.75 Gy per fraction) with concurrent daily intravenously Cisplatin (6 mg/m²). Two of those patients had stage IIIB NSCLC and 2 patients had stage IIB NSCLC. Three patients received 70 Gy in 2 Gy fractions. Ten patients were irradiated with a total dose of 67.5 Gy in 2.25 Gy per fraction. The mean dose was 77 Gy (range 60 – 94.5 Gy) (Table 1). PET positive lymphnodes were included in the gross tumour volume together with the primary tumour. Therefore these nodes were irradiated to the same dose as the primary tumour.

FDG-PET

PET imaging was performed with a median of 19 days (minimum 4, maximum 66 days) before start of treatment. Scans were performed on a dedicated ECAT EXACT HR+ PET scanner (Siemens/CTI, Knoxville, TN, USA). This scanner has an axial field of view of 15 cm, divided into 63 contiguous planes. All patients fasted for at least 6 hours before scanning. FDG was injected in the arm contra lateral to the tumour and prior to injection a blood sample was taken from this arm for the serum glucose measurement. Approximately 60 min after injection of FDG (5.5 MBq x body weight, with a minimum of 340 MBq, and a maximum of 550 MBq), an emission scan (2D mode), and a 10-15 min transmission scan were acquired. The FDG scan was corrected for dead time, decay, scatter, random coincidences and photon attenuation. Scans were reconstructed using ordered subset expectation maximization (OSEM) with 2 iterations and 16 subsets, followed by post-smoothing of the reconstructed image using a Hanning 0.5 filter. An image matrix size of 256 x 256 was used.

Standardized Uptake Value (SUV)

FDG uptake was quantified using SUV. In this study SUV_{max} was defined as the maximum tumour concentration of FDG divided by the injected dose and corrected for the body weight of the patient: [SUV = maximum activity concentration /

Chapter 2

(injected dose / body weight)]. For the determination of the SUV_{max} , the maximum FDG-uptake was searched within the region of the primary tumour on the PET image. This region was manually drawn. The mean SUV (SUV_{mean}) was defined as the mean concentration of FDG divided by the injected dose and corrected for the body weight of the patient. The mean FDG-uptake was determined by a threshold method, whereby the mean of all pixel values above 50 % of the maximum value was calculated. Assuming a normal fasting plasma glucose concentration [Glc] of 100 mg dl⁻¹ (i.e. 5.55 mmol l⁻¹), both SUVs were corrected for glucose by multiplying the SUV with the measured glucose concentration divided by this normal value [15].

Statistical analysis

For the disease-specific survival (DSS), an event was defined if lung cancer was the cause of death. One patient with a partial response developed metastasis 5 months after treatment and received palliative chemotherapy, which was complicated by renal insufficiency. For this patient renal failure was the cause of death, but it was still defined as an event in the DSS analysis. Death of any cause was defined as an event in the overall survival (OS) analysis. Survival time was defined as the time interval between the date of treatment and an event. These events were censored in the DSS analysis. Correlations between two variables were calculated with the Pearson correlation coefficient.

Logistic regression analysis was performed to assess which factors were significant explanatory variables to predict treatment response. The sensitivity and specificity of the SUV to predict therapy response was evaluated using the receiver operating characteristic (ROC) curve. Survival probabilities were estimated using the Kaplan-

Table 2. Response and follow-up data of all patients

Response Number of patients	No evidence of disease	Local progression of disease	Metastasis	Death due to disease	Death due to other cause	Median survival (months)
Complete response 15	10	1			5	38
1			1	1		
1						
Partial response 9		7		6	4	14
7			5	5	1	
5		4	4	3	1	
4						
Stable disease 2			1	1	1	11
2		2	2	1		
Progressive disease 5				4		9
Total	51	10	13	13	21	17

Meier method. Significance of the difference between groups with respect to the studied parameters was assessed using the log-rank test. To assess the joint effects and interactions of the significant variables in the univariate analysis, multivariate analysis was carried out with the Cox proportional hazards model. A significance level of 0.05 was used for covariate entry. To avoid “over-interpretation” of the SUV analysis, the median SUV was used for univariate analysis and SUV was incorporated as a continuous variable in the multivariate analysis.

Results

Treatment response and follow up

Thirty-three percent (n = 17) of the patients experienced a complete response. These patients had a median survival of 38 months. Fifty percent (n = 25) of the patients had a partial response with a median survival of 14 months. Stable disease was achieved in 8% (n = 4, 10 months median survival) of the patients and 10 % (n = 5) of the patients suffered from progressive disease (9 months median survival) (Table 2). The overall median follow-up was 17 months (range: 3 to 57 months). Of the 17 patients with a complete response (CR), one developed local progression 6 months after treatment and one patient developed distant metastasis at 24 months follow up. Sixteen of the 25 patients with partial response (PR) developed disease progression and/or metastases, diagnosed 9 months (median) after treatment. Ten months (median) after treatment, 3 of the 4 patients with stable disease (SD) developed metastases and 5 patients did not respond to therapy (progressive disease, PD). For 21 patients lung cancer was the cause of death after a median survival time of 12 months. Twelve patients died from other cause than lung cancer. Six patients died of vascular diseases, 3 patients of respiratory diseases and 3 patients from other causes. These 12 patients had a median survival of 14 months. At the end of the study the 19 surviving patients had a median survival time of 24 months.

Standardized Uptake Value

The median SUV_{max} was 15 (mean = 17, SD = 9) and the minimum and maximum SUV_{max} values were 3 and 41, respectively. No statistical correlation was observed between tumour volume and SUV_{max} (r = 0.17, p = 0.2), and between lymphnode status and SUV_{max} (r = 0.15, p = 0.3). The mean SUV_{max} for squamous cell carcinoma was 15. For adenocarcinoma and large cell carcinoma SUV_{max} was 16 and 20, respectively. The mean SUV_{max} was 17 for the 11 patients with unknown histopathology. Stage I and II patients had a mean SUV_{max} of 14. Stage III patients had a mean SUV_{max} of 16. The median SUV_{mean} was 9 (mean = 11, SD = 6) and the minimum and maximum SUV_{mean} values were 2 and 25, respectively.

Univariate response analysis

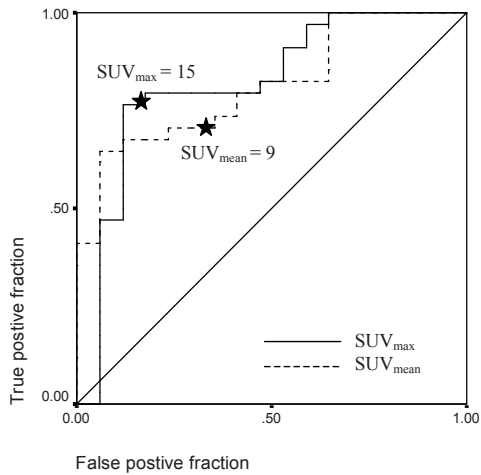


Figure 1. Receiver operating characteristics curves using standardized uptake value (SUV) to predict complete response. The maximum SUV (SUV_{max}) and the mean SUV (SUV_{mean}) were tested.

complete response, and the area under the curve was 77 % (95 % CI, 63 % - 91 %) (Figure 1).

Multivariate response analysis

To assess whether SUV was an independent predictive factor for treatment response, logistic regression analysis was used. Because the predictive value of SUV_{max} was better than the predictive value of SUV_{mean}, we included only SUV_{max} in the multivariate analysis. SUV_{max} was incorporated as a continuous parameter. Because stage was strongly correlated with the lymph node status ($r^2 = 0.86$, $p < 0.001$) only SUV_{max}, stage and performance status (and not the lymph node status) were included in this model. Stage ($p = 0.02$), performance status ($p = 0.01$) and SUV_{max} ($p = 0.05$) were independently associated with complete response (Table 3). The odds ratio (OR) of

The ability of SUV_{max} to predict initial therapy response is depicted by the receiver operating curve (ROC) curve shown in Figure 1. Using the median SUV_{max} of 15 yields a sensitivity of 77 % and specificity 84 % in predicting complete response. The area under the curve of 82 % (95 % confidence interval (CI), 69 – 95 %) is indicative for the level of accuracy (Figure 2). Stage ($p = 0.02$), performance status ($p = 0.04$) and positive lymph nodes ($p = 0.04$) were significant factors correlated with complete response. In contrast, chemotherapy, dose, tumour volume, weight loss and histology were not significant. The median SUV_{mean} had a sensitivity of 71 % and a specificity of 65 % to predict

Table 3. Logistic regression analysis to predict treatment response.

	Odds ratio	95% CI*	p
SUV _{max} **	1.13	1.01 - 1.27	0.05
Stage, I-II v III	3.29	1.23 - 8.77	0.02
Performance (WHO), 0 v 1 v 2	6.92	1.53 - 31.32	0.01

*95 % Confidence interval of the odds ratio. ** SUV_{max} is the maximum standardized uptake value within the primary tumour; SUV_{max} is incorporated as a continuous variable

SUV_{max} was 1.13, which number indicates the relative increase in odds of having no complete response when the SUV_{max} value increased by one-unit. The ORs of stage and performance status were 3.29 and 6.92, respectively (Table 3)

Univariate survival analysis

Kaplan Meier plots for the disease-specific survival (DSS) and overall survival (OS) illustrate large survival differences between patients with SUV_{max} < 15 and SUV_{max} ≥ 15 in favor of the low SUV_{max} group (Figure 2). Survival differences were statistically significant for both the DSS (p < 0.001) and OS (p < 0.001) (Table 4). The survival benefit for patients of the low SUV_{mean} group (SUV_{mean} < 9) was less significant than the survival benefit observed for the low SUV_{max} group (DSS, p = .004 and OS p = 0.02). For DSS and OS median survival times were 39 and 17 months, respectively. The 2-year survival rates for DSS and OS were 57 % and 43 %, respectively. Stage (p = 0.04), performance status (p = 0.01), lymphnode status (p = 0.04), treatment response (p = 0.02), chemotherapy (p = 0.01) and tumour volume (p = 0.03) were significantly associated with DSS. A trend for a better DSS was observed in patients irradiated with doses of 70 Gy or higher compared with patients irradiated with doses lower than 70 Gy (p = 0.06). Significant factors for OS were performance status (p = 0.04), chemotherapy (p = 0.01) and treatment response (p = 0.01) (Table 4). Weight loss and histology were not significant factors.

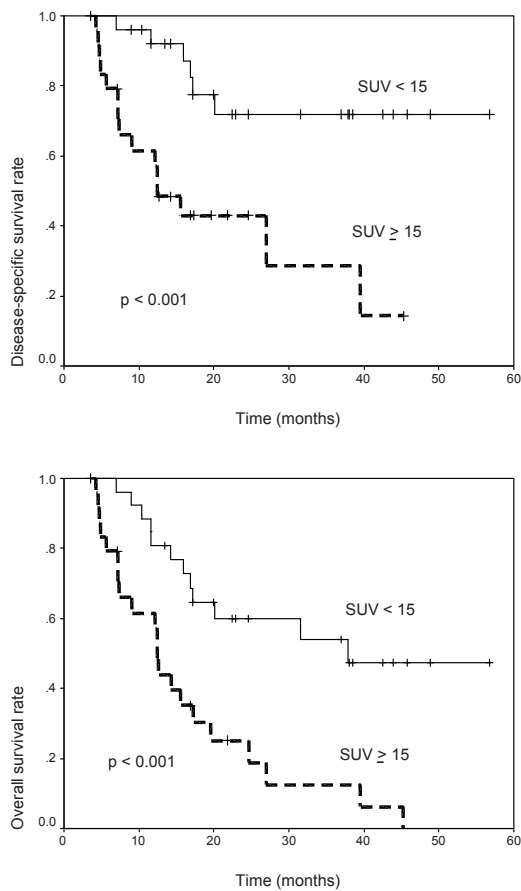


Figure 2. Kaplan–Meier survival curves for the disease-specific survival and the overall survival and the P values of the log-rank test.

Chapter 2

Table 4. Univariate analysis of the disease-specific survival and overall survival

Factor	Number of patients	Disease-specific survival			Overall survival		
		Median survival (months)	2-year survival (%)	log-rank (p)	Median survival (months)	2-year survival (%)	log-rank (p)
Total group	51	39	57		17	43	
SUV _{max}							
< 15	26	NR	72	< 0.001	38	60	< 0.001
≥ 15	25	12	43		12	27	
Treatment response							
Complete	17	NR	92	0.02	38	50	0.01
Partial	25	12	40		14	26	
Stable/Progressive disease	9	12	41		10	33	
Stage							
I, II	32	NR	68	0.04	25	50	0.3
III	19	16	41		16	32	
Performance (WHO)							
0	15	NR	81	0.01	38	61	0.04
1	33	20	51		16	39	
2	3	12	0		12	0	
N stage							
N0	23	NR	72	0.04	25	54	0.2
N+	28	16	44		16	34	
Chemotherapy							
No	41	NR	64	0.01	20	50	0.01
Yes	10	12	26		12	13	
Dose (Gy)							
< 70	17	17	42	0.06	16	37	0.4
≥ 70	34	NR	65		20	47	
Tumour volume (cm ³)							
≤ 18	17	NR	69	0.03	12	56	0.3
[19, 74]	17	NR	67		17	44	
≥ 75	17	12	36		31	34	
Weight loss (%)							
< 5	41	17	60	0.6	17	42	0.8
[5 –10]	10	40	48		17	48	
>10	0						
Histology							
Squamous	17	NR	50	0.5	14	32	0.8
Adenocarcinoma	13	27	47		20	39	
Large cell	10	20	60		17	50	
Unknown	11	NR	79		31	64	

NR = not reached.

Multivariate survival analysis

For the multivariate survival analysis the significant variables in the log-rank test ($p < 0.05$) were examined in the Cox proportional hazards model to evaluate their interaction and joint effect on DSS and OS. The SUV_{max} was included in this analysis because SUV_{max} was more significant in the log-rank test than the SUV_{mean}. This SUV_{max} was incorporated as continuous parameter. We excluded the treatment response as a parameter in the multivariate analysis, since this parameter is not known prior to therapy. Chemotherapy, tumour volume and lymph node status were not included, because of the strong correlation of these factors with stage. For

DSS, all significant factors in the univariate analysis (SUV_{max} , performance status and stage) remained significant in the Cox proportional hazard model (SUV_{max} , $p = 0.01$; performance status, $p = 0.008$; stage, $p = 0.04$, Table 5).

The hazard ratio (HR) of SUV_{max} was 1.06, which indicated that a one-unit increase of SUV_{max} correspond to a 6 % increase of hazard of lung cancer related death. The HRs for stage and performance status were 1.6 and 3.86, respectively. For OS, SUV_{max} ($p = 0.001$) and performance status ($p = 0.06$) remained significant factors in the Cox proportional hazard model (Table 6). Equally to the DSS, a one-unit increase of SUV_{max} corresponded with a 6 % increase of hazard of death due to any cause.

Table 5. Cox proportional hazards model for the disease-specific survival

	Hazard ratio	95% CI*	p
Performance (WHO), 0 v 1 v 2	3.86	1.43 - 10.43	0.008
Stage I, II v III	1.60	1.02 - 2.51	0.04
SUV_{max}^{**}	1.06	1.01 - 1.10	0.01

Table 6. Cox proportional hazards model for the overall survival

	Hazard ratio	95% CI*	p
Performance (WHO), 0 v 1 v 2	1.93	1.41 - 3.86	0.06
SUV_{max}^{**}	1.06	1.02 - 1.10	0.001

*95 % Confidence interval of the hazard ratio

** SUV_{max} is the maximum standardized uptake value within the primary tumour; SUV_{max} is incorporated as a continuous variable

Discussion

In the present study FDG SUV_{max} was predictive for treatment response and the median SUV_{max} was a good variable to predict complete response in inoperable NSCLC patients. The multivariate survival analysis proved that SUV_{max} was an explanatory prognostic factor for both disease-specific (DSS) and overall (OS) survival. We could not perform a disease free survival analysis because only 2 patients with complete response ($n = 17$) developed metastases or progression of disease.

Differences in patients selection makes it difficult to compare our results with previous studies. Most studies included mainly surgically treated NSCLC patients and observed better survival rates than in the present study [8-10]. Ahuja et al. [11] found poorer survival rates, however 20 % of those patients had stage IV disease and were treated palliatively. Only Sasaki et al. [7] evaluated the prognostic value of SUV_{max} for radiotherapy patients. They found that a cut off value of 5 (median SUV_{max} was 8) provided the most significant survival difference between patients

Chapter 2

above and below this cut off value. Their radiotherapy patients had a high 2-year OS of 71 %, which was not different from the 2-year OS of surgically treated patients. The importance of SUV for inoperable NSCLC patients was confirmed in our analysis, where SUV_{max} was statistically associated with both treatment response and survival. The lower survival rate in the present study may be explained by both higher SUV_{max} values and higher incidence of medical inoperability observed in our patients. Downey et al. [10] incorporated SUV_{max} also as a continuous variable in the Cox proportional hazards model, and observed a 7 % increase in hazard of death after a one-unit increase in SUV_{max} . This is in agreement with the present data. It is important to note that Downey et al. observed SUV_{max} values in the same range as in the present study.

Difference in PET scanning techniques is another potential problem, while comparing studies that attempt to evaluate the prognostic value of SUV. Differences in injected FDG -dose, scanning time (i.e. time after injection), reconstruction algorithms, filters, scanner characteristics, sinogram noise and quantification methods might lead to (structural) inter-institutional SUV differences [16].

Even the calculation of a SUV may differ between SUV studies. SUV_{mean} calculated with a threshold method was shown to be slightly better reproducible than the SUV_{max} . However, the SUV_{mean} might include pixel values of non-tumour tissue [17]. We observed that the SUV_{max} was better predictive for treatment response than the SUV_{mean} , which might be due to the fact that the maximum SUV represents better the most metabolic active (i.e. most aggressive) part of the tumour. Another factor that influences the SUV is the level of plasma glucose of the patient during PET scanning. Two studies observed a reduced variability and improved reproducibility of SUV after glucose correction [18, 19]. In our study we did observe a similar predictive value for both glucose corrected SUV and uncorrected SUV and also for survival analysis glucose correction did not influence the results (data not shown).

Notwithstanding the mentioned constraints of SUV, it is a clinical feasible and often used quantification parameter of PET images. Hoekstra et al. compared different SUV calculation methods with the nonlinear regression method, which is used as a golden standard to quantify FDG uptake (but this is not clinically feasible) [20]. To verify the best possible quantification method with the appropriate cut off values for NSCLC, similar studies are required with prospective clinical patients data. In addition, PET-scanning techniques and quantification methods should be more uniform, before guidelines for general use of a particular SUV can be implemented [21].

Currently, the application of FDG PET in the treatment of NSCLC patients has become increasingly important. First, detection of otherwise unknown metastases

and distinction of benign from malignant lymphnodes improves staging, and thereby potentially also the choice of treatment of NSCLC patients [22, 23]. Secondly, for inoperable NSCLC patients, the information obtained from FDG PET is important to delineate the gross tumour volume [24]. The third reason is that studies have shown that PET was a sensitive method for evaluating tumour response [25], even more accurate than response monitoring by CT [26]. Apart from these diagnostic, treatment and response monitoring purposes, the prognostic value of SUV adds another dimension to PET imaging of inoperable NSCLC patients. Prognostic information obtained from a tumour biopsy is not always available in inoperable NSCLC patients (in our study we did not have pathology in 11 patients). Pathology, tumour doubling time, glucose transporter proteins (Glut 1 and Glut 3) and proliferation markers (Ki-67) are prognostic factors obtained from biopsy material [1, 27, 28]. SUV was associated with these prognostic factors; squamous cell carcinoma did have a higher SUV than adenocarcinoma [10, 12] and strong correlations were observed between SUV and tumour doubling time, glucose transporters (Glut1 and Glut 3) and the proliferation marker Ki-67 [4, 6, 29].

SUV could have an important impact for inoperable NSCLC patients because their poor prognosis. Although the poor prognosis is also due to the co-morbidity of inoperable NSCLC patients, better selection for individually adapted treatment strategies will undoubtedly improve outcome. SUV was accurately predictive for treatment response and may contribute to select patients for the appropriate treatment strategies. Confirmation of our results by prospective clinical data is important. Quantification of PET images, in combination with conventional prognostic factors, might indicate which patients are appropriate candidates for more aggressive treatment strategies (chemo radiation, dose escalation) or should better be treated in a palliative setting.

Conclusion

FDG SUV_{max} was an important complementary prognostic factor for survival in 51 irradiated inoperable NSCLC patients. Moreover, this SUV provided good prediction of response to radiotherapy. In current diagnostic and treatment settings of (inoperable) NSCLC patients, the use of FDG PET imaging is increasing. The FDG SUV_{max} obtained from these images might help to determine the most appropriate treatment strategy, and consequently improve treatment efficiency. Because of the limited number of patients in this study a prospective clinical study, in a larger group of patients, is necessary to determine the optimal cut off values.

Chapter 2

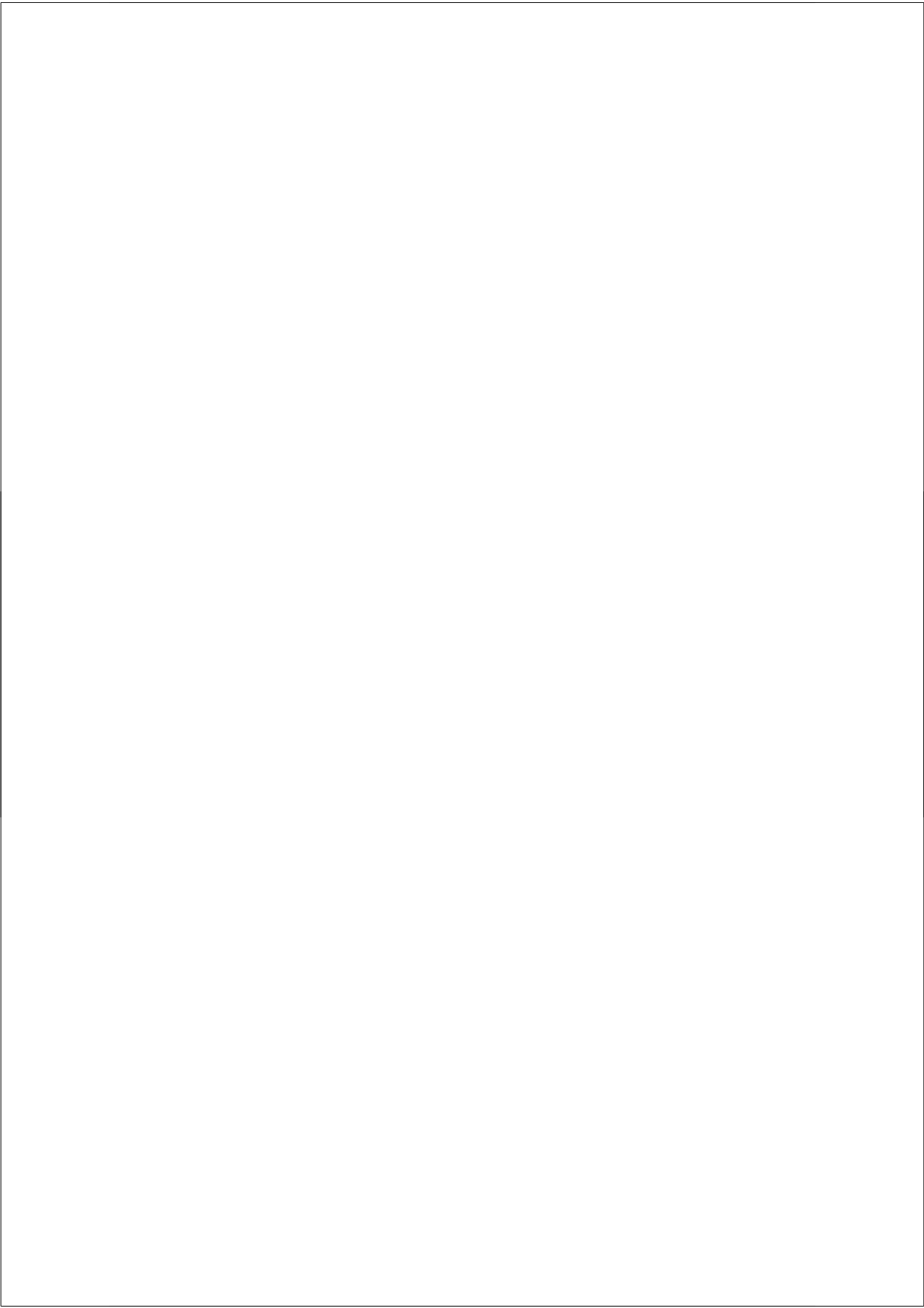
References

1. Brundage MD, Davies D, Mackillop WJ. Prognostic factors in non-small cell lung cancer: a decade of progress. *Chest* 2002; 122: 1037-1057.
2. Johnson BE. Biologic and molecular prognostic factors--impact on treatment of patients with non-small cell lung cancer. *Chest* 1995; 107: 287S-290S.
3. Pauwels EK, Ribeiro MJ, Stoot JH, McCready VR, Bourguignon M, Maziere B. FDG accumulation and tumor biology. *Nucl.Med.Biol.* 1998; 25: 317-322.
4. Duhaylongsod FG, Lowe VJ, Patz EF, Jr., Vaughn AL, Coleman RE, Wolfe WG. Lung tumor growth correlates with glucose metabolism measured by fluoride-18 fluorodeoxyglucose positron emission tomography. *Ann.Thorac.Surg.* 1995; 60: 1348-1352.
5. Higashi K, Ueda Y, Yagishita M et al. FDG PET measurement of the proliferative potential of non-small cell lung cancer. *J Nucl.Med.* 2000; 41: 85-92.
6. Vesselle H, Schmidt RA, Pugsley JM et al. Lung cancer proliferation correlates with [F-18]fluorodeoxyglucose uptake by positron emission tomography. *Clin Cancer Res.* 2000; 6: 3837-3844.
7. Sasaki R, Komaki R, Macapinlac H et al. [18F]Fluorodeoxyglucose Uptake by Positron Emission Tomography Predicts Outcome of Non-Small-Cell Lung Cancer. *J Clin Oncol* 2005; 23: 1136-1143.
8. Vansteenkiste JF, Stroobants SG, Dupont PJ et al. Prognostic importance of the standardized uptake value on (18)F-fluoro-2-deoxy-glucose-positron emission tomography scan in non-small-cell lung cancer: An analysis of 125 cases. *Leuven Lung Cancer Group. J Clin Oncol* 1999; 17: 3201-3206.
9. Higashi K, Ueda Y, Arisaka Y et al. 18F-FDG uptake as a biologic prognostic factor for recurrence in patients with surgically resected non-small cell lung cancer. *J Nucl.Med.* 2002; 43: 39-45.
10. Downey RJ, Akhurst T, Gonen M et al. Preoperative F-18 fluorodeoxyglucose-positron emission tomography maximal standardized uptake value predicts survival after lung cancer resection. *J Clin Oncol* 2004; 22: 3255-3260.
11. Ahuja V, Coleman RE, Herndon J, Patz EF, Jr. The prognostic significance of fluorodeoxyglucose positron emission tomography imaging for patients with nonsmall cell lung carcinoma. *Cancer* 1998; 83: 918-924.
12. Jeong HJ, Min JJ, Park JM et al. Determination of the prognostic value of [(18)F] fluorodeoxyglucose uptake by using positron emission tomography in patients with non-small cell lung cancer. *Nucl.Med.Commun.* 2002; 23: 865-870.
13. Therasse P, Arbuuck SG, Eisenhauer EA et al. New guidelines to evaluate the response to treatment in solid tumors. *Journal of the National Cancer Institute* 2000; 92: 205-216.
14. Belderbos JS, De Jaeger K, Heemsbergen WD et al. First results of a phase I/II dose escalation trial in non-small cell lung cancer using three-dimensional conformal radiotherapy. *Radiother.Oncol* 2003; 66: 119-126.
15. Huang SC. Anatomy of SUV. Standardized uptake value. *Nucl.Med.Biol.* 2000; 27: 643-646.
16. Boellaard R, Krak NC, Hoekstra OS, Lammertsma AA. Effects of noise, image resolution,

- and ROI definition on the accuracy of standard uptake values: a simulation study. *J Nucl.Med.* 2004; 45: 1519-1527.
17. Krak NC, Boellaard R, Hoekstra OS, Twisk JW, Hoekstra CJ, Lammertsma AA. Effects of ROI definition and reconstruction method on quantitative outcome and applicability in a response monitoring trial. *Eur J Nucl.Med.Mol.Imaging* 2004.
 18. Langen KJ, Braun U, Rota KE et al. The influence of plasma glucose levels on fluorine-18-fluorodeoxyglucose uptake in bronchial carcinomas. *J Nucl.Med.* 1993; 34: 355-359.
 19. Lindholm P, Minn H, Leskinen-Kallio S, Bergman J, Ruotsalainen U, Joensuu H. Influence of the blood glucose concentration on FDG uptake in cancer--a PET study. *J Nucl.Med.* 1993; 34: 1-6.
 20. Hoekstra CJ, Hoekstra OS, Stroobants SG et al. Methods to monitor response to chemotherapy in non-small cell lung cancer with 18F-FDG PET. *J Nucl.Med.* 2002; 43: 1304-1309.
 21. Young H, Baum R, Cremerius U et al. Measurement of clinical and subclinical tumour response using [18F]-fluorodeoxyglucose and positron emission tomography: review and 1999 EORTC recommendations. European Organization for Research and Treatment of Cancer (EORTC) PET Study Group. *Eur.J Cancer* 1999; 35: 1773-1782.
 22. Fischer BM, Mortensen J, Hojgaard L. Positron emission tomography in the diagnosis and staging of lung cancer: a systematic, quantitative review. *Lancet Oncol* 2001; 2: 659-666.
 23. Dwamena BA, Sonnad SS, Angobaldo JO, Wahl RL. Metastases from non-small cell lung cancer: mediastinal staging in the 1990s--meta-analytic comparison of PET and CT. *Radiology* 1999; 213: 530-536.
 24. Bradley J, Thorstad WL, Mutic S et al. Impact of FDG-PET on radiation therapy volume delineation in non-small-cell lung cancer. *Int.J Radiat.Oncol Biol.Phys.* 2004; 59: 78-86.
 25. Kostakoglu L, Goldsmith SJ. 18F-FDG PET evaluation of the response to therapy for lymphoma and for breast, lung, and colorectal carcinoma. *J Nucl.Med.* 2003; 44: 224-239.
 26. Mac Manus MP, Hicks RJ, Matthews JP et al. Positron emission tomography is superior to computed tomography scanning for response-assessment after radical radiotherapy or chemoradiotherapy in patients with non-small-cell lung cancer. *J Clin Oncol* 2003; 21: 1285-1292.
 27. Harpole DH, Jr., Herndon JE, Wolfe WG, Iglehart JD, Marks JR. A prognostic model of recurrence and death in stage I non-small cell lung cancer utilizing presentation, histopathology, and oncoprotein expression. *Cancer Res.* 1995; 55: 51-56.
 28. Younes M, Brown RW, Stephenson M, Gondo M, Cagle PT. Overexpression of Glut1 and Glut3 in stage I nonsmall cell lung carcinoma is associated with poor survival. *Cancer* 1997; 80: 1046-1051.
 29. Nelson CA, Wang JQ, Leav I, Crane PD. The interaction among glucose transport,

Chapter 2

- hexokinase, and glucose-6-phosphatase with respect to 3H-2-deoxyglucose retention in murine tumor models. *Nucl.Med.Biol.* 1996; 23: 533-541.
30. Solan MJ, Werner-Wasik M. Prognostic factors in non-small cell lung cancer. *Semin. Surg.Oncol* 2003; 21: 64-73.
 31. Bunn PA, Jr. Early-stage non-small-cell lung cancer: current perspectives in combined-modality therapy. *Clin Lung Cancer* 2004; 6: 85-98.
 32. Okamoto T, Maruyama R, Shoji F et al. Clinical patterns and treatment outcome of elderly patients in clinical stage IB/II non-small cell lung cancer. *J Surg.Oncol* 2004; 87: 134-138.



Prospective assessment of dosimetric/physiologic-based models for predicting radiation pneumonitis

Zafer Kocak M.D.^{1,2}, Gerben R. Borst M.D.³, Jing Zeng B.S.¹, Sumin Zhou Ph.D.¹, Donna R. Hollis M.S.⁴, Junan Zhang Ph.D.¹, Elizabeth S. Evans B.S.¹, Rodney J. Folz M.D., Ph.D.⁵, Terrence Wong M.D., Ph.D.⁶, Daniel Kahn Ph.D.¹, Jose S.A. Belderbos M.D.³, Joos V. Lebesque M.D., Ph.D.³, and Lawrence B. Marks M.D.¹

¹*Department of Radiation Oncology, Duke University Medical Center, Durham, NC;*

²*Department of Radiation Oncology, Trakya University Hospital, Edirne, Turkey;*

³*Department of Radiation Oncology, The Netherlands Cancer Institute-Antoni van Leeuwenhoek Hospital, Amsterdam, The Netherlands;*

⁴*Cancer Center Biostatistics, ⁵Pulmonary Medicine, ⁶Radiology-Nuclear Medicine Division, Duke University Medical Center, Durham, NC*

Abstract

Purpose: Clinical and 3D dosimetric parameters are associated with symptomatic radiation pneumonitis rates in retrospective studies. Such parameters include: mean lung dose (MLD), radiation (RT) dose to perfused lung (via SPECT), and pre-RT lung function. Based on prior publications, we defined pre-RT criteria hypothesized to be predictive for later development of pneumonitis. We herein prospectively test the predictive abilities of these dosimetric/functional parameters on 2 cohorts of patients from Duke and The Netherlands Cancer Institute (NKI).

Methods and Materials: For the Duke cohort, 55 eligible patients treated between 1999 and 2005 on a prospective IRB-approved study to monitor RT-induced lung injury were analyzed. A similar group of patients treated at the NKI between 1996 and 2002 were identified. Patients believed to be at high and low risk for pneumonitis were defined based on: (1) MLD; (2) OpRP (sum of predicted perfusion reduction based on regional dose-response curve); and (3) pre-RT DLCO. All doses reflected tissue density heterogeneity. The rates of grade ≥ 2 pneumonitis in the “presumed” high and low risk groups were compared using Fisher’s exact test.

Results: In the Duke group, pneumonitis rates in patients prospectively deemed to be at “high” vs. “low” risk are 7 of 20 and 9 of 35, respectively; $p = 0.33$ one-tailed Fisher’s. Similarly, comparable rates for the NKI group are 4 of 21 and 6 of 44, respectively, $p = 0.41$ one-tailed Fisher’s.

Conclusion: The prospective model appears unable to accurately segregate patients into high vs. low risk groups. However, considered retrospectively, these data are consistent with prior studies suggesting that dosimetric (e.g., MLD) and functional (e.g., PFTs or SPECT) parameters are predictive for RT-induced pneumonitis. Additional work is needed to better identify, and prospectively assess, predictors of RT-induced lung injury.

Introduction

Radiation (RT)-induced shortness of breath occurs in approximately 5–30% of patients receiving thoracic RT for lung cancer [1-8]. Despite the large number of patients receiving thoracic RT, there are currently no validated and standardized means of predicting an individual patient's risk of developing pulmonary toxicity. We and others have developed predictive models based primarily on dosimetric parameters such as the mean lung dose (MLD). Indeed, the rates of pneumonitis appear to increase with MLD in several, largely retrospective, trials [2-6][8]. Further, our data suggest that predictive models are improved if they consider both the three-dimensional (3D) dose distribution plus the pre-RT functional state [9]. Based on this, we developed a physiologic-based method to identify patients who we believe are at relatively high risk of developing clinical relevant pulmonary symptoms, based on 3D dosimetric parameters and pre-RT pulmonary function.

It is the purpose of the current study to evaluate this physiologic-based method in patients with lung cancer. Therefore, we first derived a model using the same dataset and method as previously described by Lind, selecting only the lung cancer subset[9]. Subsequently, we *prospectively* tested this approach in a new cohort of patients treated at Duke as well as in a separate group of patients treated at the Netherlands Cancer Institute. The rate of symptoms in the groups considered being at high vs. low risk was compared to assess the accuracy of the predictive model. Further, alternative dosimetric-based models are considered.

Methods and Materials

Eligibility and patient population

Between 1991 and 2005, 340 patients were enrolled into a prospective clinical study at Duke to assess RT-induced lung injury. Informed consent was obtained from all patients. Patients were eligible if they were about to receive thoracic RT for primary or metastatic disease to the thorax, with a minimum life expectancy of 6 months. Patients unable to give consent, with a history of prior RT, or who were planned to have thoracic surgery after RT, were not eligible. As part of this study, patients had pre- and post-RT assessments of lung function including symptom assessment, pulmonary function tests, computed tomography (CT), and single-photon emission computed tomography (SPECT) lung perfusion imaging.

In an analysis performed in 1999, based on 162 (62 had lung cancer and SPECT imaging) evaluable patients treated between 1991 and 1999, the risk of symptomatic radiation-induced lung injury appeared to be best predicted by a model considering the 3D dose distribution and pre-RT pulmonary function tests [9]. Based on that analysis, and other published data [3–5, 8], we defined criteria to prospectively identify patients who were believed to be at increased risk for radiation pneumonitis

(RP) (criteria defined below).

Since that analysis, 94 additional patients have been enrolled onto our study. Fifty-five of these 94 patients with lung cancer are evaluable with a minimum of 6-month post-RT follow-up. Thirty-nine patients were excluded from the analysis for the following reasons: death within 6 months after RT—18; intrathoracic disease progression within 6 months after RT—8; pulmonary emboli—1; pleural effusion—1; post-RT surgery—3; hard to score patients—5 (tumor regrowth, exacerbation of preexisting lung disease, and infection); discontinued treatment due to the bilateral diaphragmatic nerve paralysis—1; and no SPECT imaging—2. To assess the utility of these predictive models, the previously retrospective-defined predictive factors were tested in the new 55 evaluable patients.

Further, the model was also tested in a separate group of 65 patients treated for lung cancer at the NKI. These patients had medically inoperable or locally advanced disease treated between 1996 and 2002. Other inclusion criteria were a minimum 6-month post-RT follow-up, good prognostic criteria (weight loss less than 10% and ECOG performance status ≤ 2), and availability of CT and SPECT data before RT. The demographic information for the initial 62 patients who were treated at Duke, the second Duke cohort of 55 evaluable patients, and the NKI group are shown in Table 1.

Table 1. Clinical characteristics for three groups: Initial patients treated at Duke ('91-'99) and the two newer groups from Duke ('99-'05), and the NKI ('96-'02)

<i>Characteristics</i>	<i>Duke (%) (n = 55) 1999–2005</i>	<i>NKI (%) (n = 65) 1996–2002</i>	<i>Duke (%) (n = 62) 1991–1999</i>
Mean age (range)	64 (46–81)	72 (48–86)	62 (40–87)
Gender (female/male)	23/32	15/50	26/36
Histology			
Non-small cell	45 (82)	65 (100)	57 (92)
Small cell	10 (18)	—	5 (8)
Stage			
I–II	2 (4)	28 (43)	16 (26)
III–IV	48 (87)	37 (57)	41 (66)
Recurrent	5 (9)	—	5 (8)
Baseline PFTs % predicted			
Mean FEV1 (range)	68 (21–127)	63 (17–121)	62 (17–121)
Mean DLCO (range)	74 (28–129)	70 (20–128)	65 (23–114)

Table 2. Treatment characteristics for three groups: Initial patients treated at Duke ('91-'99), and the two newer groups from Duke ('99-'05), and the NKI ('96-'02)

<i>Institution</i>	<i>Radiotherapy: dose/fraction (total dose in Gy)</i>	<i>No (%)</i>	<i>Chemotherapy</i>	<i>No (%)</i>
Duke (n = 55)	1.5–1.6 (45–86.4)*	9 (16)	Pre-RT ± concurrent ± post-RT	31 (56)
(1999–2005)	1.8–2.0 (45–74)	46 (84)	Concurrent ± post-RT	19 (35)
NKI (n = 65)	2.0 (70)	34 (52)	No chemotherapy	5 (9)
(1996–2002)	2.25 (60.8–87.8)	31 (48)	No chemotherapy	65 (100)
Duke (n = 62)	1.5–1.6 (54.6–74.2)*	16 (26)	Pre-RT ± concurrent ± post-RT	22 (35)
(1991–1999)	1.8–2.0 (24–80)	45 (72)	Concurrent ± post-RT	3 (5)
	2.5 (50)	1 (2)	No chemotherapy	37 (60)

*Typically treated B.I.D

Treatment and pre- and post-RT evaluations

The treatment parameters for the three groups of patients are summarized in Table 2. At both Duke and the NKI, the patients underwent CT and SPECT imaging in the treatment position, and PFTs, before RT as previously described [10][11]. Clinical evaluation to assess for RT-induced pulmonary symptoms was performed approximately 1.5, 3, 6, 9, and 12 months post-RT, then at 6-month intervals. The average lung doses are as follows: Duke 91–99: MLD = 18.1 Gy; MpLD = 15.8 Gy; NKI: MLD = 15.5 Gy; MpLD = 14.5 Gy; Duke 99–05: MLD = 18.7 Gy; MpLD = 17.5 Gy.

Pulmonary function tests (PFTs) and scoring pulmonary symptoms

Pulmonary function tests included the forced expiratory volume (FEV1) and diffusion capacity for carbon monoxide (DLCO), and were measured as described previously [12][13]. Both were expressed as the percent of predicted value based on age, height, and gender.

Pulmonary complications were scored based on the common toxicity criteria [14]. To minimize the subjectivity, both the treating and another physician scored patients with suspected complications. The endpoint in this study was the development of grade ≥2 pneumonitis, i.e., necessitating start of steroids (Grade 2) and oxygen (Grade 3). This same scoring system was used to evaluate the patients treated at both Duke and the NKI.

Treatment planning, dose calculation, and dose-volume histogram (DVH)

The pre-treatment CT scan was performed as previously described [10][11]. At Duke, treatment planning was done using PLUNC (Plan University of North

Carolina) to define the desired beams, per the treating radiation oncologist [15]. At NKI, treatment planning was performed by using U-M plan (University of Michigan) [16]. Radiation was typically delivered with 6–15 MV photon beams by linear accelerators.

The 3D dose distributions were calculated with tissue density inhomogeneity corrections, using either an equivalent pathlength algorithm or the power law tissue-air ratio method. The dose-volume histograms were calculated based on the absolute total dose without adjustments for fraction size or overall treatment time in Duke. At NKI, all doses were corrected for fractionation. The local dose was converted to the normalized total dose, defined as the biologically equivalent dose delivered in 2 Gy/fraction. The linear quadratic model with an alpha/beta ratio of 3 Gy was used. The details of treatment planning, dose-volume histogram and calculations in both Duke and NKI were previously published [11][17][18].

Dose-function histogram (DFH) and overall perfusion weighted response parameter (OpRP)

SPECT images were obtained following i.v. injection of (99m)Tc-labeled macro aggregated albumin as previously described [13][19]. The 3D SPECT data were transferred electronically from Radiology to Radiation Oncology via an internal network, and stored on computer disk for quantitative analysis. Software in PLUNC (X Fusion) was used to visually superimpose the SPECT images with pre-RT lung contours. After a SPECT scan was adequately registered with the CT data set, the SPECT image was resampled by tri-linear interpolation to match the spatial sampling of the CT data set. The entire 3D RT dose distribution was overlaid on to the SPECT scan. The percentage of SPECT counts in each dose bin was used to generate a “dose SPECT-count histogram”. As it is assumed that perfusion is proportional to function [10][18], this histogram is termed a dose-function histogram [13][20]. In general, the bin size used for the DFH calculation is equal to the maximum radiation dose divided by 100. From the dose-function histograms, the percent of lung perfusion receiving ≥ 25 Gy, the P25, and mean-perfused lung dose (MpLD) were obtained. A similar method was used at the NKI [10][21].

A dose-response curve (DRC) for regional lung injury has been presented [18]. Briefly, for the Duke patients, 0% effect was assumed for doses < 15 Gy, and 100% effect for doses > 60 Gy. For the NKI data, the dose-effect relationship was assumed to be sigmoid-shaped according to a logistic model with a D50 of 63 Gy and k of 1.7 [21]. For the purpose of this paper (a comparison of the Duke and NKI data), the NKI data were re-analyzed using the DRC curve from Duke. Based on the DFH and DRC, the sum of expected perfusion reduction, also termed the overall perfusion weighted response parameter (OpRP) or integrated injury, is calculated as $OpRP = \sum(Pd \times Rd)$, where Pd is the percent of perfused lung irradiated to dose d, and Rd is

the expected reduction in regional perfusion at dose d (from the DRC).

Identifying patients predicted to be at “high risk”

From an analysis performed in 1999, a subgroup of 62 patients with lung cancer and the SPECT-related parameter OpRP are identified and shown in Fig. 1 [9]. Using the same methods as the prior study (bi-dimensional modeling with discriminant analysis, i.e., the Mahalanobis distances), we derived a line that segregates this subgroup of lung cancer patients into high and low-risk for pneumonitis [22]. Subsequently, we prospectively tested this model for a new cohort of patients treated at Duke as well as in a separate group of patients treated at The Netherlands Cancer Institute. Each patient’s score (i.e., high vs. low-risk for pneumonitis) was not computed during the planning/treatment process, and, therefore, patient management was not changed as a result of this study.

The association between pre-RT PFTs (y axis) and the SPECT-based overall response parameter (OpRP) (x axis) and the incidence of pneumonitis from the 62 evaluable patients with lung cancer and SPECT imaging in the 1999 analysis [9]. The line represents the “optimal” segregation of the patients with and without pneumonitis and was derived retrospectively from the data.

Assessing the concordance of the predictive model for post-RT pulmonary symptoms.

For the test patients treated at both Duke and the NKI, the rate of grade ≥ 2 RP was determined in the patient groups that were predicted to be at high and low risk. The rates of RP in the low-risk and high-risk groups were compared to assess the accuracy of the model by using a one-tailed Fisher’s exact test (since we were explicitly predicting that one group would have a higher [not just a different] rate of pneumonitis than the other group). The predictive abilities of a variety of different dosimetric/functional parameters were also tested in the patients treated in Duke and NKI using receiver operating characteristic (ROC) curves.

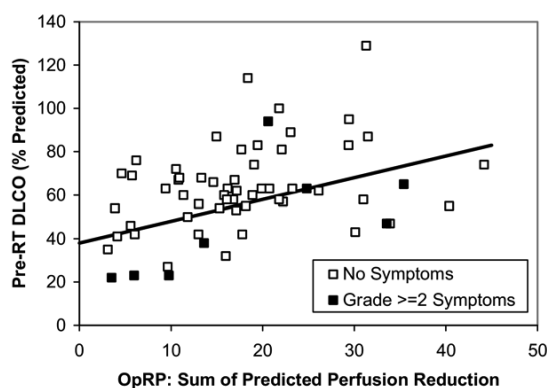


Figure 1. The association between pre-RT PFTs (y axis) and the SPECT-based overall response parameter (OpRP) (x axis) and the incidence of pneumonitis from the 62 evaluable patients with lung cancer and SPECT imaging in the 1999 analysis [9]. The line represents the “optimal” segregation of the patients with and without pneumonitis and was derived retrospectively from the data.

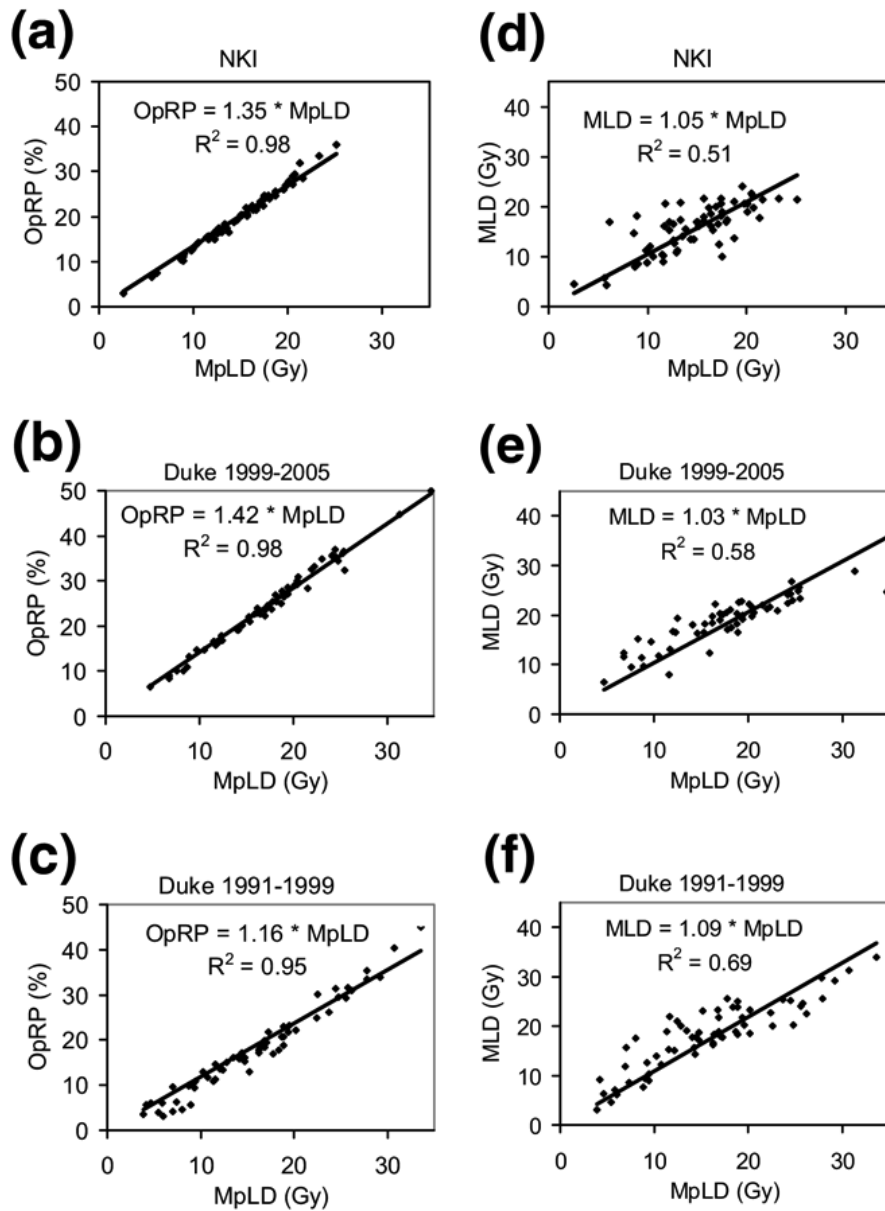


Figure 2. Comparison between different patient groups as well as dosimetric and functional parameters. Patients are divided into three groups: Duke 1991–1999 patients used to derive the model for predicting high-risk pneumonitis, and Duke 1999–2005, and NKI patients used to test the model prospectively. Panels (a) through (c) compares mean perfused lung dose (MpLD) against the overall perfusion weighted response parameter (OpRP) for the 3 patient groups. Panels (d) through (f) compares mean perfused lung dose (MpLD) against mean lung dose (MLD).

Results

Deriving a model for predicting risk of pneumonitis

The subgroup of 62 patients with lung cancer and the SPECT-related parameter OpRP treated from 1991 to 1999 is shown in Figure 1 [9]). Based on this dataset and other published works ([3-6][9]), patients are predicted to be at relatively “high risk” of post-RT pulmonary symptoms if they have: (1) An MLD of ≥ 25 Gy, or (2) A pre-RT percent predicted DLCO and OpRP that falls below the line shown in Figure 1. Mathematically, these patients have a pre-RT DLCO that is less than $(1.0 \times \text{OpRP} + 38)$, derived with bi-dimensional discriminant analysis. When this model is used in the group of patients that the model is derived from, the dividing line is highly significant with $p = 0.03$ in one-tailed Fisher’s exact test.

Comparing the different datasets

Before testing the model for predicting pneumonitis risk in a second cohort of Duke and NKI patients, a comparison between the 3 datasets is made. First, the relationship between MLD and MpLD is examined (Figure 2). The range of the MpLD and MLD for the 2 Duke datasets (1991–1999 and 1999–2005) are very similar. For the NKI data set, MpLD and MLD are restricted to values lower than 25 Gy. The correlation (R^2) between MLD and MpLD ranges from 0.51 to 0.69. The slopes of the regression lines through zero are very similar for the 3 datasets (1.09, 1.03, and 1.05 for Duke 91–99, Duke 99–05, and NKI datasets, respectively). The large spread of the data around these regression lines indicates the impact of perfusion weighting.

The relationship between the OpRPs and MpLD is also examined (Figure 2). There is a very tight correlation between the 2 parameters with R^2 ranging from 0.95 to 0.98. The slopes of the regression lines are 1.16, 1.42, and 1.35 for Duke 91–99, Duke 99–05, and NKI datasets, respectively. This means that the DRC used in the calculation of the OpRP could be well approximated by a DRC linearly dependent on the dose with a slope of 1.16, 1.42, and 1.35 for the 3 datasets, respectively.

Testing the model prospectively

The incidence of pneumonitis in the second cohort of Duke patients is illustrated in Figure 3. As shown using the line, 18 of 55 patients are *prospectively* considered high risk and 37 of 55 patients are low risk. In addition, applying the MLD >25 Gy criteria, 2 more patients from the low-risk group move into the high risk-group (shown by dashed circles in Figure 3). Therefore, 20 of 55 patients are high risk, and 35 of 55 patients are low risk. The rates of pneumonitis in the high and low-risk groups are 7 of 20 and 9 of 35, respectively, $p = 0.33$ one-tailed Fisher’s.

Similarly, the data for The Netherlands group is shown in Figure 4. No patients

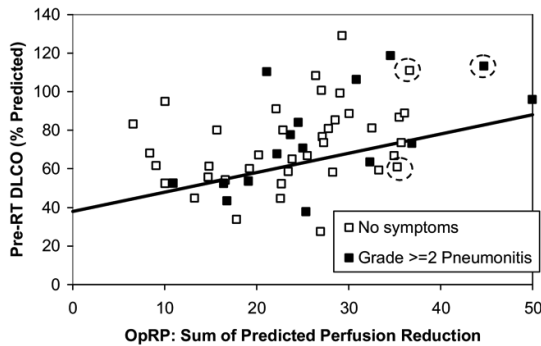


Figure 3. The relationship between the pre-RT PFTs (y axis), OpRP (x axis) and pneumonitis in the new cohort of 55 patients treated at Duke between 1999 and 2005. The line derived from the data in Figure 1 is shown. Three patients with MLD >25 Gy are indicated with dashed circles. The rates of pneumonitis in the “high” vs. “low” risk patients (high risk = below the line or MLD >25 Gy) were 7 of 20 and 9 of 35, $p = 0.33$.

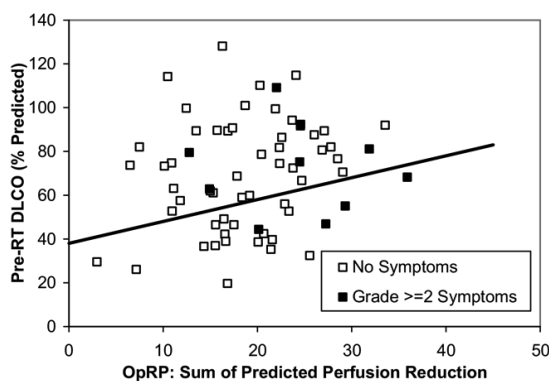


Figure 4. The relationship between the pre-RT PFTs (y axis), OpRP (x axis) and pneumonitis in the 65 patients from the NKI. The rates of pneumonitis in the “high” vs. “low” risk patients (i.e., below and above the line, respectively) were 4 of 21 and 6 of 44, $p = 0.41$.

have MLD >25 Gy in The Netherlands group. The comparable pneumonitis rates are 4 of 21 in the high-risk group and 6 of 44 in the low-risk group, $p = 0.41$ one-tailed Fisher’s.

The data from Duke, but not NKI, suggest that there is an interaction between pre-RT PFTs, OpRP, and subsequent risk of pneumonitis. This is illustrated in Figure 3. The cases of pneumonitis within the low-OpRP patients tend to have lower pre-RT DLCO. If one limits the analysis to those patients with a pre-RT DLCO >60%, the rates of radiation pneumonitis in patients with an OpRP >20 vs. ≤ 20 are 11 of 31 and 0 of 7 ($p = 0.07$), respectively. The similar rates of pneumonitis in patients with an MLD >20 Gy vs. ≤ 20 Gy were 10 of 23 vs. 1 of 18 ($p = 0.007$) for the Duke patients, and 2 of 12 vs. 5 of 29 ($p = 0.67$) for the NKI patients.

The interaction between PFTs and OpRP is also seen in the ROC analysis (Table 3). In the Duke data, bi-

parameter models considering both a dosimetric DVH/DFH-based parameter and the PFT parameter FEV1 tend to have higher ROC areas than the corresponding uni-parameter models (0.65–0.72 vs. 0.56–0.62, respectively). However, bi-parameter models using DLCO do not perform better than uni-parameter models. For the NKI data, bi-parameter models have equivalent ROC areas as uni-parameter models, both for FEV1 and DLCO. In fact, bi-dimensional modeling with OpRP and DLCO

Table 3. Area under the ROC curves for uni- and bi-parameter-based models predicting radiation pneumonitis

Parameter	Area under the ROC curve	
	Duke (1999–2005)	NKI
<u>Pulmonary function tests (%)</u>		
Pre-RT DLCO	0.53	0.52
Pre-RT FEV1	0.61	0.53
<u>Single DVH-based parameters</u>		
V20	0.54	—
V25	0.52	—
V30	0.51	—
MLD	0.62	0.61
<u>Single SPECT-based parameters</u>		
P20	0.55	—
P25	0.54	—
P30	0.54	—
MpLD	0.59	0.71
OpRP	0.56	0.72
<u>Multiparameter-based models</u>		
MLD and DLCO	0.62	0.60
MLD and FEV1	0.72	0.62
MpLD and DLCO	0.59	0.71
MpLD and FEV1	0.65	0.70
OpRP and DLCO	0.56	0.72
OpRP and FEV1	0.65	0.72

leads to less significant results ($p = 0.04$) compared to OpRP alone ($p = 0.01$).

Furthermore, in the Duke data, perfusion weighted parameters have lower ROC areas than nonperfusion weighted parameters (0.62–0.72 for MLD models, 0.56–0.65 for MpLD and OpRP models). This is in contrast to the NKI data, where models using MpLD and OpRP have higher ROC areas than models using MLD (0.70–0.72 vs. 0.60–0.62, respectively). In the NKI data, OpRP and MpLD also appear as the most significant predictors in uni-dimensional modeling ($p = 0.01$ and 0.03, respectively), better than the nonperfusion weighted parameters OpRP ($p = 0.3$) and MLD ($p = 0.4$).

If the Duke 1999–2005 and NKI data are examined again *retrospectively*, new segregating lines that optimally divide patients into high and low risk for pneumonitis can be calculated. For the Duke data, the best discriminant line retrospectively is shown in Figure 5 as the

dashed line with equation $DLCO = (4 * OpRP - 10)$. For the NKI dataset, a new discriminant line that uses both OpRP and DLCO could be drawn, but it is nearly vertical because only the OpRP contributes to the discriminant value (Figure 6). The better predictive value of OpRP alone is also displayed in Figure 6.

Discussion

The prospective identification of patients at relatively high risk for RP is challenging since a variety of treatment/patient-related factors appear to influence this risk.

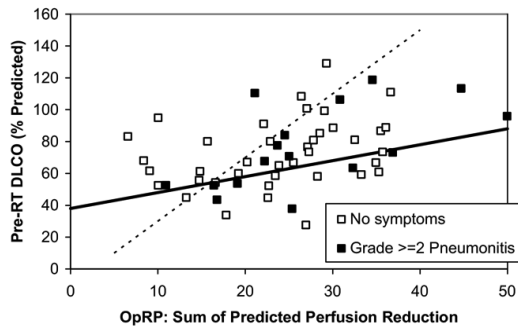


Figure 5. The data shown in Figure 3 is reproduced here. As noted, the solid line illustrate the challenges associated with prospectively identifying specific high- and low-risk groups of patients. If done retrospectively, one could define the dashed line as a “new” PFT/OpRP ratio that well segregates patients into high vs. low risk ($DLCO = 4 * OpRP - 10$).

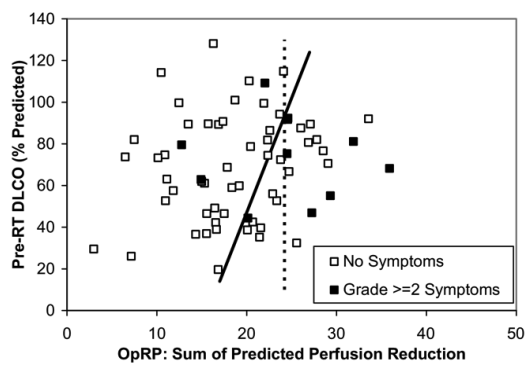


Figure 6. The data shown in Figure 4 is reproduced here, with retrospectively-defined new segregations lines that are superior to the prospective line in Figure 4. The solid line ($DLCO = 11 * OpRP - 173$) considers both the OpRP and DLCO in segregating patients into high and low risk, the dashed line ($OpRP = 24$) uses only the OpRP.

In particular, dosimetric parameters, such as the mean lung dose, have been most consistently linked with the risk of pneumonitis in many studies [2-6][8]. Furthermore, several studies suggest that patients with relatively poor pre-RT lung function are more likely to experience toxicity than are patients with better lung function [7][9][23][24]. Based on a 1999 analysis of the patients treated at Duke [6][9], and the data from others [3-5], we developed a functional/dosimetric model to attempt to prospectively segregate patients into high- and low-risk groups. The present report demonstrates that the model was unsuccessful when applied to a set of new patients treated at Duke, and a contemporaneous group from the NKI. The selection of the line in Figure 1 is central to the results. The line herein used was derived from bi-dimensional discriminant analysis using Mahalanobis distances. We recognize there are alternative methods to select

an appropriate “division line”. Further, we have reassessed the 1991–1999 data and identified additional lines that might have been considered “optimal” based on visual inspection or ROC curves. The use of alternative discriminant lines was still unable to accurately segregate patient outcomes in the more recent dataset (2000–2005). While unsuccessful, the Duke data show that combining dosimetric parameters with FEV1 might improve outcome prediction compared to the use of dosimetric parameters alone, although this is not seen with DLCO. The NKI data shows no improvement when PFTs are combined with dosimetric parameters, although

prediction does improve with the use of functional/perfusion imaging (vs. CT-based dosimetric parameters). The present analysis highlights the challenges of the prospective identification of high- vs. low-risk patients.

The present analysis is not contradictory with prior studies from our group and others. The patients with the highest MLD are at greater risk of pneumonitis than are patients with lower MLD. In the Duke data, patients with low pre-RT pulmonary function have a higher rate of pneumonitis at low lung doses than do patients with better pre-RT lung function. Thus, if we were to analyze these patients “retrospectively” the conclusions would be similar to what we and others have noted before. However, the present analysis demonstrates the challenges associated with prospectively identifying specific high- and low-risk groups of patients. Indeed, if done retrospectively, one could define the dashed line on Figure 5 as a “new” PFT/OpRP ratio that well segregates Duke patients into high vs. low risk.

One factor that contributed to this present study’s inability to prospectively segregate patients into high- and low-risk groups is that we are underpowered. The prospective model is derived from the first group of Duke patients (1991–1999), where pneumonitis rates are 26% and 5% in the high- and low-risk groups, respectively. For a study to have 80% power to detect a 20% difference between the high- and low-risk groups, approximately 80 patients are needed for the 2 arms (assuming $\alpha = 0.05$ for one-sided test). The second group of Duke patients (2000–2005) has 20 high-risk patients and 35 low-risk patients, and the NKI group has 21 high-risk patients and 44 low-risk patients. The 2 groups each have approximately 70% power to detect a 20% difference. There is certainly a trend in both the Duke and NKI groups toward a higher pneumonitis rate in the high-risk group compared to the low-risk group, but the trend is not statistically significant. Combining the data from Duke 1999–2005 and the NKI to increase the power yields pneumonitis rates in the high-risk and low-risk groups of 11 of 41 vs. 15 of 79; $p = 0.22$; one-tailed Fisher’s exact tests.

A tool to prospectively identify patients at increased risk for pneumonitis would be extremely useful. Presently, there are interventions that may reduce patients risk for pneumonitis (e.g., Amifostine). However, the toxicity of such interventions has, at least in part, hindered its widespread use. If patients at particularly high-risk for pneumonitis could be identified, such interventions might be effectively applied in particular patient subgroups. On the other hand, patients who are deemed to be at a relatively low risk for pneumonitis might be candidates for dose escalation.

There have been very few attempts to prospectively identify patients’ risk for radiation-induced lung injury [2][3]. The University of Michigan is performing a dose escalation study wherein the prescribed dose is dependent on the anticipated normal tissue complication probability (NTCP). In this study, the observed and predicted complication rates were fairly divergent [2]. Among patients with a predicted >95%

risk for pneumonitis, only 5 of 13 developed clinical pneumonitis. Nevertheless, the patients that they deemed to be at “high risk” for pneumonitis did have a higher rate of pneumonitis than did the patients that they deemed to be at low risk. However, the absolute magnitude of the predicted vs. observed rates were different. Similarly, Oetzel et al. noted the rates of pneumonitis to be 13% and 29% for patients with a calculated NTCP of $<30\%$ and $\geq 30\%$, respectively [3]. In this regard, these findings are similar to ours. On the other hand, in the dose escalation study by Belderbos et al., the observed incidence of radiation pneumonitis was not statistically different from the estimated probability using results from Kwa et al. [4][25]. However, the authors do comment that the observed data seemed to indicate a higher incidence of RP than predicted, but the difference is not statistically significant due to the limited number of cases.

The model we used to identify patients at high vs. low risk for pneumonitis may seem cumbersome. We used a 2-threshold approach. Patients were considered to be at high risk if their MLD exceeded 25 Gy. This threshold was selected based on studies from multiple institutions [3][4]. Among patients who had MLD below 25 Gy, they were expected to be at high risk for pneumonitis if their pre-RT lung function was poor relative to the planned radiation dose distribution. In other words, patients were considered “high risk” if their PFTs were relatively low compared to the anticipated degree of lung injury (OpRP). This relationship between pre-RT lung function and expected lung injury is the second component of our prospective model, and is more difficult to explain and apply clinically than the MLD. Nevertheless, we believe that this second component is, in many ways, more physiologically sound than the MLD alone. The MLD considers only the radiation dose distribution, and ignores the possible impact of pre-RT lung function distribution. Indeed, in our initial data set, from which the threshold PFT/OpRP ratio was defined (i.e., the line in Figure 1), we did not observe a strong impact of MLD alone. The MLD threshold was included due to the number of studies that show the importance of this parameter [2-6][8]. Similarly, we elected to use the OpRP as our dosimetric parameter to compare to the PFTs since we believe that the OpRP provides a useful metric of anticipated global lung effects. However, the simpler parameter MpLD could probably have been used instead of the OpRP, given the very tight correlations between these 2 parameters (Figure 2). Prior studies from Duke and the NKI have suggested that SPECT-based dosimetric parameters may predict RT-induced symptomatic lung injury better than CT-based dosimetric parameters that do not incorporate functional information. This trend continues to be seen in the NKI data in this study but not the Duke data [9][21]. One could have defined similar ratios between the PFTs and other dosimetric parameters such as V20 or MLD.

To further test the applicability of such predictive models in another venue, we also studied patients irradiated at the NKI. Similar methods were used to compute

radiation dose, define the overall response parameter, and assess pre-RT pulmonary function. As was the case with the Duke test set, the model was not able to accurately identify patients at high vs. low risk in the NKI data set. While it is clearly important to demonstrate the utility of a prognostic factor in diverse patient population, applying predictive model developed at one institution to a second institution is potentially problematic. For example, several studies demonstrated an association between a variety of dosimetric parameters and the incidence of pneumonitis. We and others have suggested that the precise dosimetric parameter selected is not critical as there is a strong correlation between the different dosimetric parameters. For example, in the study by Graham et al. from

Mallinckrodt, the correlation coefficient between V20 and MLD was 0.94 [5]. Correlation coefficients between other parameters were similarly high in the studies by Kwa [4] and Fan et al. [18]. These dosimetric parameters tend to be highly correlated with each as long as the radiation technique being used is relatively uniform across patients. However, the associations become less strong when a more varied radiation technique is used. For example, most of the patients in the Duke series were treated with fairly conventional beams (e.g., AP/PA followed by off cord oblique

opposed fields). Within that construct, there is a strong association between the different dosimetric parameters. When more varied beam arrangements are used, e.g., 5 or 7 non-opposed beams, the V20 tends to decrease, but the MLD stays relatively constant. Thus the V5 and V10 tend to increase. It appears reasonable to consider The Netherlands data in this context since the radiation techniques used at the NKI and Duke are similar. An important difference in the 2 institutions is that 91% of patients treated in Duke were given chemotherapy, but none in the NKI.

The dosimetric parameters for the initial 62 Duke patients are somewhat different than the subsequent group from Duke and the NKI patients. Our original prospective model used an MLD greater than 25 Gy to define high risk. In the subsequent groups, very few patients had this high dosimetric parameter (3 of 55 and 0 of

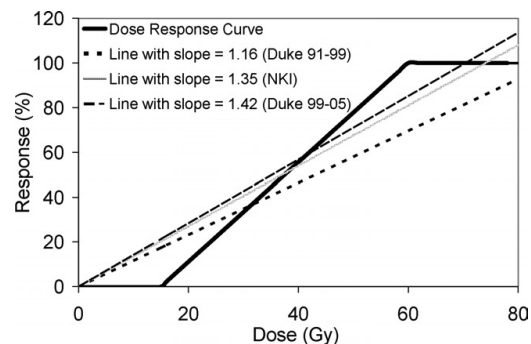


Figure 7. The dose-response curve used in this study, compared against 3 linear approximations based on the 3 patient groups in this study (Duke 1991–1999, Duke 1999–2005, and NKI). The linear approximations are derived from the relationship between the OpRP and MplD, shown in Figure 2. A line with a smaller slope means more patients in that dataset were treated with higher doses, which flattens out the line since the DRC flattens out at >60 Gy.

65 at Duke and NKI, respectively). This difference in the patient groups appears reflected in slopes of the OpRP vs. MpLD plots (Figure 2). The slopes of these plots are mathematically equal to the linear approximation of the DRC curve underlying the OpRP calculation. Since the DRC used to compute the OpRP has a threshold at low doses (<15 Gy), and a plateau at high dose (>60 Gy), the slope of the MpLD vs. OpRP graphs differ from one. The linear approximation of the Duke DRC had a slope of 1.16 for the Duke 91-99 data, whereas the slopes for the Duke 99-05 and NKI data were steeper (1.42 and 1.35, respectively). A flatter slope is consistent with a larger portion of the lung being treated to a higher dose (because the DRC saturates at 100% when doses > 60 Gy), and/or a larger portion of the lung being treated to <15 Gy (due to the threshold). Indeed, a relatively large fraction of the Duke 91-99 patients were treated to higher doses (i.e. beyond saturation), and/or received a concurrent BID boost technique that typically increases the fraction of irradiated lung exposed to low doses of RT. Thus, the differences in slope of the MpLD vs. OpRP graphs reflect differences in the RT doses and techniques used.

One variable that may be predictive of radiation pneumonitis that was not taken into consideration in this study is the effect of the region of lung irradiated. A number of clinical studies, including Yorke et al. from Memorial and Seppenwoolde et al. from NKI, have shown that radiation dose to the lower lung may be more associated with lung injury than radiation dose to the upper lung [16][26]. Other studies such as Hope et al. from Washington University and Yamada et al. from Japan have found that the incidence of pneumonitis is higher in patients with lower lobe tumors [27][28]. Our group has also looked for this effect in our data and has not seen this [29]. We are uncertain why we achieve different results in this regard, and this is a topic of ongoing study. A number of other research groups also did not find different rates of pneumonitis based on tumor location [7][30][31]. The model tested in this study was DVH-based, which discards all spatial information. Alternative predictive models that consider such spatial information can certainly be developed and tested. The diagnostic uncertainty of radiation pneumonitis may be a factor that makes the prediction of RT-induced lung injury difficult. In a study of 251 lung cancer patients treated with RT at Duke between 1991 and 2003, 47 of 251 (19%) were thought to have RP and 13 of 47 (28%) had concurrent medical diagnoses (e.g., possible infection, exacerbation of pre-existing lung disease, tumor regrowth/progression, and/or cardiac disease) that confounded the diagnosis [32].

In conclusion, the prospective model was unable to accurately segregate patients into high- vs. low-risk groups. However, the data continue to suggest that dosimetric (e.g., MLD) and functional (e.g., PFT) parameters are potentially important in the prospective identification of patients at high and low risk of RP. Additional work is needed to better identify, and prospectively assess, predictors of RT-induced lung injury.

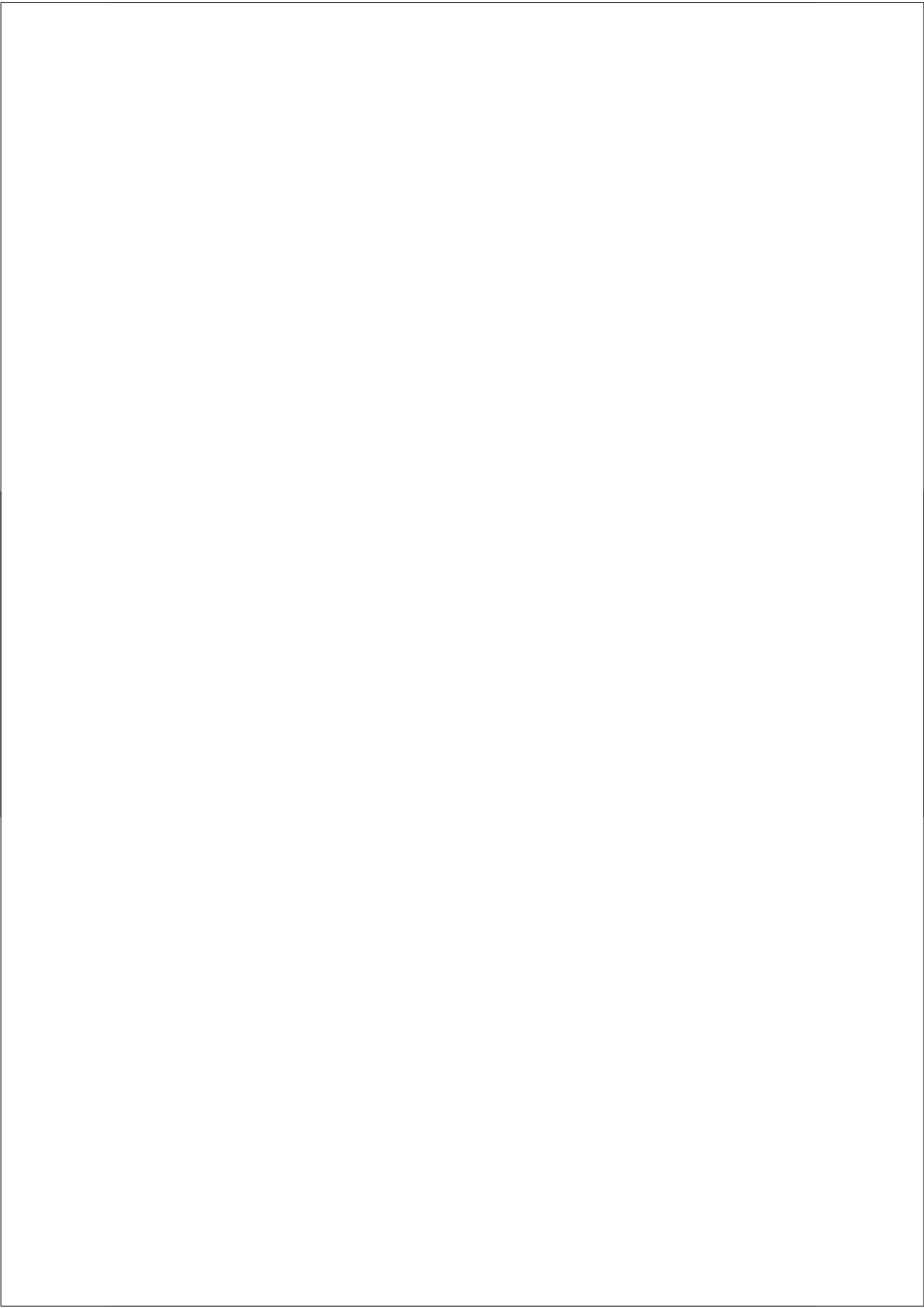
References

1. McDonald S, Rubin P, Phillips TL, et al. Injury to the lung from cancer therapy: Clinical syndromes, measurable endpoints, and potential scoring systems. *Int J Radiat Oncol Biol Phys* 1995;31:1187–1203.
2. Martel MK, Ten Haken RK, Hazuba MB, et al. Dose-volume histogram and 3-D treatment planning evaluation of patients with pneumonitis. *Int J Radiat Oncol Biol Phys* 1994;28:575–581.
3. Oetzel D, Schraube P, Hensley F, et al. Estimation of pneumonitis risk in three-dimensional treatment planning using dose-volume histogram analysis. *Int J Radiat Oncol Biol Phys* 1995;33:455–460.
4. Kwa SL, Lebesque JV, Theuws JC, et al. Radiation pneumonitis as a function of mean lung dose: An analysis of pooled data of 540 patients. *Int J Radiat Oncol Biol Phys* 1998;42:1–9.
5. Graham MV, Purdy JA, Emami B, et al. Clinical dose-volume histogram analysis for pneumonitis after 3D treatment for non-small cell lung cancer (NSCLC). *Int J Radiat Oncol Biol Phys* 1999;45:323–329.
6. Hernando ML, Marks LB, Bentel GC, et al. Radiation-induced pulmonary toxicity: A dose-volume histogram analysis in 201 patients with lung cancer. *Int J Radiat Oncol Biol Phys* 2001; 51:650–659.
7. Robnett TJ, Machtay M, Vines EF, et al. Factors predicting severe radiation pneumonitis in patients receiving definitive chemoradiation for lung cancer. *Int J Radiat Oncol Biol Phys* 2000;48:89–94.
8. Seppenwoolde Y, Lebesque JV, de Jaeger K, et al. Comparing different NTCP models that predict the incidence of radiation pneumonitis. Normal tissue complication probability. *Int J Radiat Oncol Biol Phys* 2003;55:724–735.
9. Lind PA, Marks LB, Hollis D, et al. Receiver operating characteristic curves to assess predictors of radiation-induced symptomatic lung injury. *Int J Radiat Oncol Biol Phys* 2002; 54:340–347.
10. Boersma LJ, Damen EM, de Boer RW, et al. A new method to determine dose-effect relations for local lung-function changes using correlated SPECT and CT data. *Radiother Oncol* 1993; 29:110–116.
11. Marks LB, Hollis D, Munley M, et al. The role of lung perfusion imaging in predicting the direction of radiation-induced changes in pulmonary function tests. *Cancer* 2000; 88:2135–2141.
12. Borst GR, De Jaeger K, Belderbos JS, et al. Pulmonary function changes after radiotherapy in non-small-cell lung cancer patients with long-term disease-free survival. *Int J Radiat Oncol Biol Phys* 2005;62:639–644.
13. Marks LB, Munley MT, Spencer DP, et al. Quantification of radiation-induced regional lung injury with perfusion imaging. *Int J Radiat Oncol Biol Phys* 1997;38:399–409.
14. Common Toxicity Criteria Version 2.0, in Cancer Therapy Evaluation Program. 1998, National Cancer Institute.
15. Sailer SL, Chaney EL, Rosenman JG, et al. Treatment Planning at the University of

- North Carolina at Chapel Hill. *Semin Radiat Oncol* 1992;2:267–273.
16. Seppenwoolde Y, De Jaeger K, Boersma LJ, *et al.* Regional differences in lung radiosensitivity after radiotherapy for nonsmall-cell lung cancer. *Int J Radiat Oncol Biol Phys* 2004;60:748–758.
 17. Lebesque JV, Keus RB. The simultaneous boost technique: The concept of relative normalized total dose. *Radiother Oncol* 1991;22:45–55.
 18. Fan M, Marks LB, Hollis D, *et al.* Can we predict radiation-induced changes in pulmonary function based on the sum of predicted regional dysfunction? *J Clin Oncol* 2001;19:543–550.
 19. Marks LB, Spencer DP, Bentel GC, *et al.* The utility of SPECT lung perfusion scans in minimizing and assessing the physiologic consequences of thoracic irradiation. *Int J Radiat Oncol Biol Phys* 1993;26:659–668.
 20. Marks LB, Spencer DP, Sherouse GW, *et al.* The role of three dimensional functional lung imaging in radiation treatment planning: The functional dose-volume histogram. *Int J Radiat Oncol Biol Phys* 1995;33:65–75.
 21. De Jaeger K, Seppenwoolde Y, Boersma LJ, *et al.* Pulmonary function following high-dose radiotherapy of non-small-cell lung cancer. *Int J Radiat Oncol Biol Phys* 2003;55:1331–1340.
 22. Rao CR. Contributions to statistics. Presented to PC Mahalanobis on the occasion of his 70th birthday. New York: Pergamon Press; 1965.
 23. Choi NC, Kanarek DJ, Kazemi H. Prospective study of pulmonary tolerance to radiotherapy or radiotherapy plus multi multidrug chemotherapy for loco-regional lung carcinoma. *Antibiot Chemother* 1988;41:213–219.
 24. Marks LB, Munley MT, Bentel GC, *et al.* Physical and biological predictors of changes in whole-lung function following thoracic irradiation. *Int J Radiat Oncol Biol Phys* 1997;39: 563–570.
 25. Belderbos JS, De Jaeger K, Heemsbergen WD, *et al.* First results of a phase I/II dose escalation trial in non-small cell lung cancer using three-dimensional conformal radiotherapy. *Radiother Oncol* 2003;66:119 –126.
 26. Yorke ED, Jackson A, Rosenzweig KE, *et al.* Correlation of dosimetric factors and radiation pneumonitis for non-smallcell lung cancer patients in a recently completed dose escalation study. *Int J Radiat Oncol Biol Phys* 2005;63:672– 682.
 27. Hope AJ, Lindsay PE, El Naqa I, *et al.* Modeling radiation pneumonitis risk with clinical, dosimetric, and spatial parameters. *Int J Radiat Oncol Biol Phys* 2006;65:112–124.
 28. Yamada M, Kudoh S, Hirata K, *et al.* Risk factors of pneumonitis following chemo radiotherapy for lung cancer. *Eur J Cancer* 1998;34:71–75.
 29. Yu X, Zhou S, Kahn D, *et al.* Relating RT-induced pulmonary symptoms based on the dose to the superior vs. inferior lung in patients irradiated for lung cancer. *Int J Radiat Oncol Biol Phys* 2003;57:S415.
 30. Tsujino K, Hirota S, Endo M, *et al.* Predictive value of dose-volume histogram parameters for predicting radiation pneumonitis after concurrent chemoradiation for lung cancer. *Int J Radiat Oncol Biol Phys* 2003;55:110 –115.
 31. Fay M, Tan A, Fisher R, *et al.* Dose-volume histogram analysis as predictor of radiation

Prospective assessment of models for predicting radiation pneumonitis

- pneumonitis in primary lung cancer patients treated with radiotherapy. *Int J Radiat Oncol Biol Phys* 2005;61:1355–1363.
32. Kocak Z, Evans ES, Zhou SM, *et al.* Challenges in defining radiation pneumonitis in patients with lung cancer. *Int J Radiat Oncol Biol Phys* 2005;62:635– 638.



**Radiation pneumonitis for patients treated for
malignant pulmonary lesions with
stereotactic body radiation therapy**

Gerben R. Borst M.D.¹, Masayori Ishikawa Ph.D.², Jasper Nijkamp M.Sc.¹,
Michael Hauptmann Ph.D.³, Hiroki Shirato M.D. Ph.D.², Rikiya Onimaru
M.D.², Michel M. van den Heuvel M.D. Ph.D.⁴, Jose Belderbos M.D.
Ph.D.¹, Joos V. Lebesque M.D. Ph.D.¹, Jan-Jakob Sonke Ph.D.¹

¹*Department of Radiation Oncology, The Netherlands Cancer Institute-Antoni van Leeuwenhoek
Hospital, Amsterdam, The Netherlands*

²*Department of Radiation Oncology, Hokkaido University School of Medicine, Sapporo, Japan.*

³*Department of Bioinformatics and Statistics,* ⁴*Department of Thoracic Oncology,
The Netherlands Cancer Institute - Antoni van Leeuwenhoek Hospital, Amsterdam, The Netherlands.*

Abstract

Purpose: We evaluated the relationship between the mean lung dose (MLD) and the incidence of radiation pneumonitis (RP) after SBRT and compared this with conventional fractionated radiation therapy (CFRT).

Material and Methods: For both SBRT (n=128) and CFRT (n=142) patients, RP grade ≥ 2 was scored. Toxicity models predicting the probability of RP as a function of the MLD were fitted using maximum log likelihood analysis. The MLD was NTD (Normalized Total Dose) corrected using an α/β ratio of 3 Gy.

Results: SBRT patients were treated with 6 Gy to 12Gy per fraction with a median MLD of 6.4 Gy (range:1.5 Gy to 26.5 Gy). CFRT patients were treated with 2 Gy or 2.25Gy per fraction, the median MLD was 13.2Gy (range:3.0Gy to 23.0 Gy). The crude incidence rates of RP were 10.9% and 17.6% for the SBRT and CFRT patients, respectively. A significant dose-response relationship for RP was found after SBRT that was not significantly different from the dose-response relationship for CFRT (p=0.18).

Conclusion: We derived from clinical data a significant dose-response relationship between the risk of RP and the MLD for SBRT. This relation was not significantly different from the dose-response relation for CFRT although statistical analysis was hampered by the low number of patients in the high dose range.

Introduction

Stereotactic body radiation therapy (SBRT) for pulmonary lesions is becoming more widely used following the first clinical experiences described by Blomgren et al. in 1995 [1]. Collaboration of Japanese radiation departments resulted in the publication of encouraging outcomes among stage I lung cancer patients after SBRT [2,3]. In addition, SBRT proved to be an effective treatment for metastases in lung and liver with high tumour control rates being achieved [4,5]. With respect to healthy tissue injury, Timmerman et al. [6] observed a significantly higher toxicity for centrally located tumours compared to peripherally located tumours using similar irradiation schedules. In an analysis of Lagerwaard et al. [7], lowering the fraction dose for centrally located tumours resulted in similar toxicity for central and peripheral tumours. A recent review of Brock et al. [8] evaluating SBRT studies showed limited toxicity whereas between these studies a large heterogeneity of treatment techniques, dose parameters and clinical endpoints is observed. To extend the applicability of SBRT, knowledge of the dose-toxicity relationship is necessary. However, dose response evaluations are hampered by the restricted dose range and (consequently) the low number of toxicity events following SBRT. Moreover, the influence of larger fraction dose, shorter overall treatment time and differences in dose distribution on existing radiobiological models is rather unknown. In addition, patients receiving pulmonary SBRT are a select group of patients with a high comorbidity.

Radiation pneumonitis (RP) is a serious complication which was fatal after SBRT in 3 of the 25 patients in a recent study of Yamashita et al [9] after 48Gy in 4 fractions. The incidence of RP requiring clinical intervention ranges from 0% to 29% after SBRT [9-14]. Unfortunately, no predictive model to assess the probability of RP is available for SBRT.

The goal of our study was to evaluate the relation between the radiation dose and the occurrence of RP after SBRT. In addition, since for CFRT the relation between lung dose and radiation pneumonitis (RP) is extensively evaluated (e.g. [15]), we compared the dose relationship of SBRT and CFRT patients.

Material & Methods

Patients

SBRT patients were irradiated with hypofractionated schedules at the Department of Radiation Medicine of the Hokkaido University School of Medicine, Sapporo, Japan. Clinical data and treatment plans were retrievable for 128 patients, treated between April 1998 and December 2005. Follow up was performed at the outpatient clinic of the Department of Radiation Medicine. Irradiation regimens were 35 Gy in 4 fractions, 40 Gy in 4 fractions, 48 Gy in 8 fractions, 60 Gy in 8 fractions and 48 Gy in 4 fractions. A subgroup of these patients with a schedule of 40 Gy and 48 Gy in

Chapter 4

4 fractions (n = 41) was previously described in a tumour dose-response study [16]. The approach to define appropriate doses and margins for the SBRT patients can be described as a continuous reassessment approach which was dependent on tumour control and toxicity. This has been accurately described previously [16]. Patients with a schedule of 35 Gy in 4 fractions, 48 Gy and 60 Gy in 8 fractions (irradiated before 2000) and patients treated for multiple targets were treated in a similar manner. Ninety-five SBRT patients were irradiated on one single target. The treatment schedule, diagnosis of RP and the MLD of these patients are given in Table 1. Thirty-three patients received irradiations on multiple targets. For 20 patients,

Table1. The total dose, fraction dose, median tumor volume, median MLD and the incidence of RP for each treatment schedule of the SBRT patients.

Number of patients	Total dose (Gy)	Fraction dose (Gy)	Median tumor volume (cm ³)	Median MLD (Gy)	Number of RP
3	35	8.75	32.8	5.1	1
29	40	10	15.9	5.4	2
15	48	6	12.0	5.5	0
39	48	12	7.7	7.0	4
9	60	7.5	2.6	3.5	0
20	≥ 2 successively treated lesions		19.5	10.1	5
13	≥ 2 treated lesions (minimum time interval of 2.8 months)		30.6	7.5	2

the initial radiation treatment consisted of multiple targets that were successively treated (Table 2). For 13 patients a new treatment plan was made some time after the initial treatment because of additional pulmonary lesions (Table 3). No time-related recovery of lung tissue was taken into account for these 13 patients. These 33 patients received an individually adapted (i.e. restricted) dose schedule. For all plans (and summed plans in case of re-irradiations) a maximum dose of 46 Gy and 60 Gy (recalculated into 2 Gy per fraction with an α/β ratio of 2 Gy) for the spinal cord and oesophagus, respectively was allowed. A total dose of 60 Gy/8 fr or equivalent dose calculated using LQ model with an α/β ratio = 2 Gy was allowed as maximum dose in the lung.

Patients with a conventional dose per fraction (CFRT) schedule were treated at the Department of Radiation Oncology of the Netherlands Cancer Institute – Antoni van Leeuwenhoek Hospital (NKI-AVL), Amsterdam, The Netherlands. We updated our previous analysis (with 106 patients) by Seppenwoolde [17] to a total of 142

Table2. Treatment schedule, number of irradiated targets, diagnosis of RP and the MLD of SBRT patients with multiple targets incorporated in one single treatment plan.

Pt	No. of targets	D 1 (Gy)	fr 1	D 2 (Gy)	fr 2	D 3 (Gy)	fr 3	RP	MLD (Gy)
1	2	48	8	48	12				5.5
2	2	40	4	35	4			+	8.0
3	2	48	8	48	8				16.1
4	2	48	4	48	4			+	15.8
5	2	48	4	48	8			+	19.2
6	2	40	4	40	4				17.0
7	2	48	4	48	4				11.0
8	2	40	4	40	4				11.0
9	2	40	4	40	4				8.9
10	2	35	4	35	4				3.7
11	2	35	4	45	15				6.4
12	2	60	8	60	8				4.5
13	2	40	4	50	16				6.9
14	2	48	4	40	8				11.1
15	2	48	8	48	8				10.7
16	2	48	4	60	8			+	10.3
17	2	48	4	48	4				6.9
18	2	48	8	48	8			+	16.2
19	3	40	4	40	4	48	8		5.3
20	3	40	8	35	4	35	4		7.1

Table3. Treatment schedule, time between subsequent treatments, diagnosis of RP and the MLD of SBRT patients with multiple targets incorporated in different treatment plans.

Pt	No. of treatments	D 1 (Gy)	fr 1	D 2 (Gy)	fr 2	Time 2 (mths)	D 3 (Gy)	fr 3	Time 3 (mths)	D 4 (Gy)	fr 4	Time 4 (mths)	RP	MLD (Gy)
1	2	48	8	30	8	13.3								7.6
2	2	35	4	40	4	9.8								8.9
3	2	40	4	30	8	8.3							+	7.5
4	2	40	4	35	4	4.4								9.2
5	2	60	8	40	4	2.8								8.6
6	3	48	8	35	8	6.3	48	8	6.7				+	18.1
7	3	48	4	30	10	1.4	48	8	13.2					20.6
8	3	60	8	60	8	0.6	60	8	9.1					9.7
9	3	48	8	25	5	0.1	25	5	16.9					8.4
10	4	60	8	40	4	0.7	48	8	10.8	25	5	15.7		13.3
11	4	60	8	35	4	9.7	35	4	9.7	35	4	9.7		10.6
12	4	40	4	40	4	0.1	40	4	0.6	40	4	3.3		26.5
13	4	60	8	48	8	0.0	48	8	21.5	35	4	28.8		13.5

patients. Our update included 86 patients of the dose escalation (DE) study of Belderbos et al [17]) (with 88 patients). For 2 patients included in this study dose data were lost. Of the 58 non-DE patients included in the Seppenwoolde study, we excluded 2 patients, of which the treatment was interrupted and not finished. Therefore, we were able to include 86 patients of the DE study (who were irradiated to a dose of 60.8 and 94.5 Gy with 2.25 Gy per fraction) and 56 patients who were irradiated with a dose of 70 Gy in 2 Gy per fraction).

Chapter 4

For both SBRT and CFRT patients, three dimensional (3-D) treatment plans were made. To correct for the effect of dose per fraction, the local dose was converted to the 2 Gy equivalent Normalized Total Dose (NTD) [18] using the linear quadratic (LQ) model [19] with an α/β ratio of 3 Gy. The α/β ratio of 3 Gy was used because a detailed analysis (see companion paper [20]) revealed that for SBRT this was the best value to correct for the dose per fraction evaluating RP. For the 33 SBRT patients irradiated on multiple lesions, individual plans were summed after NTD corrections and image registration had been performed. From the 3-D dose data, the MLD was calculated as the average corrected dose over the total lung volume (based on CT) excluding the gross tumour volume.

For the SBRT plans, a convolution superposition algorithm for tissue density heterogeneity was used. For the CFRT patients the inhomogeneity correction was performed using the equivalent-path length inhomogeneity-correction (EPL). The MLD_{EPL} was converted to the MLD according to convolution superposition algorithm using the conversion factor determined by De Jaeger et al ($MLD = 0.64(MLD_{EPL})^{1.10}$) [21].

The dose response relationship in the lungs between RP and MLD was modelled by a sigmoid-shaped relation according to Lyman [22] using the TD_{50} representing the dose for a 50 % complication probability. The slope of the dose response relationship is proportional to the reciprocal value of $m \cdot TD_{50}$. Using this model and parameter values, the normal tissue complication probability (NTCP) (i.e. RP) can be calculated from the MLD [23].

$$NTCP = \frac{1}{\sqrt{2\pi}} \int_{-\infty}^t e^{-\frac{x^2}{2}} dx \quad \text{with} \quad t = \frac{MLD - TD_{50}}{m \cdot TD_{50}}$$

Radiation pneumonitis (RP) was prospectively scored for both SBRT and CFRT patients and classified according to the NCI-CTC (CTC 2.0) or SWOG criteria. Grade 2 RP was scored for both SBRT and CFRT after steroids had been prescribed for RP symptoms. Grade 3 RP was scored after oxygen was required and grade 4 for assisted ventilation. Grade 5 was scored after death due to RP.

None of the included SBRT patients that were scored with RP grade 2 used steroids for other pulmonary morbidities than RP before or after the irradiation. For the CFRT patients, information on pre-treatment use of steroids was not available. For all patients the diagnosis and grade of RP was determined by the radiation oncologist and a pulmonologist experienced in the diagnosis of RP.

Statistics

By maximizing the logarithm of the likelihood function of a dataset containing N patients where P_i ($i=1, \dots, N$) represents the NTCP of a patient i , and e_{p_i} is the binary outcome (0=no RP, 1=RP), the parameters TD_{50} and m of the NTCP model

were estimated.

$$\ln(L) = \ln\left(\prod_{i=1}^N L_i\right) = \sum_{i=1}^N \ln(L_i) = \sum_{i=1}^N [ep_i \ln(P_i) + (1 - ep_i) \ln(1 - P_i)]$$

95% confidence intervals around m and TD_{50} were calculated using a profile likelihood approach [22]. For each parameter, the confidence interval includes a certain value if twice the difference of the log likelihood evaluated at the maximum likelihood estimate and at the value of interest do not exceed the quantile of a chi-square (χ^2) distribution with one degree of freedom [24]. To determine the confidence interval of the NTCP curve, a similar approach was performed, however, this test was performed with two degrees of freedom.

To test the difference between the fitted NTCP model of SBRT and CFRT the data of both models was pooled. The NTCP model based on the pooled data (i.e. one TD_{50} and one m) was compared to the NTCP model whereby the data set-specific optimized parameters of SBRT and CFRT were included in a 2 degree of freedom likelihood ratio test [22]. We also compared the empirical incidence of RP across data sets for several non-overlapping dose intervals using Fisher's exact test.

The Hosmer-Lemeshow Goodness-of-Fit Test [25] was used to estimate the goodness of the fit of the fitted NTCP model. Patients were divided into 10 equal bins in increasing order of the estimated NTCP. The chi square test statistic was calculated

by
$$\chi^2_{HL} = \sum_{i=1}^{10} \frac{(O_i - N_i \cdot \overline{NTCP}_i)^2}{N_i \cdot \overline{NTCP}_i \cdot (1 - \overline{NTCP}_i)}$$
 where N_i is the total number of patients in

the i^{th} group, O_i is the total number of events in the i^{th} group, and \overline{NTCP}_i is the mean calculated NTCP in the i^{th} group. The test statistic is compared to chi square distribution with 8 degrees of freedom (by definition of the Hosmer-Lemeshow goodness of the fit test). The null hypothesis is that there is no difference between the observed and expected values of RP. (i.e. large values of chi square (and small p values) indicate a lack of fit by the model). A two-tailed $p < 0.05$ was considered to be statistically significant.

Results

Radiation Pneumonitis

Median follow up was 16.1 months for the SBRT patients and 13.0 months for the CFRT patients. All 39 events occurred within 6.2 months following treatment for both SBRT and CFRT within a similar time frame. Within this period 4 SBRT and 18 CFRT patients were censored (Figure 1).

For the SBRT the crude incidence of RP grade 2 or higher was 10.9% (14 events in the group of 128 patients). Only 1 SBRT patient was diagnosed with grade

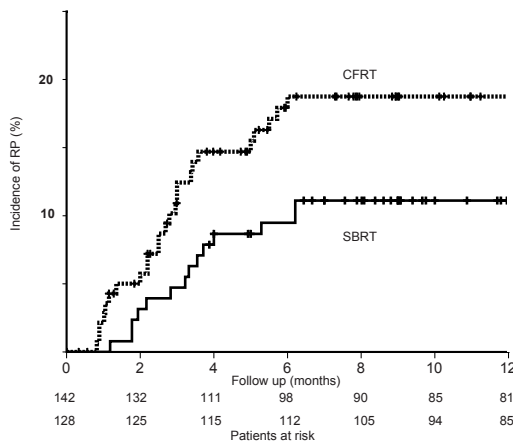


Figure 1. The incidence of RP as a function of the follow up (months). Vertical axis: one minus the cumulative RP free survival. Censored patients are indicated by crosses. The follow up is given in months on the horizontal axis.

3 RP. Three SBRT patients included in the analysis, received oxygen within the first year after irradiation and were not scored as having RP because of the uncertainty of diagnosis (one patient had cardiac problems, one patient had a medical history of receiving oxygen before treatment and one patient had fibrosis and tumour progression). For CFRT the crude incidence of RP was 17.6 % (25 events in the group of 142 patients). Four CFRT patients experienced a grade 3 RP and one patient died due to pulmonary toxicity (grade 5 RP).

Tumour volume and Mean Lung Dose

The median MLD for SBRT was 6.4 Gy (range: 1.5 Gy to 26.5 Gy). The median tumour volume of the SBRT patients was 9.6 cm³ (range: 0.2 cm³ to 106.9 cm³). For CFRT patients, the median MLD was 13.2 Gy (range: 3.0 Gy to 23.0 Gy) and the median tumour volume was 61.2 cm³ (range: 3.8 cm³ to 789.9 cm³).

Normal Tissue Complication Probability

SBRT

For SBRT the observed incidence of RP as a function of the MLD is plotted in Figure 2a. The error bars represent the 68% confidence interval (CI) of the observed incidence in 4 Gy dose bins. The observed number of RP and the total number of patients within each dose bin are indicated. The solid line represents the best fit of the NTCP model based on the MLD. The best parameter values of the NTCP model were TD₅₀ = 19.6 Gy (95%CI: 16.0 Gy to 30.0 Gy) and m=0.43 (95%CI: 0.33 to 0.59). The dashed lines represent the 68% CI of the fitted curve.

CFRT

For the CFRT the observed incidence of RP as a function of the MLD is plotted in Figure 2b. The optimal fit of the NTCP model using MLD resulted in a TD₅₀ of 28.6Gy (95%CI: 21.5 Gy to 125.0 Gy) and an m value of 0.56 (95%CI: 0.39 to 0.99).

Radiation pneumonitis for Patients Treated for Malignant Pulmonary Lesions with SBRT

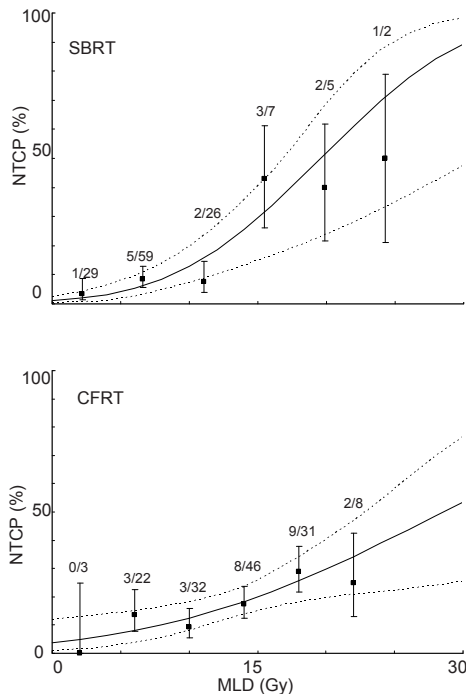


Figure 2 a + b. The incidence of grade ≥ 2 RP of SBRT (2a) and CFRT (2b) irradiated patients as a function of the MLD. The error bars represent the 68 % confidence intervals (CI) of the observed incidence. The solid lines represent the probability of RP accordingly to the NTCP model with the optimized parameters m and TD_{50} (as shown in Table 5). The dotted lines represent the 68 % CI of the fitted NTCP curve.

SBRT versus CFRT

Both the SBRT model and the CFRT model fitted the clinical data well ($\chi^2_{HL}=8.27$, $p=0.41$ and $\chi^2_{HL}=4.36$, $p=0.82$, respectively).

A comparison of the dose-specific observed RP incidence between SBRT and CFRT revealed that there was no significant difference for any of the 6 dose ranges covering 4 Gy each. However, RP occurred more frequently in the 2 highest dose ranges for SBRT compared to CFRT but this difference was not significant (Table 4). Importantly, lower numbers of patients were included in the higher dose ranges for both SBRT and CFRT limiting the power of statistical comparison of these particular high dose groups.

Evaluating the whole dose range, the NTCP curve of SBRT is steeper for the high dose range suggesting an increased risk for RP after SBRT compared to CFRT for patients with a higher MLD. However, there was no statistical evidence that the fitted NTCP model (with the parameters

Table 4. Incidence of RP by MLD range and treatment type (SBRT, CFRT).

Dose bin (Gy)	SBRT	CFRT	<i>p</i> -value Fisher's exact test
	Number of RP events / total number of patients	Number of RP events / total number of patients	
0 - 4	0/23 (0%)	0/3 (0%)	0.99
4 - 8	4/60 (7%)	3/22 (14%)	0.38
8 - 12	4/28 (14%)	3/32 (9%)	0.70
12 - 16	1/8 (13%)	4/46 (9%)	0.99
16 - 20	4/7 (57%)	9/31 (29%)	0.20
20 - 28	1/2 (50%)	2/8 (25%)	0.46

m and TD_{50}) differed between SBRT and CFRT ($p=0.37$, likelihood ratio test). Again, we would like to stress that the statistical power was limited due to lower number of patients in the high dose range.

The optimal fit of the SBRT and CFRT together resulted in a TD_{50} of 24.4 Gy (95%CI: 21.0Gy to 32.0Gy) and m of 0.49 (95%CI: 0.42 to 0.61) (Figure 3).

Discussion

A significant relationship between the MLD and the incidence of RP following SBRT was observed. Moreover, the NTCP model fitted the SBRT data well. We observed no significant difference between the NTCP models predicting RP in SBRT and CFRT patients. Furthermore, no significant difference between SBRT and CFRT was observed in the incidence of RP in any dose range. Nevertheless, an increased risk for SBRT in higher dose ranges was suggested by both the NTCP model fit and the observed RP incidences. However, because fewer patients were available in the high dose range no firm conclusions can be made concerning these differences.

At the Department of Radiation Medicine of the Hokkaido University School of Medicine, different SBRT dose schedules have been used since 1998. The first applied schedule was 35 Gy in 4 fractions that was escalated to 48 Gy in 4 fractions. Between these schedules, interim doses of 40 Gy in 4 fractions and 48 Gy and 60 Gy in 8 fractions were given. In addition, tumours located near to critical structures were more fractionated than peripheral tumours. The absence of severe toxicity strengthened the approach of re-treating patients with tumour recurrence or irradiating multiple lesions sequentially. Consequently, a dose-response analysis could be performed with a dose range similar to the dose range of the CFRT. The comparison of SBRT with

CFRT was performed with an update of previously evaluated NKI-AVL CFRT patients. As expected, the m and TD_{50} for these CFRT patients were similar to a previous publication [18] and the meta-analysis of Semenenko et al. [15].

Previous SBRT studies reported a 0 % to 29 % incidence of RP grade 2 or higher [3,9-14,26]. Unfortunately, only a limited number of studies reported

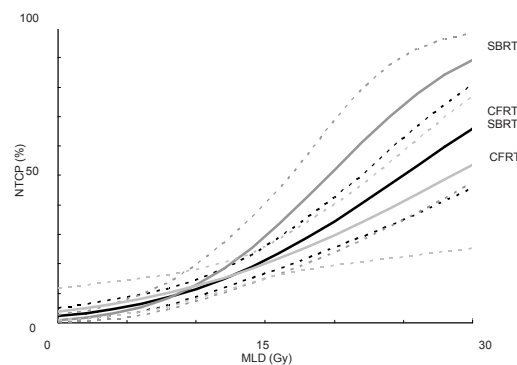


Figure 3. Fitted NTCP curves (solid lines) and their 68 % confidence intervals (CI) intervals (dashed lines) as a function of the MLD for SBRT (dark grey), CFRT (grey) and combined data (black).

dose parameters to describe the lung dose. Yamashita et al [9] reported a high incidence of RP grade 2 or higher in 7 of the 25 patients treated with 48 Gy in 4 fractions. The mean MLD was only 4.3 Gy (ranging from 1.72 Gy to 5.85 Gy). However, for the calculation of the lung dose, which was not NTD corrected, not only the tumour volume was subtracted from the total lung volume but also an extra margin surrounding the tumour, resulting in an underestimation of the lung dose. Nagata et al [13] reported a 4 % incidence of RP grade 2 in patients treated with 48 Gy in 4 fractions with a mean V20 (percentage volume of the whole lung receiving more than 20 Gy) in this patient group of only 4.5 %. In the study by Ng et al. [26], no RP grade 2 or higher was observed. However, this study included only 20 patients with 80 % of the patients having a V20 < 20 % (GTV ranged from 4.27 cm³ to 74 cm³).

The clinical applicability of our results in relation to other SBRT schedules may be questionable as many institutions in Europe and the USA use fraction doses of 18 Gy or 20 Gy. In our study, 48 Gy in 4 fractions was the most commonly used fractionation schedule having 8 different beam angles (i.e. 1.5 Gy per beam). For fraction doses of 18 Gy, at least 12 different beam angles are used [6], which results also 1.5 Gy per beam. Therefore, the major part of the lung tissue will receive equivalent doses per fraction. Moreover, in the 18 Gy or 20 Gy per fraction schedule, the percentage of lung tissue receiving the highest proportion of the dose is small because smaller dose planning margins of 5 mm to 10 mm around the tumour are used [6] (most of our patients had 11 mm to 13 mm margins [16]). Therefore, large deviations in the lung tissue response of these hypofractionated schedules are not expected.

Because the collaboration encompassed two different radiotherapy departments, a lot of effort was invested in standardizing methods for dose planning and dose calculation between the patient groups. A recent study by Gershkevish [27] showed that deviations between different treatment planning systems decrease with the use of more advanced calculation algorithms. For all patients included in this analysis, the superposition or collapsed cone algorithm was used for treatment planning. The clinical variability in the prescribing of steroids between the two institutes was limited as only patients who were diagnosed by both radiotherapists and pulmonologists experienced with the diagnosis of radiation pneumonitis were included. Patients were excluded if the diagnosis of RP was hampered or accompanied by pulmonary comorbidity (e.g. infection, tumour progression, previous use of oxygen). Nevertheless, the uncertainties of including patients from 2 different institutes should be taken into account, and a similar one single-institute validation would be of interest.

We observed a similar time frame for RP occurrences in both SBRT and CFRT; RP occurred several weeks to 6 months after irradiation as both Guckenberger et

al. [10] and Yamshita et al. [9] reported for SBRT and Graham et al. [28] reported for CFRT. Further toxicity may be observed with a longer follow up. In the study by Timmerman [6] et al. four of the six treatment related deaths occurred after 12 months. Four of the patients suffered from a bacterial pneumonia and 1 patient experienced tumour recurrence adjacent to the carina. Evidently, both short and long term toxicity may conceivably be obscured by pulmonary comorbidity or tumour progression. Therefore, these patients, who are often suffering from pulmonary comorbidities, should be intensively followed by both radiation oncologists and pulmonologists.

For lung cancer patients or patients with pulmonary metastases, the critical prognostic importance of controlling RP risks must be balanced against not only the patient's physical condition, but also against tumour control. A strong consequential component between acute and long term pulmonary toxicity after lung irradiation is observed in animal studies [29,30]. Consequently, even though grade 2 RP might not be life-threatening, it may substantially contribute to a cascade of pulmonary deterioration in patients with pulmonary comorbidity. Moreover, a long-term dose dependent progressive decline of pulmonary function is observed in patients treated with CFRT [31] with MLD up to 21.9 Gy (mean MLD 13.9 Gy). In a recently published SBRT phase II study [32] no relationship was observed between toxicity and lung dose. In this study a mean MLD of 7 Gy for 60 patients was found. Our retrospective study encompassed a larger dose range for a larger number of patients but no pulmonary function data or follow up CT's were evaluated. A prospective study with a large dose range with long term follow up should reveal the predictability of any radiation induced toxicity after hypofractionated schedules.

To date, there is no clinical data available which compares the prognosis (survival) of lung cancer patients experiencing clinical relevant radiation induced toxicity versus non-symptomatic patients. With regards to the optimal treatment, the clinical evaluation of the risk of tumour recurrence and the probability of toxicity is a matter of concern in a patient group with a poor tumour related prognosis and a high incidence of co-morbidity. Our retrospective evaluation can serve as a guideline estimating the probability of RP for the clinical decision making (i.e. staying on the safe side for pulmonary compromised or palliative patients and accepting a higher risk of toxicity for curable patients without pulmonary comorbidities). Nevertheless, prospective studies are needed to reveal the relation of short and long term toxicity and tumour control.

Time related recovery of lung tissue was not taken into account in our patients who had received multiple treatment schemes. A mouse study by Terry et al. [33] showed that irradiation induced lung injury tissue could (partly) recover, suggesting an early target cell depletion and regeneration which was dependent on the size of the initial injury (i.e. dose). For a single dose of 10 Gy, less recovery was observed than for 6 Gy.

Clinical studies, evaluating toxicity after re-irradiations for lung cancer patients are limited due to poor prognosis. Okamoto et al. [34] studied 34 lung cancer patients re-irradiated because of a local recurrence. The large number of patients (19 patients, i.e. 56%) experiencing grade 2 or higher RP suggest limited (or no) time related recovery. Moreover, from the long term survivors (20 to 58 months after re-irradiation) 71% of the patients experienced a grade 2 RP. However, no lung dose characteristics were reported and RP risk estimating could therefore not be performed.

To predict normal tissue complication probabilities (NTCP) after radiotherapy treatment, the delivered dose has to be re-calculated into a biological-effective dose using a mathematical model (Linear Quadratic model) [35,36] derived from in-vitro and animal studies [37]. The clinical applicability of this model is a historical cornerstone in assessing tumour doses and dose tolerance of normal tissues. Although the use of SBRT is increasing, no study validated the clinical applicability of the LQ model for SBRT. We evaluated the applicability of the LQ model in this patient group in the accompanying paper [20].

Although there were numerous limitations in our study we were able to show a relationship between the lung dose and the incidence of RP for SBRT that was not significantly different from CFRT.

Chapter 4

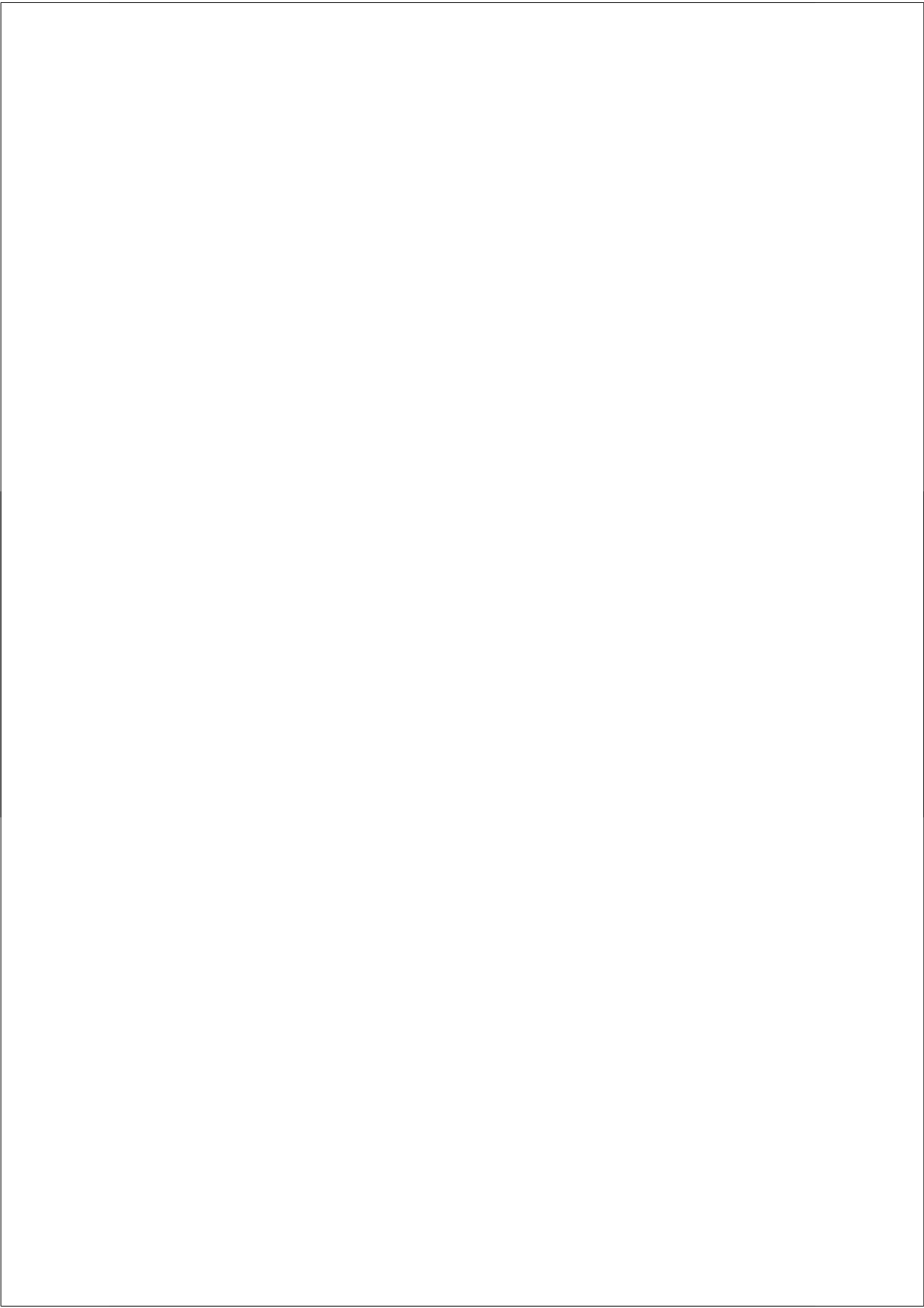
References

1. Blomgren H, Lax I, Naslund I et al. Stereotactic high dose fraction radiation therapy of extracranial tumors using an accelerator. Clinical experience of the first thirty-one patients. *Acta Oncol* 1995;34:861-870.
2. Onishi H, Araki T, Shirato H et al. Stereotactic hypofractionated high-dose irradiation for stage I nonsmall cell lung carcinoma: clinical outcomes in 245 subjects in a Japanese multiinstitutional study. *Cancer* 2004;101:1623-1631.
3. Onishi H, Shirato H, Nagata Y et al. Hypofractionated stereotactic radiotherapy (HypoFXSRT) for stage I non-small cell lung cancer: updated results of 257 patients in a Japanese multi-institutional study. *J Thorac Oncol* 2007;2:S94-100.
4. Wulf J, Haedinger U, Oppitz U et al. Stereotactic radiotherapy for primary lung cancer and pulmonary metastases: a noninvasive treatment approach in medically inoperable patients. *Int J Radiat Oncol Biol Phys* 2004;60:186-196.
5. Timmerman RD, Kavanagh BD, Cho LC et al. Stereotactic body radiation therapy in multiple organ sites. *J Clin Oncol* 2007;25:947-952.
6. Timmerman R, McGarry R, Yiannoutsos C et al. Excessive toxicity when treating central tumors in a phase II study of stereotactic body radiation therapy for medically inoperable early-stage lung cancer. *J Clin Oncol* 2006;24:4833-4839.
7. Lagerwaard FJ, Haasbeek CJ, Smit EF et al. Outcomes of risk-adapted fractionated stereotactic radiotherapy for stage I non-small-cell lung cancer. *Int J Radiat Oncol Biol Phys* 2008;70:685-692.
8. Brock J, Ashley S, Bedford J et al. Review of hypofractionated small volume radiotherapy for early-stage non-small cell lung cancer. *Clin Oncol (R Coll Radiol)* 2008;20:666-676.
9. Yamashita H, Nakagawa K, Nakamura N et al. Exceptionally high incidence of symptomatic grade 2-5 radiation pneumonitis after stereotactic radiation therapy for lung tumors. *Radiat Oncol* 2007;2:21-
10. Guckenberger M, Heilman K, Wulf J et al. Pulmonary injury and tumor response after stereotactic body radiotherapy (SBRT): results of a serial follow-up CT study. *Radiother Oncol* 2007;85:435-442.
11. Zimmermann FB, Geinitz H, Schill S et al. Stereotactic hypofractionated radiotherapy in stage I (T1-2 N0 M0) non-small-cell lung cancer (NSCLC). *Acta Oncol* 2006;45:796-801.
12. Aoki T, Nagata Y, Negoro Y et al. Evaluation of Lung Injury after Three-dimensional Conformal Stereotactic Radiation Therapy for Solitary Lung Tumors: CT Appearance *Radiology* 2003;
13. Nagata Y, Takayama K, Matsuo Y et al. Clinical outcomes of a phase I/II study of 48 Gy of stereotactic body radiotherapy in 4 fractions for primary lung cancer using a stereotactic body frame. *Int J Radiat Oncol Biol Phys* 2005;63:1427-1431.
14. McGarry RC, Papiez L, Williams M et al. Stereotactic body radiation therapy of early-stage non-small-cell lung carcinoma: phase I study. *Int J Radiat Oncol Biol Phys* 2005;63:1010-1015.
15. Semenenko VA, Li XA. Lyman-Kutcher-Burman NTCP model parameters for radiation

- pneumonitis and xerostomia based on combined analysis of published clinical data. *Phys Med Biol* 2008;53:737-755.
16. Onimaru R, Fujino M, Yamazaki K et al. Steep dose-response relationship for stage I non-small-cell lung cancer using hypofractionated high-dose irradiation by real-time tumor-tracking radiotherapy. *Int J Radiat Oncol Biol Phys* 2008;70:374-381.
 17. Belderbos JS, Heemsbergen WD, De Jaeger K et al. Final results of a Phase I/II dose escalation trial in non-small-cell lung cancer using three-dimensional conformal radiotherapy. *Int J Radiat Oncol Biol Phys* 2006;66:126-134.
 18. Lebesque JV, Keus RB. The simultaneous boost technique: the concept of relative normalized total dose. *Radiother Oncol* 1991;22:45-55.
 19. Douglas BG, Fowler JF. The effect of multiple small doses of x rays on skin reactions in the mouse and a basic interpretation. *Radiat Res* 1976;66:401-426.
 20. Borst GR, Ishikawa M, Nijkamp J et al. Linear Quadratic Model Corrected Lung Dose Predicting Radiation Pneumonitis after Hypofractionated Lung Irradiation? submitted 2008;
 21. De Jaeger K, Hoogeman MS, Engelsman M et al. Incorporating an improved dose-calculation algorithm in conformal radiotherapy of lung cancer: re-evaluation of dose in normal lung tissue. *Radiother Oncol* 2003;69:1-10.
 22. Clayton D, Hills M. *Statistical Models in Epidemiology*. Oxford University Press. New York.; 1993.
 23. Seppenwoolde Y, Lebesque JV, De Jaeger K et al. Comparing different NTCP models that predict the incidence of radiation pneumonitis. Normal tissue complication probability. *Int J Radiat Oncol Biol Phys* 2003;55:724-735.
 24. D.J.Venzon, S.H.Moolgavkar. A Method for Computing Profile-Likelihood-Based Confidence Intervals. *Applied Statistics* 1988;37:87-94.
 25. Hosmer D, Lemeshow S. Goodness of fit tests for the multiple logistic regression model. *Communications in Statistics - Theory and models* 1980;A9:1043-1069.
 26. Ng AW, Tung SY, Wong VY. Hypofractionated stereotactic radiotherapy for medically inoperable stage I non-small cell lung cancer--report on clinical outcome and dose to critical organs. *Radiother Oncol* 2008;87:24-28.
 27. Gershkevitch E, Schmidt R, Velez G et al. Dosimetric verification of radiotherapy treatment planning systems: Results of IAEA pilot study. *Radiother Oncol* 2008;
 28. Graham MV, Purdy JA, Emami B et al. Clinical dose-volume histogram analysis for pneumonitis after 3D treatment for non-small cell lung cancer (NSCLC). *Int J Radiat Oncol Biol Phys* 1999;45:323-329.
 29. Franko AJ, Sharplin J. Development of fibrosis after lung irradiation in relation to inflammation and lung function in a mouse strain prone to fibrosis. *Radiat Res* 1994;140:347-355.
 30. Trott KR, Herrmann T, Kasper M. Target cells in radiation pneumopathy. *Int J Radiat Oncol Biol Phys* 2004;58:463-469.
 31. Borst GR, De Jaeger K, Belderbos JS et al. Pulmonary function changes after radiotherapy in non-small-cell lung cancer patients with long-term disease-free survival. *Int J Radiat Oncol Biol Phys* 2005;62:639-644.

Chapter 4

32. Baumann P, Nyman J, Hoyer M et al. Stereotactic body radiotherapy for medically inoperable patients with stage I non-small cell lung cancer - a first report of toxicity related to COPD/CVD in a non-randomized prospective phase II study. *Radiother Oncol* 2008;88:359-367.
33. Terry NH, Tucker SL, Travis EL. Residual radiation damage in murine lung assessed by pneumonitis. *Int J Radiat Oncol Biol Phys* 1988;14:929-938.
34. Okamoto Y, Murakami M, Yoden E et al. Reirradiation for locally recurrent lung cancer previously treated with radiation therapy. *Int J Radiat Oncol Biol Phys* 2002;52:390-396.
35. Fowler JF. The first James Kirk memorial lecture. What next in fractionated radiotherapy? *Br J Cancer Suppl* 1984;6:285-300.
36. Tucker SL. Tests for the fit of the linear-quadratic model to radiation isoeffect data. *Int J Radiat Oncol Biol Phys* 1984;10:1933-1939.
37. Steel GG. *Basic Clinical Radiobiology*, Text book. 3ed. 1997.



**Pulmonary function changes after radiotherapy in
non-small cell lung cancer patients with a
long-term disease free survival**

Gerben R. Borst, M.D.¹, Katrien De Jaeger, M.D.¹, José S.A. Belderbos,
M.D.¹, Sjaak A. Burgers, M.D., Ph.D.¹, Joos V. Lebesque, M.D., Ph.D.¹

¹*Department of Radiation Oncology, ²Department of Thoracic Oncology, The Netherlands Cancer Institute - Antoni van Leeuwenhoek Hospital, Amsterdam, The Netherlands.*

International Journal of Radiation Oncology*Biography*Physics
Volume 62, Issue 3,1 July 2005, Pages 639-644

Abstract

Purpose: To evaluate the changes in pulmonary function after high-dose radiotherapy (RT) for non-small-cell lung cancer in patients with a long-term disease-free survival.

Methods and Materials: Pulmonary function was measured in 34 patients with inoperable non-small-cell lung cancer before RT and at 3 and 18 months of follow-up. Thirteen of these patients had a pulmonary function test (PFT) 36 months after RT. The pulmonary function parameters (forced expiratory volume in 1 s [FEV1], diffusion capacity [Tlco], forced vital capacity, and alveolar volume) were expressed as a percentage of normal values. Changes were expressed as relative to the pre-RT value. We evaluated the impact of chronic obstructive pulmonary disease, radiation pneumonitis, mean lung dose, and PFT results before RT on the changes in pulmonary function.

Results: At 3, 18, and 36 months, a significant decrease was observed for the Tlco (9.5%, 14.6%, and 22.0%, respectively) and the alveolar volume (5.8%, 6.6%, and 15.8%, respectively). The decrease in FEV1 was significant at 18 and 36 months (8.8% and 13.4%, respectively). No recovery of any of the parameters was observed. Chronic obstructive pulmonary disease was an important risk factor for larger PFT decreases. FEV1 and Tlco decreases were dependent on the mean lung dose.

Conclusion: A significant decrease in pulmonary function was observed 3 months after RT. No recovery in pulmonary function was seen at 18 and 36 months after RT. The decrease in pulmonary function was dependent on the mean lung dose, and patients with chronic obstructive pulmonary disease had larger reductions in the PFTs.

Introduction

Lung cancer is still one of the leading causes of cancer mortality [1]. About 80 % of these tumors are histologically non-small cell lung cancers (NSCLC). Eighty percent of these NSCLC patients receive radiotherapy because many patients are inoperable due to metastases, loco regional spread (technically inoperable) or because of a poor pulmonary function (medically inoperable) [2].

Radiotherapy to the thoracic region is associated with important side effects. Several investigators found various parameters such as the Mean Lung Dose (MLD), or the percentages of lung volume receiving more than a threshold dose of 13 Gy, 20 Gy or 30 Gy to be predictive for radiation pneumonitis [3-7]. These parameters can currently be taken into account to estimate the risk of this type of complication.

It is more complicated to estimate graded responses in the lung such as changes in pulmonary function. For patients with healthy lungs (breast cancer and lymphoma patients) Theuws et al. [8] was able to show a significant recovery in pulmonary function tests (PFTs) at 18 months after an initial reduction at 3 months following irradiation. For lung cancer patients it is more difficult to estimate PFT changes. First, lung cancer patients are often suffering from pulmonary comorbidities such as chronic obstructive pulmonary disease (COPD) and emphysema, mainly due to the high incidence of smokers. These underlying lung diseases increase the variability of PFTs [9], and therefore makes it more difficult to objectify the pulmonary toxicity of irradiation. Secondly, the estimation of pulmonary function changes on the long term is hampered by the poor prognosis of NSCLC patients.

Radiotherapy modalities, such as dose escalation [10-13] and combined chemoradiation [14-18] may improve local control and even the prognosis of NSCLC patients. Long-term toxicity following irradiation in medically inoperable NSCLC patients is of great interest, especially if tumor control improves in these patients. Long-term follow-up data are however scarce for this group of patients. Seven patients experienced a progressive decrease of PFTs 3 years after radiotherapy in a study by Miller et al. [7]. But clearly, data of more patients is needed to clarify the respiratory condition following irradiation of inoperable NSCLC patients with a long-term disease free survival.

To investigate the development of pulmonary function in the long term, we evaluated the PFT changes of inoperable NSCLC patients with locally controlled disease with at least a follow up of 18 months. We investigated the impact of patient- and treatment- related factors on the PFTs.

Material and Methods

Patient, tumor, and treatment characteristics

Patients with baseline pulmonary function tests (PFTs) 2 weeks before the start of

Chapter 5

radiotherapy, and at 3 and 18 months follow up were included. Patients with tumor recurrence, progression and/or metastases were excluded. One hundred and sixty-nine patients with medically or technically inoperable non-small cell lung cancer (NSCLC) were referred to the department for radical or curative RT between 1996 and 2002. According to these inclusion criteria, 34 patients were eligible. In 13 of these 34 patients PFTs were evaluated at 36 months, as well.

Patient and tumor characteristics are shown in Table 1. The majority of patients were former (47 %) or current (41 %) smokers. Half of the patients suffered from chronic obstructive pulmonary disease (COPD). COPD was diagnosed according to the Global Initiative for Obstructive Lung Disease (GOLD) criteria [19]. COPD was defined in patients having symptoms of cough, sputum production, or dyspnea, and/or a history of exposure to risk factors (smoking) for the disease. A postbronchodilator forced expiratory volume (FEV₁) of less than 80 % and a ratio of FEV₁/ forced vital capacity (FVC) of less than 70 % can confirm the diagnosis.

Thirteen patients received a standard radiotherapy regimen of 70 Gy delivered in 35 fractions in 7 weeks. The remaining 21 patients were included in a Phase I/II dose escalation study (10) and were treated with doses between 60.8 and 94.5 Gy (2.25 Gy per fraction, fixed overall treatment time of 6 weeks).

Three radiotherapy patients received chemotherapy, which was administered at least 6 weeks before the start of the irradiation. Radiation pneumonitis (RP) was scored according to the Southwest Oncology Group (SWOG) toxicity criteria. Five patients developed RP grade 2 and one patient developed grade 3 RP (grade 2 is scored when steroids are required for treatment, grade 3 is scored when oxygen is needed).

Pulmonary function tests

Pulmonary function tests (PFTs) were performed using the Jaeger Masterlab equipment (Würzburg, Germany). In this study, we evaluated the FEV₁, forced vital capacity (FVC), transfer factor for carbon monoxide corrected for the actual hemoglobin (Hb) level in the peripheral blood (Tlcoc) and the alveolar volume (VA) The transfer factor for carbon monoxide (Tlco) was corrected for the actual hemoglobin (Hb) level according to the formula $Tlcoc = Tlco * (6.12 + Hb) / (1.7 * Hb)$ [mmol / min/ kPa]. PFTs were expressed as a percentage of the normal value (based on weight, height and gender) [20]. Changes of the PFTs 3, 18 and 36 months post-RT were expressed as the difference between the pre-RT and post-RT PFT relative to the pre-RT value: $(PFT_{pre} - PFT_{post}) / PFT_{pre}$ (%).

Lung dose

CT based dose calculations were performed as previously described [21] using a 3-D treatment planning system [U-Mplan, University of Michigan]. Corrections for tissue inhomogeneities were based on an equivalent path length algorithm.

Table 1. Patient, tumor, and treatment characteristics

Age (y)	
Median	72.5
Range	48–82
Gender (n)	
Male	23
Female	11
Smoking history (n)	
Current smoker	14
Former smoker	16
Nonsmoker	4
COPD (n)	
Yes	15
No	19
Radiation pneumonitis (n)	
SWOG Grade 2	5
SWOG Grade 3	1
SWOG Grade 4	0
Tumor stage (n)	
I	11
II	5
III	18
Tumor location (n)	
Right upper lobe	15
Right middle lobe	2
Left upper lobe	14
Left lower lobe	2
Main bronchus	1
Total tumor dose (Gy)	
Median	74.3
Range	60.8–94.5
Mean lung dose (Gy)	
Mean	13.9
Range	2.9–21.9

Abbreviations: COPD = chronic obstructive pulmonary disease; SWOG = Southwest Oncology Group.

All doses reported in this paper were corrected for fractionation. The local dose was converted to the normalized total dose (NTD) [22], defined as the biologically equivalent dose delivered in 2 Gy per fraction. The linear quadratic model with an α/β ratio of 3 Gy was used [23]. For calculating the mean lung dose (MLD), the gross target volume (GTV) was excluded from total volume of both lungs. The lung was defined on the CT scan by a binary threshold. The mean perfusion weighted lung dose (MpLD), a parameter correlating better with PFT changes at 3 months compared to the MLD [24], was not evaluated because perfusion data were not available for a significant number of patients.

Statistical analysis

To evaluate changes in the PFT parameters following irradiation, we compared the pre-RT values with the 3, 18 and 36 months follow-up values using the paired t-test. To study whether a parameter remained constant or changed after 3 months, we compared the values at 18 months with both pre-RT and 3-month values. Similarly, the values at 36 months were compared with the measurements at earlier points (i.e. pre-RT, 3 months and 18 months). To investigate whether PFT values and the PFT changes were different between specific subgroups, the unpaired t-test was used.

To assess the impact of various parameters on the change of the PFTs, an univariate linear regression analysis was performed. Significant (and borderline significant) factors in the univariate analysis were explored in the multivariate linear regression analyses to evaluate their association with PFT changes. A stepwise backward approach was used. Differences were considered significant when the p-value was < 0.05. Analyses were carried out using SPSS version 10.0.0 (statistical package for the social sciences).

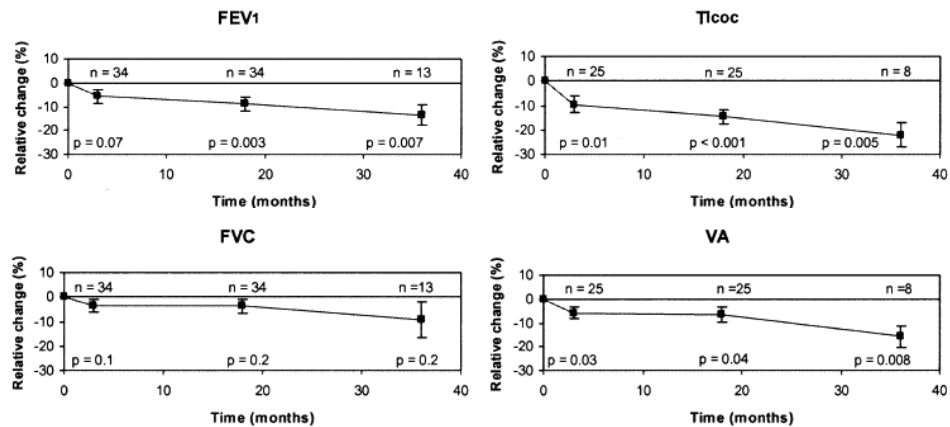


Figure 1. Mean relative change of the FEV₁, Tlcoc, FVC and VA values at 3, 18 and 36 months following irradiation. The error bars indicate the standard error of the mean. n = number of patients, p = significance of the paired t-test.

Results

Pulmonary function before radiotherapy

Values for the FEV₁ and FVC were available for all patients. The Tlcoc and VA values were available in 25 of the 34 patients. The absolute FEV₁ values ranged between 0.7 to 3.7 L/s. The mean values for FEV₁, FVC, Tlcoc and VA were 60 %, 84 %, 69 % and 85 %, respectively.

Pulmonary function after radiotherapy

The mean values for FEV₁, FVC, Tlcoc and VA, 3 months following irradiation, were 56 %, 80 %, 62 % and 80 %, respectively. Eighteen months after radiotherapy the mean values for FEV₁, FVC, Tlcoc and VA were 54 %, 80 %, 59 % and 80 %, respectively. For the PFT at 36 months the mean values for FEV₁, FVC, Tlcoc and VA were 56 %, 76 %, 58 % and 75 %, respectively. The time trend of the mean relative change of all the different PFT parameters is illustrated in Figure 1. Tlcoc and VA showed a statistically significant decrease at all points compared to the pre-RT values. The FEV₁ decreased significant at 18 and 36 months. The FVC did not decrease significant.

In addition, the PFT values at 18 and 36 months were compared with the PFT values of previous PFTs (i.e. 3 and 18 months, respectively), using the paired t-test. Decreases were observed for all parameters although these decreases were not significant with respect to each other in the period from 3 to 36 months.

Patients with an improvement or deterioration of more than 10 % of the PFT parameters after 18 and 36 months are indicated in Figure 2.

Long-term pulmonary function changes after RT in NSCLC patients

A change of 10 % was regarded as no change, since the reproducibility of PFT measurements is approximately 10 % (20,25). For Tlcoc and FEV₁, the majority of the patients showed a decrease of more than 10 %. After 36 months none of the patients showed an improvement in Tlcoc, FEV₁ and VA of 10 % or more, but the number of patient was smaller.

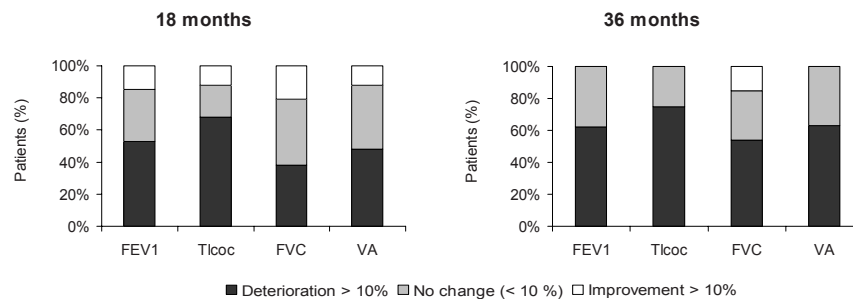


Figure 2. Bar graphs of the relative pulmonary function changes at 18 and 36 months following irradiation.

Changes of PFT parameters and patient related factors

The pulmonary function of COPD patients was worse than that of non-COPD patients. The mean pre-RT FEV₁ was as expected, statistically significantly different in COPD vs. non-COPD patients (50 % and 67 %, respectively, $p = 0.006$). The FEV₁ also remained significantly different between the non-COPD and COPD patients at 3 (43 % vs. 67 %, $p < 0.001$), 18 (42 % vs. 64 %, $p < 0.001$) and 36 months (45 % vs. 66%, $p = 0.03$). For the FVC and Tlcoc, at all time periods, the mean values were lower for COPD patients compared to non-COPD patients. The difference was significant for FVC at 18 months (72 % vs. 87 %, $p = 0.02$) and for the Tlcoc at 36 months (44 % vs. 72 % $p = 0.03$). For the VA a significantly lower mean value was observed for COPD compared to non-COPD patients at 36 months (62 % vs. 87 %, $p = 0.03$).

In Figure 3, the mean of the relative changes for COPD and non-COPD patients is given. For the FEV₁ a (borderline) significant larger decrease for COPD patients compared to non-COPD patients was observed at 3 months 13 % vs. 0 % ($p = 0.02$), at 18 months 14 % vs. 4 % ($p = 0.09$) and at 36 months 23 % vs. 5% ($p = 0.03$). The difference between the relative Tlcoc changes in COPD vs. non-COPD patients showed a trend at 3 months (18 % vs. 5 %, $p = 0.09$), 18 months (19 % vs. 12 %, $p = 0.3$) and at 36 months (33 % vs. 11 %, $p = 0.01$). The difference between the relative FVC changes in COPD versus non-COPD patients was significant at 3 months ($p = 0.04$) and at 18 months ($p = 0.008$) and for the VA at 36 months ($p = 0.03$).

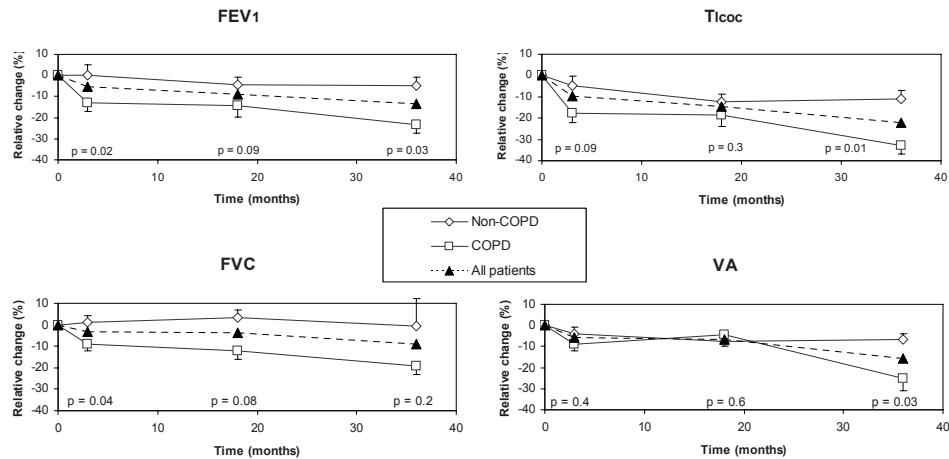


Figure 3. Mean relative change of the FEV₁, Tlcoc, FVC and VA values for COPD and non-COPD patients. The error bars indicate the standard error of the mean. The indicated p-values are calculated with the unpaired t-test comparing the changes of the COPD patients with the changes of the non-COPD patients.

We compared patients with pre-RT FEV₁ values above the median to patients with pre-RT FEV₁ values below the median value. The median FEV₁ before treatment was 57 %. The higher FEV₁ pre-RT group experienced a (borderline) significant decrease for 18 and 36 months for all parameters ($p = 0.01 - 0.08$) except for the FVC. However, these decreases were not significantly larger than the decreases of the lower FEV₁ pre-RT group. The decreases for the lower pre-RT FEV₁ were significant for the FEV₁ and FVC at 36 months ($p = 0.05$ and $p = 0.02$, respectively) and for the Tlcoc at 18 months ($p = 0.003$).

Patients who developed radiation pneumonitis did not experience a larger decrease of the pulmonary function at any of the follow-up PFTs. No conclusion can be made because of the small number of radiation pneumonitis events. No analyses could be performed to evaluate the influence of smoking on PFT changes because only 4 patients were non-smokers.

Changes of PFT parameters and treatment related factors.

The average of the mean lung dose (MLD) was 13.9 Gy (range 2.9 - 21.9 Gy). A statistically significant correlation was found between the MLD and the decrease in FEV₁ at 3 ($p = 0.03$) and 18 months ($p = 0.01$). The same correlation, but not significant, was found at 36 months (Figure 4). The correlation between the MLD and decrease in Tlcoc was (borderline) significant at 3 ($p = 0.03$) and 36 ($p = 0.06$) months, but not significant at 18 months (Figure 4). For the FVC and VA no significant correlations were observed. No analyses could be performed to evaluate

the influence of chemotherapy because only 3 patients received chemotherapy.

Estimation of PFT changes

For the time periods where a trend was observed between the PFT changes and the variables MLD and COPD a multivariate analysis was performed to test their joint effect on the reduction of the PFTs (Table 2). The decrease of FEV₁ remained dependent of the MLD and COPD at 3 and 18 months following irradiation. Regarding the Tlcoc changes, a trend was observed for the MLD and COPD at 3 months (p = 0.08) and at 36 months (p = 0.07), respectively. Because the reductions of FVC and VA were only correlated with COPD, no multivariate analyses were performed for these parameters.

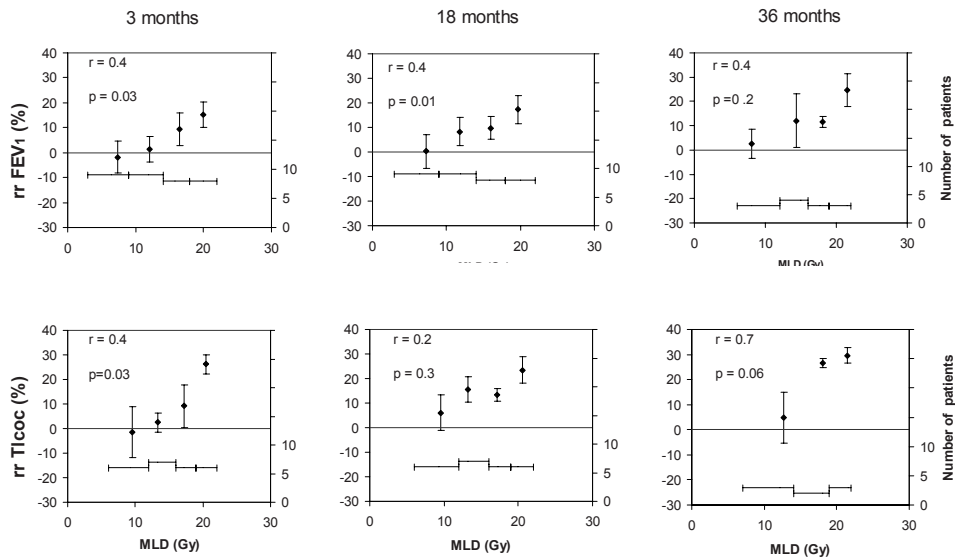


Figure 4. Correlation of the relative reduction (rr) of FEV₁ and Tlcoc and the mean lung dose (MLD) at 3, 18 and 36 months following irradiation. Positive values indicate an impairment of pulmonary function. The correlation coefficient (r), and p-value are shown. The number of patients in each dose bin is indicated on the right vertical axis.

Discussion

Non-small cell lung cancer (NSCLC) patients referred for curative radiotherapy experienced a statistically significant decrease of their pulmonary function following irradiation. The decrease observed 3 months following irradiation was additional to a relative poor pulmonary function. Our data showed that the pulmonary function did not recover in patients with a long-term disease free survival. This long-term information is extremely important for inoperable NSCLC patients, especially for

patients with a poor pulmonary function. In the long-term study of Miller *et al.* [7], a significant progressive decrease was reported for 7 patients with a follow-up of 3 to 8 years. This decrease was observed after a partial recovery, or plateau, by 12 months. We did not observe this phenomenon in our larger patient group.

We observed a significant decrease of the FEV₁ and Tlcoc at 18 and 36 months in patients with higher pre-RT FEV₁ which was also observed by Choi *et al.* [26]. They observed a significant decrease at 12 months following irradiation in patients with a pre-RT FEV₁ value > 50 %. We did not observe a significant difference between the decreases of the FEV₁ for the two pre-RT FEV₁ subgroups as was observed by Gopal *et al.* [27]. They observed a significant difference between the FEV₁ decrease of 9.9 % for patients with a pre-RT FEV₁ ≥ 50 % and the increase of 8.4 % for patients with a pre-RT FEV₁ ≤ 50 %. Both the studies of Choi *et al.* and Gopal *et al.* used a pre-RT FEV₁ of 50 % as cut off value which was not feasible in our study because the low number of patients with a FEV₁ < 50 %. In our study, 10 of the 15 COPD patients were in the lower pre-RT FEV₁ group. These 10 patients might be responsible for observing no significant difference between the pre-RT FEV₁ groups.

COPD is a common co-morbidity in NSCLC patients. COPD is a progressive disease characterized by obstructive pulmonary function. Chronic inflammation, oxidative stress and an imbalance of proteinases and antiproteinases are present throughout the airway, parenchyma, and pulmonary vessels. The significant lower baseline FEV₁ in COPD patients is the consequence of the airflow limitation characteristic for COPD. The significant larger decrease of the FEV₁ at 36 months could be due to the progression of COPD. However, the larger decrease of FEV₁ and Tlcoc in COPD patients at 3 months may not (because of the small time interval) be due to COPD alone. Only a very few studies evaluated the influence of COPD on pulmonary function after treatment in lung cancer patients. Maas *et al.* [28] did not observe a different PFT outcome for COPD patients compared to non-COPD patients after three cycles of gemcitabine and cisplatin in NSCLC patients. This suggests that COPD did not have an influence on PFTs following this particular chemotherapy. The pathogenesis of COPD might reinforce the damage caused by irradiation. Radiation injury, responsible for an early inflammatory and a late fibrotic response in normal lung tissue might be more pronounced in patients suffering from COPD. It could explain both, the significant correlation between COPD and radiation pneumonitis in the study of Rancati *et al.* [29] and the initial large decrease in FEV₁ and Tlcoc already 3 months following irradiation, observed in our study.

We observed that patients receiving a high MLD, experienced a decrease of the FEV₁ and Tlcoc in the order of 1 % per Gy MLD at all follow-up periods. A similar relation was found for the Tlcoc by Theuws *et al.* [30] for 81 lymphoma and breast cancer patients. They observed a Tlcoc reduction at 3 months (1.1 % per Gy MLD) that remained unchanged at 18 months (0.9 % per Gy MLD). The decrease of the

Long-term pulmonary function changes after RT in NSCLC patients

volume parameters (FEV₁, VA and FVC) at 3 months (0.8 – 0.9 % per Gy MLD) improved significantly at 18 months (0.3 – 0.4 % per Gy MLD) for these lymphoma and breast cancer patients. We did not observe a recovery for any of the parameters for our lung cancer patients at 18 or 36 months.

The NSCLC patients experienced a significant decrease of the pulmonary function following irradiation. The decrease was observed in the acute phase following irradiation and did not recover after a longer follow-up. Dose-escalation and chemoradiation trials show promising results with better tumor control for inoperable NSCLC patients. For these patients, a sufficient respiratory outcome is important to ensure a satisfying quality of life. The respiratory condition of inoperable NSCLC patients should be optimized before and after radiotherapy and more consideration is required for patients with pulmonary comorbidities like COPD.

Conclusion

A significant decrease of the pulmonary function was observed 3 months following irradiation. There was no recovery at 18 and 36 months after radiotherapy. The decrease in pulmonary function was dependent on the mean lung dose and patients with pre-existing lung disease (COPD) had larger reductions in PFTs.

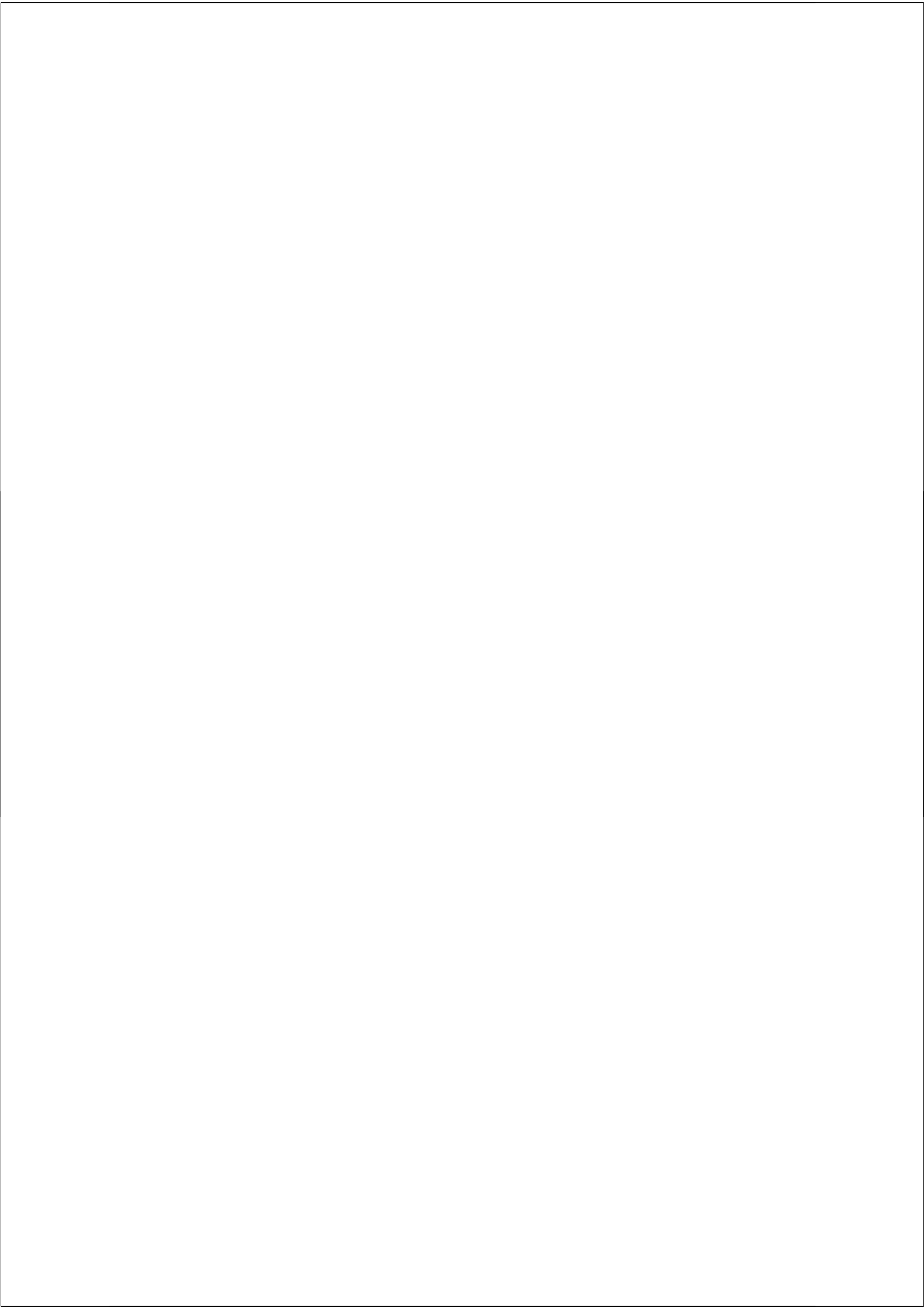
Chapter 5

Reference

1. Ferlay J, Bray F, Pisani P et al: Globocan 2000 Cancer Incidence, Mortality and Prevalence Worldwide. *International Agency for Research on Cancer, World Health Organization*. 2001.
2. Spira A, Ettinger DS: Multidisciplinary management of lung cancer. *N Engl J Med*. 2004;350:379-392.
3. Armstrong J, Raben A, Zelefsky M et al: Promising survival with three-dimensional conformal radiation therapy for non-small cell lung cancer. *Radiother Oncol*. 1997;44:17-22.
4. Graham MV, Purdy JA, Emami B et al: Clinical dose-volume histogram analysis for pneumonitis after 3D treatment for non-small cell lung cancer (NSCLC). *Int J Radiat Oncol Biol Phys*. 1999;45:323-329.
5. Kwa SL, Lebesque JV, Theuws JC et al: Radiation pneumonitis as a function of mean lung dose: an analysis of pooled data of 540 patients. *Int J Radiat Oncol Biol Phys*. 1998;42:1-9.
6. Marks LB, Munley MT, Bentel GC et al: Physical and biological predictors of changes in whole-lung function following thoracic irradiation. *Int J Radiat Oncol Biol Phys*. 1997;39:563-570.
7. Miller KL, Zhou SM, Barrier RC, Jr. et al: Long-term changes in pulmonary function tests after definitive radiotherapy for lung cancer. *Int J Radiat Oncol Biol Phys*. 2003;56:611-615.
8. Theuws JC, Muller SH, Seppenwoolde Y et al: Effect of radiotherapy and chemotherapy on pulmonary function after treatment for breast cancer and lymphoma: A follow-up study. *J Clin Oncol*. 1999;17:3091-3100.
9. Punjabi NM, Shade D, Patel AM et al: Measurement variability in single-breath diffusing capacity of the lung. *Chest*. 2003;123:1082-1089.
10. Belderbos JS, De Jaeger K, Heemsbergen WD et al: First results of a phase I/II dose escalation trial in non-small cell lung cancer using three-dimensional conformal radiotherapy. *Radiother Oncol*. 2003;66:119-126.
11. Hayman JA, Martel MK, Ten Haken RK et al: Dose escalation in non-small-cell lung cancer using three-dimensional conformal radiation therapy: update of a phase I trial. *J Clin Oncol*. 2001;19:127-136.
12. Wu KL, Jiang GL, Liao Y et al: Three-dimensional conformal radiation therapy for non-small-cell lung cancer: a phase I/II dose escalation clinical trial. *Int J Radiat Oncol Biol Phys*. 2003;57:1336-1344.
13. Narayan S, Henning GT, Ten Haken RK et al: Results following treatment to doses of 92.4 or 102.9 Gy on a phase I dose escalation study for non-small cell lung cancer. *Lung Cancer*. 2004;44:79-88.
14. Chen Y, Okunieff P: Radiation and third-generation chemotherapy. *Hematol Oncol Clin North Am*. 2004;18:55-80.
15. Cohen EE, Vokes EE: Induction chemotherapy and radiotherapy in locally advanced non-small cell lung cancer. *Hematol Oncol Clin North Am*. 2004;18:81-90.
16. Curran WJ, Scott CB, Langer CJ et al: Long-term benefit is observed in a phase III

Long-term pulmonary function changes after RT in NSCLC patients

- comparison of sequential vs concurrent chemo-radiation for patients with unresected stage III nscl: RTOG 9410. *Proc Am Soc Clin Oncol.* 2003; 22: 621.
17. Dhital K, Saunders CA, Seed PT et al: [(18)F]Fluorodeoxyglucose positron emission tomography and its prognostic value in lung cancer. *Eur J Cardiothorac Surg.* 2000;18:425-428.
 18. Dillman RO, Seagren SL, Propert KJ et al: A randomized trial of induction chemotherapy plus high-dose radiation versus radiation alone in stage III non-small-cell lung cancer. *N Engl J Med.* 1990;323:940-945.
 19. Global Initiative for Chronic Obstructive Lung Disease (GOLD). Global Strategy for the Diagnosis, Management, and Prevention of Chronic Obstructive Pulmonary Disease. Executive Summary updated 2004. www.goldcopd.com. 143. 2004.
 20. Quanjer PH, Andersen LH, Tammeling GJ: Clinical respiratory physiology. *Bull Eur Physiopathol Respir.* 1983;19:11-21.
 21. Boersma LJ, Damen EM, de Boer RW et al: Dose-effect relations for local functional and structural changes of the lung after irradiation for malignant lymphoma. *Radiother Oncol.* 1994;32:201-209.
 22. Lebesque JV, Keus RB: The simultaneous boost technique: the concept of relative normalized total dose. *Radiother Oncol.* 1991;22:45-55.
 23. Van Dyk J, Mah K, Keane TJ: Radiation-induced lung damage: dose-time-fractionation considerations. *Radiother Oncol.* 1989;14:55-69.
 24. De Jaeger K, Seppenwoolde Y, Boersma LJ et al: Pulmonary function following high-dose radiotherapy of non-small-cell lung cancer. *Int J Radiat Oncol Biol Phys.* 2003;55:1331-1340.
 25. American Thoracic Society, Committee on Proficiency Standards for Clinical Pulmonary Laboratories: Single-breath Carbon Monoxide Diffusing Capacity (Transfer Factor) Recommendations for a Standard Technique- 1995 Update. *Am J Respir Crit Care Med.* 1995;Vol 152:2185-2198.
 26. Choi NC, Kanarek DJ: Toxicity of thoracic radiotherapy on pulmonary function in lung cancer. *Lung Cancer.* 1994;10 Suppl 1:S219-S230.
 27. Gopal R, Starkschall G, Tucker SL et al: Effects of radiotherapy and chemotherapy on lung function in patients with non-small-cell lung cancer. *Int J Radiat Oncol Biol Phys.* 2003;56:114-120.
 28. Maas KW, van der Lee I, Bolt K et al: Lung function changes and pulmonary complications in patients with stage III non-small cell lung cancer treated with gemcitabine/ cisplatin as part of combined modality treatment. *Lung Cancer.* 2003;41:345-351.
 29. Rancati T, Ceresoli GL, Gagliardi G et al: Factors predicting radiation pneumonitis in lung cancer patients: a retrospective study. *Radiother Oncol.* 2003;67:275-283.
 30. Theuws JC, Kwa SL, Wagenaar AC et al: Prediction of overall pulmonary function loss in relation to the 3-D dose distribution for patients with breast cancer and malignant lymphoma. *Radiother Oncol.* 1998;49:233-243.



Radiation Pneumonitis after Hypofractionated Radiotherapy: Evaluation of the LQ(L) model and different dose parameters

Gerben R. Borst M.D.¹, Masayori Ishikawa Ph.D.², Jasper Nijkamp M.Sc.¹, Michael Hauptmann Ph.D.³, Hiroki Shirato M.D. Ph.D.², Gerard Bengua Ph.D.b, Rikiya Onimaru M.D.², Josien A. de Bois R.T.T.¹, Joos V. Lebesque M.D. Ph.D.¹, Jan-Jakob Sonke Ph.D.¹

¹*Department of Radiation Oncology, ²Department of Bioinformatics and Statistics, The Netherlands Cancer Institute - Antoni van Leeuwenhoek Hospital, Amsterdam, The Netherlands.*

³*Department of Radiology, Hokkaido University School of Medicine, Sapporo, Japan*

**Accepted for publication in the
International Journal of Radiation Oncology**Biology**Physics,**

Abstract

Purpose: To evaluate the Linear Quadratic (LQ) model for hypofractionated radiotherapy (RT) within the context of predicting radiation pneumonitis (RP) and to investigate the effect if a linear model in the high region (LQL model) is used.

Methods and Materials: The radiation dose of 128 patients treated with hypofractionated RT was converted to the equivalent dose given in fractions of 2Gy for a range of α/β ratios (1Gy to infinity) according to the LQ(L) model. For the LQL model different cut off values between the LQ model and the linear component were used. The Lyman model parameters were fitted to the events of RP grade 2 or higher to derive the Normal Tissue Complication Probability (NTCP). The lung dose was calculated as the mean lung dose (MLD) and as percentages of lung volume receiving doses higher than a threshold dose xGy (V_x)

Results: The best NTCP fit was found if the MLD or V_x was calculated with an α/β ratio of 3 Gy. The NTCP fits of other α/β ratios and the LQL model were worse but within the 95%CI of the NTCP fit of the LQ model with an α/β ratio of 3 Gy. The V_{50} NTCP fit was better compared to the NTCP fit of lower threshold doses.

Conclusion: For high fraction doses, the LQ model with an α/β ratio of 3 Gy was the best method for converting the physical lung dose to predict RP.

Introduction

An increasing number of radiotherapy departments implement hypofractionated radiotherapy (RT) regimens for pulmonary malignant lesions, encouraged by reports of good tumor control and little toxicity. Consequently, clinical questions concerning the normal tissue tolerance dose, the possibility to include multiple targets or to irradiate larger lung volumes (e.g. applying multiple treatments or irradiation of larger tumors) are important.

For conventional fractionated radiotherapy the physical dose can be converted into a biological equivalent dose using the linear quadratic (LQ) model[1,2]. Historically, the strength of the LQ model for conventional fraction doses is twofold. First, it is a simple mathematical model fitting log cell survival data as function of the dose. Secondly, this model enables iso-effect calculations of fractionation schemes with different doses per fraction. However, already in 1954 Puck et al. observed that for the high dose regions the log cell survival was linear[3]. As a result, some modifications have been derived from NSCLC cell lines[4] and other tumor cell lines and animal iso-effect data[5]. In general, a non-linear part (LQ) in the low dose region and a linear (L) part for the high dose region differentiated by a transition dose (d_T) was proposed (i.e. LQL model)[6]. Since clinical data is lacking, the clinical iso-effect calculations by the LQ model at higher fraction doses remains uncertain as was comprehensively discussed previously[7-11]. Using the LQ model with an α/β ratio of 3Gy, it was observed that the normal tissue complication probability (NTCP) model predicting radiation pneumonitis (RP) after hypofractionated RT was not different compared to the NTCP model after conventional fractionated RT[12]. For conventional fractionated RT, the relation between lung dose and radiation pneumonitis (RP) is extensively evaluated (e.g.[13]). RP is a serious complication after irradiation, and also after hypofractionated schemes fatal RP toxicities are observed[14].

To evaluate the applicability of the LQ(L) model and normal tissue complication models for higher dose per fraction, we evaluated the prediction of RP after hypofractionated RT. Different α/β ratios and different d_T values of the LQ(L) models were analyzed modeling the probability of RP after hypofractionated RT as function of the dose.

Material & Methods

Patients

Patients and treatment schedules were comprehensively described elsewhere[12]. In summary, 128 patients irradiated with hypofractionated RT at the Department of Radiation Medicine of the Hokkaido University School of Medicine, Sapporo, Japan, with 35 Gy in 4 fractions, 40 Gy in 4 fractions, 48 Gy in 8 fractions, 60 Gy

Chapter 6

in 8 fractions and 48Gy in 4 fractions. Twenty patients had multiple targets in one treatment plan (18 patients had 2 targets, 2 patients had 3 targets). For 13 patients multiple treatment plans were made for different targets because of metastasis or recurrence (5 patients had 2 plans, 4 patients had 3 plans and 4 patients had 4 plans) (for time schedule, dose schedule and tolerated maximum dose for organs at risk see[12]).

Toxicity

Radiation pneumonitis (RP) was prospectively scored according to the NCI-CTC version 2, whereby grade 2 RP is scored after prescribing steroids for treatment related toxicity. Grade 3 RP is scored after requiring. None of the patients scored with RP grade 2 used steroids before. Radiation pneumonitis (RP) was prospectively scored according to the NCI-CTC version 2 whereby grade 2 RP is scored after prescribing steroids for treatment related toxicity, like progressive shortness of breath combined with typical RP changes on the X-thorax . Grade 3 RP is scored after requiring oxygen. None of the patients scored with RP grade 2 used steroids before radiotherapy. For all patients the diagnosis and grade of RP was determined by the radiation oncologist and a pulmonologist experienced in the diagnosis of RP. Patients whereby the diagnosis of RP was unlikely were not included (progressive cardiac problems, medical history of receiving oxygen before treatment, tumor progression).

Dose

Three dimensional (3-D) treatment plans were made using Focus (CMS, St Louis, MO), XiO (CMS) or Pinnacle. A convolution superposition algorithm for tissue density heterogeneity was used (plans initially planned with the Clarkson method were re-calculated). Normal lung tissue was defined in the CT scan by binary thresholding (thus excluding the gross tumor volume). Both lungs together were considered as one organ. Four to six non-coplanar beams were used. The beam energy was 4, 6 or 10MV. Plans were further analyzed with in-house developed software. The physical dose-distribution was converted into the Normalized Total Dose (NTD) distribution[15] using the linear quadratic (LQ) model. The NTD is defined as the equivalent total dose given in fractions of 2 Gy:

$$NTD = D \frac{d + \alpha/\beta}{2 + \alpha/\beta} \quad (1)$$

whereby the total dose (D) is the number of fractions multiplied by the dose per fraction (d).

The dose distributions were converted according to formula (1) for α/β ratios of 1Gy, 2 Gy, 3 Gy, 4 Gy, 5 Gy, 7.5 Gy, 10 Gy and infinity (i.e. physical dose) to evaluate the effect of different α/β ratios. After this conversion for the dose per fraction,

we determined different dose-volume parameters from the dose volume histograms (DVHs): the mean lung dose (MLD) and the lung volume percentage receiving doses higher than 5 Gy(V_5), 13 Gy(V_{13}), 20 Gy(V_{20}), 40 Gy(V_{40}) and 50 Gy(V_{50}) or in general higher than x Gy(V_x). For the 33 patients irradiated on multiple lesions, individual plans were summed after NTD corrections and image registration had been performed. Time-related recovery of lung tissue was not taken into account for multiple treatments.

The dose response relation between RP and MLD was modelled by a sigmoid shaped dose effect relation according to Lyman[16]. The normal tissue complication probability (NTCP) can be calculated from the MLD[17] according to

$$NTCP = \frac{1}{\sqrt{2\pi}} \int_{-\infty}^t e^{-\frac{x^2}{2}} dx \quad \text{with} \quad t = \frac{MLD - TD_{50}}{m \cdot TD_{50}} \quad (2)$$

whereby the TD_{50} represents the dose for a 50 % NTCP and m is the (inverse) steepness parameter in the standard formulation of the Lyman model. Similar for the V_x parameter, formula (2) was used with

$$t = \frac{V_x - V_{x50}}{m \cdot V_{x50}} \quad \text{whereby the } V_{x50} \text{ represents the } V_x \text{ for a 50 \% NTCP.}$$

Modification of the LQ model to the LQL model

We adapted the LQ model (LQL) by applying a two component model proposed by Park et al[4] (Figure 1). For the low dose range, the total dose is corrected according to the LQ model using equation (1)

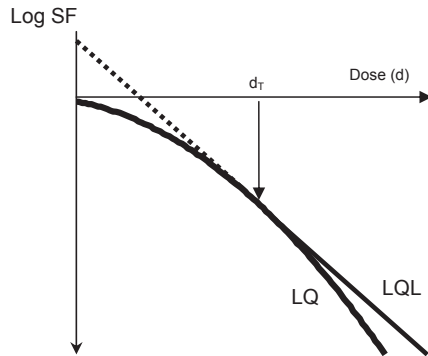


Figure 1. Schematic representation of the log survival curve as a function of the dose according to the LQL model. Below the transition dose (d_T) the curve is linear quadratic (the LQ model). Above d_T the log survival curve is linear whereby the slope is determined by the asymptote of the LQ model at dose d_T .

according to the best α/β ratio. For the high dose range, the log survival curve is assumed to be linear. The slope of the linear part is determined by the derivative of the LQ curve at the cut off value between the linear-quadratic part and the linear part (i.e. the transition dose d_T) (Figure 1 and Appendix) resulting in

$$NTD = D \frac{\alpha/\beta + 2d_T - \frac{d_T^2}{d}}{2 + \alpha/\beta} \quad (3)$$

In contrast to the literature, we propose to use the denotation of a lower case letter (d_T) because this transition dose refers the dose per fraction correction.

We converted the dose distributions for d_T values of 0 Gy, 5 Gy, 7 Gy and 9 Gy and subsequently calculated the MLD (not the V_x) from these dose distributions (i.e. MLD_{LQL}).

Statistics

The TD_{50} and m were estimated by maximizing the logarithm of the likelihood function [17]

$$\ln(L) = \ln\left(\prod_{i=1}^N L_i\right) = \sum_{i=1}^N \ln(L_i) = \sum_{i=1}^N [ep_i \ln(P_i) + (1 - ep_i) \ln(1 - P_i)] \quad (4)$$

where P_i ($i = 1, \dots, N$) represents the predicted NTCP and ep_i is the observed binary outcome ($0 = RP \leq$ grade 1, $1 = RP \geq$ grade 2) for patient i . The confidence intervals (CI) of the fitted parameters were calculated using the profile likelihood method[18]. These CI were calculated by finding the points in the parameter space where the $\ln(L)$ values are $\Delta \ln(L)$ lower than $\ln(L_{max})$ (e.g. for the 95%CI the value of $\Delta \ln(L)$ is 1.92 corresponding to half of the 95% percentile of the cumulative chi-square value for one degree of freedom).

In order to evaluate which α/β ratio would give the maximum likelihood estimation, a profile likelihood approach of the best NTCP fit was performed according to α/β ratios in the range of 1 Gy up to infinity. This analysis was only performed for the

MLD (i.e. the corrected mean lung dose (MLD_{LQ})).

Converting the dose according to the LQL model, we used an α/β ratio of 3 Gy. The LQ and the LQL model are nested since the 3-parameter (TD_{50} , m and d_T) MLD_{LQL} model reduces to the 2-parameter (TD_{50} , m) MLD_{LQ} model when d_T goes to infinity (or at least becomes higher than the highest dose per fraction value in the data set) (see Figure 1). According to the LQL model, the doses were converted with d_T values of 0, 5, 7 and 9 Gy. The NTCP model fit using the MLD_{LQL} was compared to the NTCP model fit with the MLD_{LQ} using the maximum likelihood ratio test since the 2 models were nested [19]. For this analysis this requires that twice the difference of

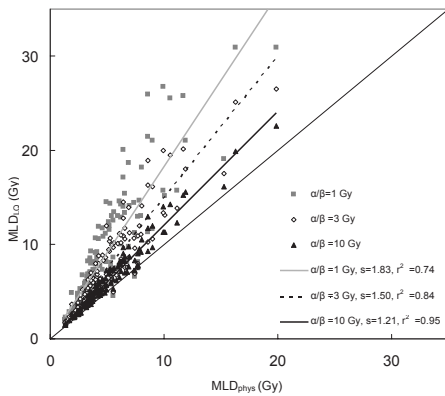


Figure 2. The MLD_{LQ} calculated according to the LQ model with α/β ratios of 1 Gy (grey squares), 3 Gy (open diamonds), 10 Gy (black triangles) plotted as function of the MLD_{phys} . The straight line with a slope 1 represents the equivalent line where MLD_{LQ} equals MLD_{phys} . The other lines represent the best fit through the data with a zero intercept (see legend in Figure); s represents the slope and r the regression coefficient.

the log likelihoods between the two models should be larger than the quantile of a chi-square distribution with one degree of freedom (i.e. 3.84/2) to be significantly different. For regression analysis, the slope of the linear regression (s) with a zero intercept was used to assess the relation between different parameters. A two-tailed $p < 0.05$ was considered to be statistically significant.

Results

The crude incidence of RP was 10.9% (14 events in the group of 128 patients). One patient was observed with grade 3 RP, all other patients were diagnosed with grade 2 RP.

MLD corrected for different α/β ratios

The relationships between the MLD calculated with an α/β ratio of infinity (MLD_{phys}) and of 1Gy(MLD_1), 3Gy(MLD_3) and 10Gy(MLD_{10}) are illustrated in Figure 2. The MLD_{LQ} calculated with a low α/β ratio is higher than the MLD_{LQ} calculated with a higher α/β ratio, as expected. A linear fit of the data (with zero intercept) resulted in the following relations and correlations; $MLD_1 = 1.83 \times MLD_{phys}$ ($r^2 = 0.74$), $MLD_3 = 1.50 \times MLD_{phys}$ ($r^2 = 0.84$) and $MLD_{10} = 1.21 \times MLD_{phys}$ ($r^2 = 0.95$), respectively. Two patients were located under the equality line. These two patients were also irradiated at a target in the mediastinum with a more fractionated scheme whereby the high dose region in the lung tissue received less than 2Gy.

To evaluate the effect of the dose per fraction, the MLD_1 and the MLD_3 were plotted as a function of the MLD_{phys} (Figure 3) for each dose per fraction separately for patients irradiated on one single target. Because only 3 patients received 35 Gy/4fr,

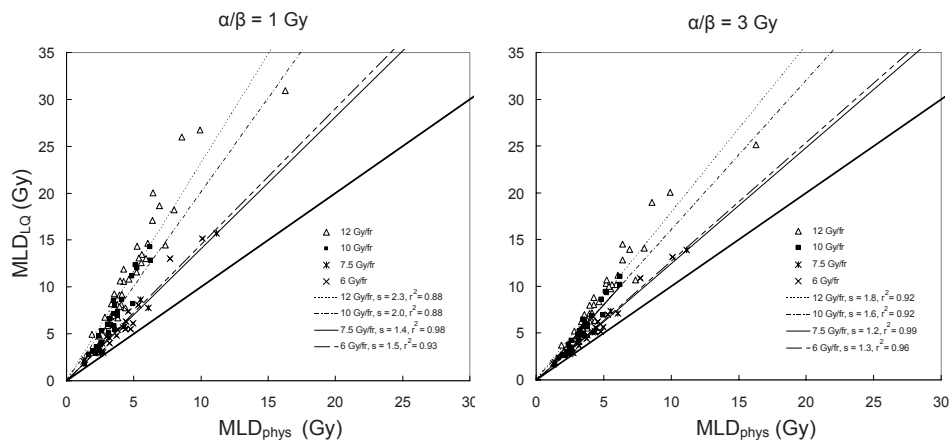


Figure 3. The MLD_1 and MLD_3 as a function of the MLD_{phys} plotted for different fractionation schemes (see legend Figure). The straight line with a slope 1 represents the equivalent line where MLD_{LQ} equals MLD_{phys} . The other lines represent the best fit through the data with a zero intercept (see legend in Figure); s represents the slope and r the regression coefficient.

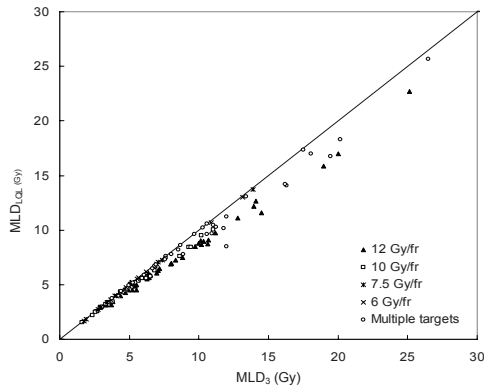


Figure 4. The MLD_{LQL} as a function of MLD_3 plotted for different fractionation schemes (see legend in Figure). The straight line with a slope 1 represents the equivalent line where MLD_{LQL} equals MLD_3 .

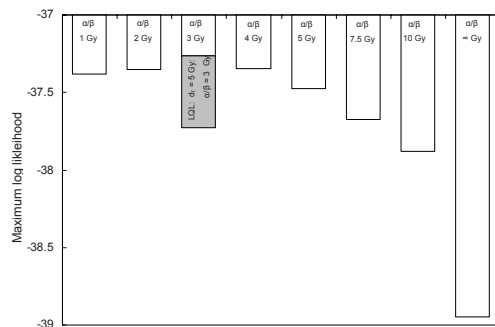


Figure 5. The maximum log likelihood of the NTCP fit for the MLD calculated for different α/β ratios. The maximum log likelihood of the NTCP fit based on the MLD calculated with the LQL model (with α/β ratio of 3 Gy and d_T of 5 Gy) is indicated next to the MLD_3 .

[12]¹). All other evaluated α/β ratios had lower maximum log likelihoods (Figure 5) but were within the 95%CI of the NTCP fit with an α/β ratio of 3Gy. The largest difference was found between the NTCP fit with an α/β ratio of 3 Gy and the NTCP fit with an α/β ratio of infinity (i.e. physical dose) (with $TD_{50}=14.6$ Gy and $m=0.48$) but this was not significant ($p=0.07$) (Figure 6).

Evaluating the NTCP model according to the LQL model with $d_T = 5$ Gy, the maximum log likelihood was lower than the MLD_3 NTCP LQ model fit. The LQL

¹These parameter values and the data points in Figure 6a are slightly different from the values and data points in reference [12] because of a dose recalculation error of one patient.

these patients were excluded. As expected, the slopes of the linear regression of the higher dose per fraction schedules (10 Gy and 12 Gy per fraction) were higher than for the lower dose per fraction schedules (6Gy and 7.5 Gy per fraction). In addition, the slope s for the $\alpha/\beta = 1$ Gy was higher than the s for the $\alpha/\beta = 3$ Gy for each dose per fraction. All correlations were significant with $p<0.001$.

The MLD calculated according to LQL model (MLD_{LQL}) with a d_T of 5 Gy is shown as a function of the MLD_3 in Figure 4. For patients with a high MLD_3 and irradiated with a high dose per fraction, larger differences between the MLD_3 and MLD_{LQL} were observed than for other patients (Figure 4).

NTCP for different α/β ratios and the LQL and V_x models

Optimizing the LQ NTCP model as a function of the m , TD_{50} and α/β ratio, revealed that the highest maximum log likelihood was found at an α/β ratio of 3Gy (with $TD_{50}=20.8$ Gy and $m=0.45$

NTCP fit parameters TD_{50} of 19.5Gy and $m=0.46$ were not significantly different from the LQ fit parameters ($p=0.28$). The NTCP model according to the LQL model with $d_T=7$ Gy and $d_T=9$ Gy was approaching the MLD_3 NTCP LQ model fit as expected, because only a limited part of the distribution of doses per fraction was larger than these d_T values. The NTCP according to the LQL model with $d_T=0$ Gy was as expected similar to the MLD_{phys} NTCP LQ model fit. For the V_x (calculated with the LQ model with an α/β ratio of 3Gy), the maximum likelihood profile approach revealed that the highest likelihood (i.e. best fit) is achieved with a threshold dose of 50Gy. The V_{50} calculated with the LQL model had lower log likelihoods (worse fits) although these differences were not significant ($p=0.16$ for $d_T=5$ Gy and $p=0.21$ for $d_T=7$ Gy). For all other V_x values similar results were observed (data not shown). The V_5 , V_{13} and V_{20} were outside the 95%CI of the V_{50} (Table 1). Because one patient had 0% of the lung volume receiving doses higher than 60Gy (corrected for an α/β ratio of 3Gy) we did not evaluate V_x values higher than 50Gy.

Table 1.

V_x	V_{x50} (%)	m	Maximum log likelihood
V_5	65.4 (49.0 - 121.0)	0.46 (0.34 - 0.66)	-39.40
V_{13}	39.2 (30.0 - 77.0)	0.48 (0.36 - 0.67)	-39.77
V_{20}	30.6 (23.0 - 57.0)	0.50 (0.37 - 0.68)	-39.63
V_{40}	15.9 (13.0 - 27.0)	0.48 (0.37 - 0.65)	-38.12
V_{50}	13.1 (11.0 - 21.0)	0.48 (0.37 - 0.65)	-37.04

The TD_{50} , V_{x50} and m optimized with the 95 % confidence intervals for the general parallel model (with optimized D_{50} (i.e. $D_{50} = \infty$ Gy) and k (i.e. $k = 1.3$)), MLD , V_5 , V_{13} , V_{20} and V_{40} . Maximum log likelihood and the p-value of the NTCP models compared to the reference model are given. Note that the upper bound of 95 % CI of the V_5 exceeds the 100% lung volume due to the approximation in the statistical method applied whereas in mathematical and clinical terms the upper limit is 100%.

Discussion

Our results showed that the NTD corrected MLD_{LQ} , calculated with an α/β ratio of 3Gy was the best parameter to fit the NTCP model to the observed incidence of RP after hypofractionated RT. These data suggest that a correction for the dose per fraction after hypofractionated radiotherapy should be performed similar to conventional fractionated schemes (i.e. LQ model and an α/β ratio of 3Gy (e.g. [20])). Other tested α/β ratios, or a modification of the LQ model (by introducing a linear relation after a threshold dose d_T of 5 Gy or higher) deteriorated the predictive value of the lung dose but were within the 95% CI of the NTCP LQ model fit with an α/β ratio of 3Gy. The not significant differences in the NTCP fits might be explained by the strong correlations between the corrected dose parameters.

Since the dose per fraction in hypofractionated RT is considerably larger than 2 Gy, a substantial volume of lung tissue received more than 2 Gy per fraction. Because

the MLD_{LQ} is expressed as 2 Gy equivalents, the MLD_{LQ} is therefore expected to be larger than the MLD_{phys} . Evaluating different α/β ratios resulted in different relations between the MLD_{LQ} and the MLD_{phys} . By nature of the LQ model, for lower α/β ratios and higher fraction doses the difference between the MLD_{LQ} and MLD_{phys} increased, and for higher α/β ratios the MLD_{LQ} approached the MLD_{phys} . Because of the strong correlation between the MLD_{LQ} and the MLD_{phys} it might be questioned whether the physical dose can be used to estimate complication probabilities. However, our results confirm that also after hypofractionation the physical dose should not be used for calculation of toxicity probabilities.

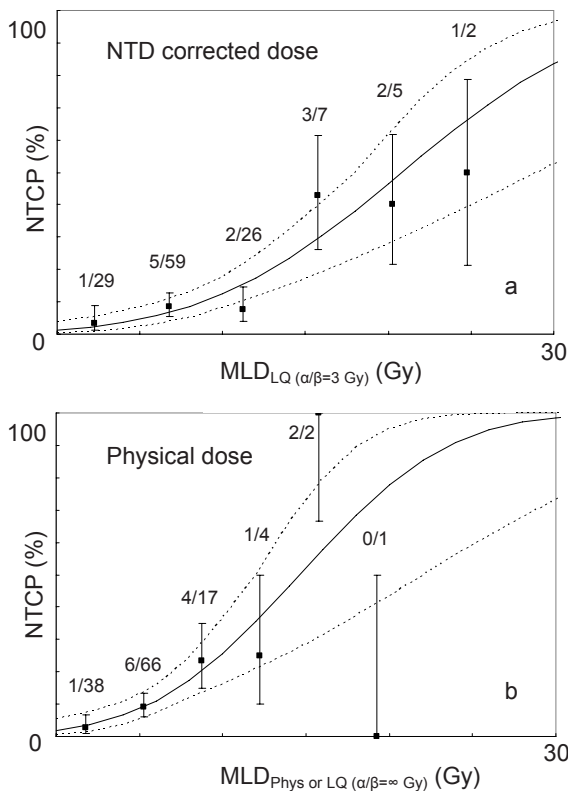


Figure 6. a: The NTCP fit (solid line) as function of the MLD calculated according to the LQ model and an α/β ratio of 3 Gy with the 68% CI (dotted lines) (TD50=20.8Gy, $m=0.45$). The number of events and number of patients are indicated. b: The NTCP fit (solid line) as function of the physical MLD (i.e. LQ model and an α/β ratio of infinity) with the 68% CI (dotted lines) (TD50=14.6Gy, $m=0.48$). The number of events and number of patients are indicated.

By calculating the MLD, the local dose in the lungs is weighted according to a linear local dose-effect relation. In contrast, for the V_x , the local dose-effect relation is considered as a binary effect whereby no damage is taken into account below the threshold dose of xGy and a full damage above the threshold dose of xGy. Different dose volume parameters and their mutual relations have not previously been evaluated for hypofractionated RT. Since the dose effect relation expressed by the MLD and V_x are based on different parameters (i.e. models are not nested), a direct comparison of the NTCP fits via a log likelihood ratio approach is not possible. Including these parameters (MLD, V_5 , V_{13} , V_{20} , and V_{40}) in a multivariate logistic regression analysis revealed that only the MLD was significantly associated

with RP (data not shown). However, these data should be interpreted with caution since it is known from studies with conventional fractionated RT evaluating clinical and dose factors predicting RP that there is a large heterogeneity of results[21-32] whereby no validation was performed. One collaborative study from the Duke University and the Netherlands Cancer Institute developed a prospective method to predict radiation pneumonitis from dose and clinical parameters in one group of patients but validation failed in another group of patients [33].

The validity of the LQ model for both clonogenic cell survival as clinical iso-dose calculations for higher dose per fraction was discussed previously; Hall and Brenner[11] estimated from the iso-effect data of van der Kogel[34] (late-responding damage to the rat spinal cord) and Douglas and Fowler[35] (acute damage to the mouse skin) that the LQ model would be valid for single doses up to 20Gy. According to this estimation, Fowler et al.[9] extrapolated the relation between RP and MLD, as determined for conventional treated patients, to hypofractionated schemes. Unfortunately, clinical data was lacking to validate such an extrapolation. Concerning RP (or other clinical toxicity endpoints), it might be questioned whether the applicability of the LQ model for these fraction doses can be answered by clinical studies. For example, the high number of (non-coplanar) beams results in an irradiation dose to healthy (lung) tissue that will be much smaller than the maximum dose. In addition, the relative volume of healthy tissue receiving such a high dose is limited by current advanced radiotherapy techniques (e.g. IMRT and IGRT). Moreover, the purpose of these techniques is to avoid high doses in normal tissues.

Guerrero et al[5] developed a modification of the LQ model by extending the LQ model with a protraction factor, based on the Lethal-Potentially Lethal (LPL) model which is supposed to be superior describing log cell survival data in the higher dose region[36]. This modification was based on cell survival and animal toxicity data. They observed a wide range of dose values where the LQ started to deviate from the LPL model (cell lines 0.6 Gy to 37.7 Gy, animal toxicity data 2.6 Gy to 100 Gy). It was shown that this modification results in a LQ model with a linear extension of the log cell survival as function of the dose for the high dose range by Carlone et al[6] and they proposed to name this model the linear-quadratic-linear (LQL) model. Elaborating this discussion in the clinical setting, we evaluated the LQL model with clinical data using a more simple but similar method proposed by Park et al[4] using a linear extension of the log cell survival as function of the dose for doses higher than a threshold (i.e. transition dose d_T). For a d_T of 5 Gy we observed a (non-significant) worse NTCP fit. For higher d_T values the LQL NTCP fit approached to the LQ NTCP fit; the differences between the MLD_{LQL} and MLD_{LQ} are becoming smaller because less lung tissue dose will be recalculated according to the linear part of the LQL model (dose larger than the d_T). Lastly, if the d_T is larger than the largest fraction

doses the MLD_{LQL} equals the MLD_{LQ} . Another mathematical model to describe the cellular response as function of the irradiation dose is the Linear Quadratic Cubic (LQC)[37] model whereby the cubic term is negative. This LQC model has also a (more) linear response in the high dose region approximating the LPL model. As the LQL model, the LQC model is mathematically more simple compared to the LPL model with only one additional parameter (as in the LQL model).

At the NKI (and many other institutes) the hypofractionated schedule that is mainly given is 3 x 18 Gy. Unfortunately, the patients treated at the NKI could not be included in the current analysis. The first reason for this is the limited follow up of a substantial part of these patients. Secondly, the patients with sufficient follow up (>1 year) had only lung doses in the lower MLD range resulting in low incidences of RP. Consequently, these patients cannot be of additional value for this type of analysis. However, the relation between the MLD_{LQL} as a function of the MLD_{LQ} for higher transition doses than used in current analysis could be evaluated. As illustrated in Figure 7, only a d_T of about 10 Gy or lower results in a difference between the MLD_{LQL} and the MLD_{LQ} . Introduction of a higher d_T would lead to imperceptible differences between the MLD_{LQ} and MLD_{LQL} . Consequently, it might be questioned whether a higher d_T can be clinically evaluated with respect to RP in the future due to limited amount of lung tissue receiving high doses. Irradiation of healthy lung tissue of animals with increasing fraction sizes, which could be possible in the future with advances in preclinical irradiation techniques, might facilitate resolving this issue.

We evaluated the LQL model, using an α/β ratio of 3 Gy which did not improve the NTCP fit to the data. Although the slope of the linear component is dependent of both the d_T and the α/β ratio, we did not analyse the LQL model with other α/β values. The first reason for this is that evaluations of the LQL model with α/β ratios close to 3Gy would not affect the NTCP fit significantly according to current data. Secondly, for (much) higher α/β values the LQL model approaches the LQ model (for α/β equal to infinity the LQL and LQ model both are becoming the L (linear) model). Thirdly, for lung tissue an α/β value of 3-4 Gy is an accepted value converting doses in the lower dose range[38-42].

Predictive models based on clinical data are as good as the clinical data. Consequently, the limitations of this study should be stressed. We discussed the clinical limitations of our study comprehensible previously[12]. First, the study was a retrospective univariate analysis evaluating RP grade \geq 2. Secondly, although the assessment of RP was carefully performed, the prescription of steroids and oxygen is relying on the intention to treat of the physician. Thirdly, only one grade 3 RP was scored and the duration of the RP grade 2 treatment was not registered. Therefore, no dose response analysis could be performed regarding the severity of the radiation induced toxicity. Another discussion point is whether the time interval between the subsequent

treatments should be taken into account. As discussed previously[12], we did not consider any repair between the treatments. A mouse study suggested that for higher doses per fraction less recovery might be expected[43]. Moreover, limited clinical data showed that patients are experiencing a high probability of RP after re-irradiation[44].

Besides the reliability of NTCP modeling on the robustness of the clinical data, some assumptions have to be made for (NTCP) modeling in general. First, a NTCP model based on one (dose) characteristic disregard all other factors influencing the probability to develop toxicity (e.g. genetic variability and/or comorbidity) for one individual patient. Secondly, to evaluate clinically applicable dose parameters, DVHs are reduced to simple parameters (e.g. MLD and V_x) whereby a (biological) background is assumed but questionable. Thirdly, the limited number of patients included in the current study might have caused that a real intrinsic difference between these parameters was not apparent with statistical significance.

In conclusion, with our study we provide clinical toxicity data for the discussion of the applicability of current radiobiological models for higher doses per fraction. We observed that the LQ model was valid (with an α/β ratio of 3 Gy for lung tissue) to recalculate the physical dose into biological equivalent dose and that the biological dose should be used for estimating toxicity probabilities. The LQL model did not improve the prediction of RP. This might be due to the limitations of our study and/or to (still) unknown fundamental mechanisms complicating the translation of mathematical models developed with cell survival data into clinical data. With currently used fraction doses of up to 18 Gy, substantially different results are not expected, but this should be confirmed in future evaluations.

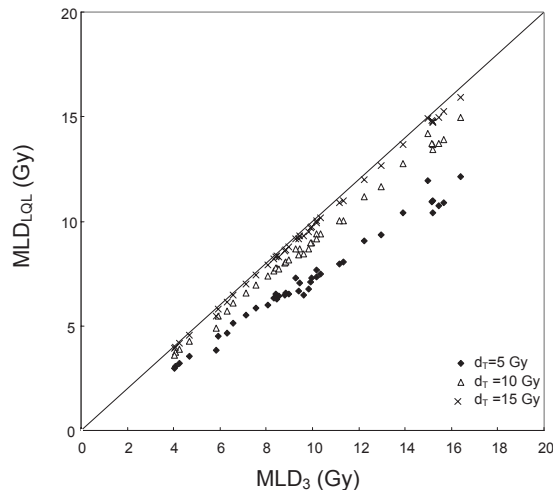


Figure 7. For patients treated at the NKI-AVL the MLD_{LQL} is plotted as a function of MLD_3 for d_T of 5 Gy (closed diamonds), d_T of 10 Gy (open triangles) and d_T of 15 Gy (crosses). The straight line with a slope 1 represents the equivalent line where MLD_{LQL} equals MLD_3 .

Chapter 6

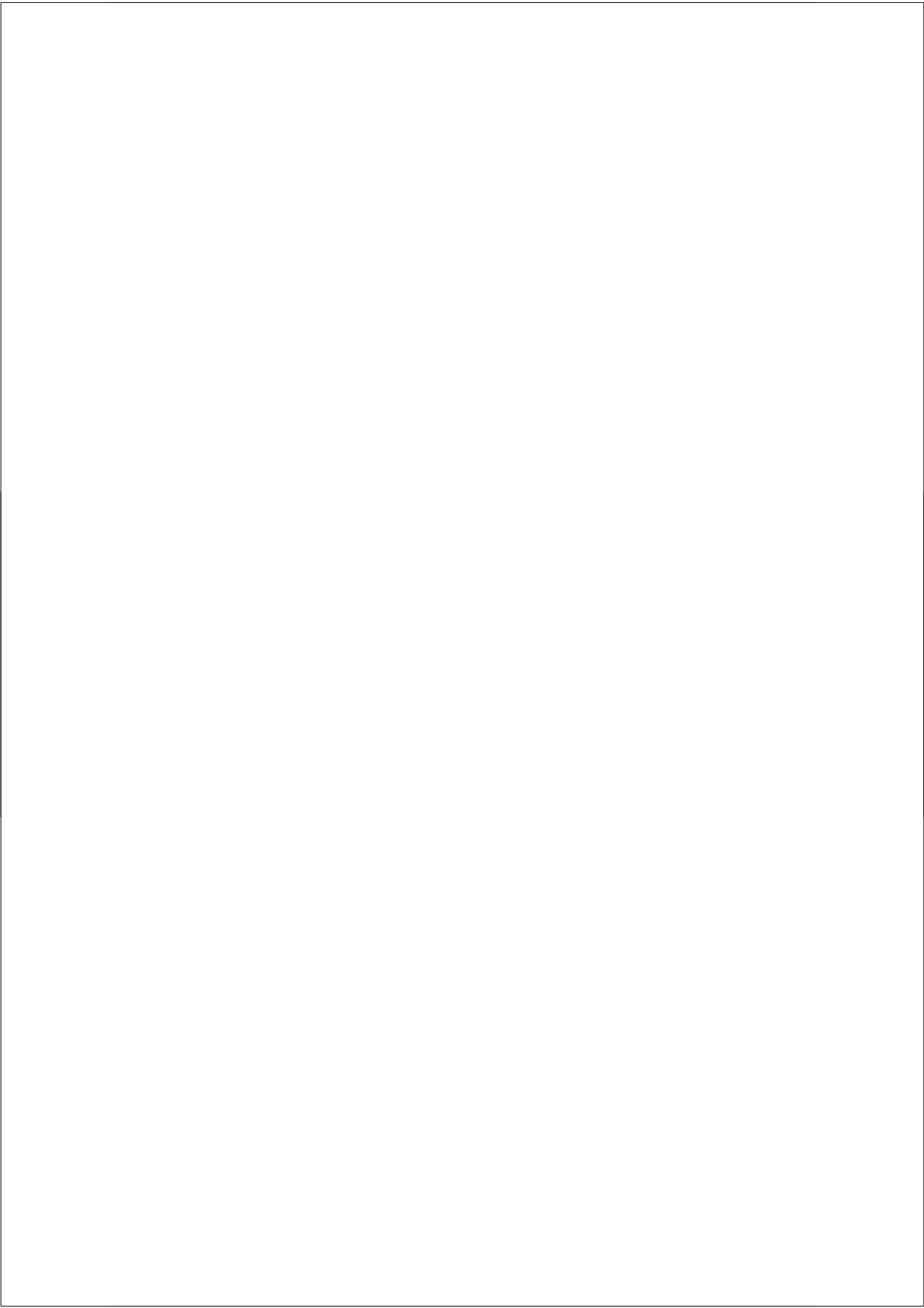
References

1. Fowler JF. The first James Kirk memorial lecture. What next in fractionated radiotherapy? *Br J Cancer Suppl* 1984;6:285-300.
2. Tucker SL. Tests for the fit of the linear-quadratic model to radiation isoeffect data. *Int J Radiat Oncol Biol Phys* 1984;10:1933-1939.
3. Puck T, Marcus P. Action of x-rays on mammalian cells. *J Exp Med* 1956;103:653-666.
4. Park C, Papiez L, Zhang S et al. Universal survival curve and single fraction equivalent dose: useful tools in understanding potency of ablative radiotherapy. *Int J Radiat Oncol Biol Phys* 2008;70:847-852.
5. Guerrero M, Li XA. Extending the linear-quadratic model for large fraction doses pertinent to stereotactic radiotherapy. *Phys Med Biol* 2004;49:4825-4835.
6. Carlone M, Wilkins D, Raaphorst P. The modified linear-quadratic model of Guerrero and Li can be derived from a mechanistic basis and exhibits linear-quadratic-linear behaviour. *Phys Med Biol* 2005;50:L9-13.
7. Barendsen GW. Dose fractionation, dose rate and iso-effect relationships for normal tissue responses. *Int J Radiat Oncol Biol Phys* 1982;8:1981-1997.
8. Denekamp J, Waites T, Fowler JF. Predicting realistic RBE values for clinically relevant radiotherapy schedules. *Int J Radiat Biol* 1997;71:681-694.
9. Fowler JF, Tome WA, Fenwick JD et al. A challenge to traditional radiation oncology. *Int J Radiat Oncol Biol Phys* 2004;60:1241-1256.
10. Hall EJ, Brenner DJ. The radiobiology of radiosurgery: rationale for different treatment regimes for AVMs and malignancies. *Int J Radiat Oncol Biol Phys* 1993;25:381-385.
11. Marks LB. Extrapolating hypofractionated radiation schemes from radiosurgery data: regarding Hall et al., *IJROBP* 21:819-824; 1991 and Hall and Brenner, *IJROBP* 25:381-385; 1993. *Int J Radiat Oncol Biol Phys* 1995;32:274-276.
12. Borst GR, Ishikawa M, Nijkamp J et al. Radiation pneumonitis in patients treated for malignant pulmonary lesions with hypofractionated radiation therapy. *Radiother Oncol* 2009;91:307-313.
13. Semenenko VA, Li XA. Lyman-Kutcher-Burman NTCP model parameters for radiation pneumonitis and xerostomia based on combined analysis of published clinical data. *Phys Med Biol* 2008;53:737-755.
14. Yamashita H, Nakagawa K, Nakamura N et al. Exceptionally high incidence of symptomatic grade 2-5 radiation pneumonitis after stereotactic radiation therapy for lung tumors. *Radiat Oncol* 2007;2:1-11.
15. Lebesque JV, Keus RB. The simultaneous boost technique: the concept of relative normalized total dose. *Radiother Oncol* 1991;22:45-55.
16. Lyman JT. Complication probability as assessed from dose-volume histograms. *Radiat Res Suppl* 1985;8:S13-S19.
17. Seppenwoolde Y, Lebesque JV, De Jaeger K et al. Comparing different NTCP models that predict the incidence of radiation pneumonitis. Normal tissue complication probability. *Int J Radiat Oncol Biol Phys* 2003;55:724-735.
18. D.J.Venzon, S.H.Moolgavkar. A Method for Computing Profile-Likelihood-Based Confidence Intervals. *Applied Statistics* 1988;37:87-94.

19. Clayton D, Hills M. *Statistical Models in Epidemiology*. Oxford University Press. New York.; 1993.
20. Kwa SL, Theuws JC, Wagenaar A et al. Evaluation of two dose-volume histogram reduction models for the prediction of radiation pneumonitis. *Radiother Oncol* 1998;48:61-69.
21. Claude L, Perol D, Ginestet C et al. A prospective study on radiation pneumonitis following conformal radiation therapy in non-small-cell lung cancer: clinical and dosimetric factors analysis. *Radiother Oncol* 2004;71:175-181.
22. Fujino M, Shirato H, Onishi H et al. Characteristics of patients who developed radiation pneumonitis requiring steroid therapy after stereotactic irradiation for lung tumors. *Cancer J* 2006;12:41-46.
23. Hernando ML, Marks LB, Bentel GC et al. Radiation-induced pulmonary toxicity: a dose-volume histogram analysis in 201 patients with lung cancer. *Int J Radiat Oncol Biol Phys* 2001;51:650-659.
24. Inoue A, Kunitoh H, Sekine I et al. Radiation pneumonitis in lung cancer patients: a retrospective study of risk factors and the long-term prognosis. *Int J Radiat Oncol Biol Phys* 2001;49:649-655.
25. Kim TH, Cho KH, Pyo HR et al. Dose-volumetric parameters for predicting severe radiation pneumonitis after three-dimensional conformal radiation therapy for lung cancer. *Radiology* 2005;235:208-215.
26. Moreno M, Aristu J, Ramos LI et al. Predictive factors for radiation-induced pulmonary toxicity after three-dimensional conformal chemoradiation in locally advanced non-small-cell lung cancer. *Clin Transl Oncol* 2007;9:596-602.
27. Oh D, Ahn YC, Park HC et al. Prediction of radiation pneumonitis following high-dose thoracic radiation therapy by 3 Gy/fraction for non-small cell lung cancer: analysis of clinical and dosimetric factors. *Jpn J Clin Oncol* 2009;39:151-157.
28. Rancati T, Ceresoli GL, Gagliardi G et al. Factors predicting radiation pneumonitis in lung cancer patients: a retrospective study. *Radiother Oncol* 2003;67:275-283.
29. Rodrigues G, Lock M, D'Souza D et al. Prediction of radiation pneumonitis by dose - volume histogram parameters in lung cancer--a systematic review. *Radiother Oncol* 2004;71:127-138.
30. Schallenkamp JM, Miller RC, Brinkmann DH et al. Incidence of radiation pneumonitis after thoracic irradiation: Dose-volume correlates. *Int J Radiat Oncol Biol Phys* 2007;67:410-416.
31. Tucker SL, Liu HH, Liao Z et al. Analysis of radiation pneumonitis risk using a generalized Lyman model. *Int J Radiat Oncol Biol Phys* 2008;72:568-574.
32. Willner J, Jost A, Baier K et al. A little to a lot or a lot to a little? An analysis of pneumonitis risk from dose-volume histogram parameters of the lung in patients with lung cancer treated with 3-D conformal radiotherapy. *Strahlenther Onkol* 2003;179:548-556.
33. Kocak Z, Borst GR, Zeng J et al. Prospective assessment of dosimetric/physiologic-based models for predicting radiation pneumonitis. *Int J Radiat Oncol Biol Phys* 2007;67:178-186.

Chapter 6

34. van der Kogel AJ. Chronic effects of neutrons and charged particles on spinal cord, lung, and rectum. *Radiat Res Suppl* 1985;8:S208-S216.
35. Douglas BG, Fowler JF. The effect of multiple small doses of x rays on skin reactions in the mouse and a basic interpretation. *Radiat Res* 1976;66:401-426.
36. Curtis SB. Lethal and potentially lethal lesions induced by radiation--a unified repair model. *Radiat Res* 1986;106:252-270.
37. Joiner MC. Quantifying cell kill and cell survival. In: van der Kogel AJ, Joiner MC, editors. *Basic Clinical Radiobiology*. 4 ed. Hodder Arnold; 2009. p. 42-55.
38. Fowler JF. The linear-quadratic formula and progress in fractionated radiotherapy. *Br J Radiol* 1989;62:679-694.
39. Kwa SL, Lebesque JV, Theuws JC et al. Radiation pneumonitis as a function of mean lung dose: an analysis of pooled data of 540 patients. *Int J Radiat Oncol Biol Phys* 1998;42:1-9.
40. Thames HD, Bentzen SM, Turesson I et al. Time-dose factors in radiotherapy: a review of the human data. *Radiother Oncol* 1990;19:219-235.
41. Van Dyk J, Mah K, Keane TJ. Radiation-induced lung damage: dose-time-fractionation considerations. *Radiother Oncol* 1989;14:55-69.
42. Bentzen SM, Joiner MC. The linear-quadratic approach in clinical practice. In: van der Kogel AJ, Joiner MC, editors. *Basic Clinical Radiobiology*. 4 ed. Hodder Arnold; 2009. p. 120-134.
43. Terry NH, Tucker SL, Travis EL. Residual radiation damage in murine lung assessed by pneumonitis. *Int J Radiat Oncol Biol Phys* 1988;14:929-938.
44. Okamoto Y, Murakami M, Yoden E et al. Reirradiation for locally recurrent lung cancer previously treated with radiation therapy. *Int J Radiat Oncol Biol Phys* 2002;52:390-396.



**Kilo-voltage cone beam CT setup measurements for
lung cancer patients; first clinical results and
comparison with electronic portal-imaging device**

Gerben R. Borst, M.D., Jan-Jakob Sonke, Ph.D., Anja Betgen, R.T.T., Peter Remeijer, Ph.D., Marcel van Herk, Ph.D., Joos V. Lebesque, M.D., Ph.D.

*Department of Radiation Oncology, The Netherlands Cancer Institute-Antoni van Leeuwenhoek
Hospital, Amsterdam, The Netherlands.*

**International Journal of Radiation Oncology*Biography*Physics,
Volume 68, Issue 2, 1 June 2007, Pages 555-561**

Abstract

Purpose: Kilovoltage cone-beam computed tomography (CBCT) has been developed to provide accurate soft-tissue and bony setup information. We evaluated clinical CBCT setup data and compared CBCT measurements with electronic portal imaging device (EPID) images.

Material and Methods: The setup error for CBCT scans at the treatment unit relative to the planning CT was measured for 62 patients (524 scans). For 19 of these patients (172 scans) also portal images were made. The mean, systematic setup error (Σ) and random setup error (σ) were calculated for the CBCT and the EPID. Also the differences between CBCT and EPID and the rotational setup error derived from the CBCT were evaluated.

An offline SAL correction protocol, based on the CBCT measurements, was used to reduce systematic setup errors and the impact of this protocol was evaluated.

Results: The CBCT setup errors were significantly larger than the EPID setup errors for the CC and AP directions ($p < 0.05$) due to discrepancy of the setup errors by the EPID relative to CBCT. The mean overall setup errors after correction measured with the CBCT were 0.2 mm ($\Sigma = 1.6$ mm, $\sigma = 2.9$ mm) in the left-right, -0.8 mm ($\Sigma = 1.7$ mm, $\sigma = 4.0$ mm) in cranial-caudal and 0.0 mm ($\Sigma = 1.5$ mm, $\sigma = 2.0$ mm) in the anterior-posterior direction. Using our correction protocol only two patients had mean setup errors larger than 5 mm, without this correction protocol more than 51 % of the patients would have had a setup error larger than 5 mm.

Conclusion: Three-dimensional kilovoltage CBCT scans provided more accurate information concerning the setup of lung cancer patients than was available with prior techniques.

Introduction

Correct target positioning is of major concern in the delivery of radiotherapy. However, the position of the target is subject to geometric uncertainties due to variability in patient positioning and internal organ motion [1]. Awareness of these uncertainties in the planning of radiotherapy is essential. Appropriate margins for an adequate coverage of the target volume have to be taken into account. 3D conformal planning techniques improve dose distributions by sharpening dose gradients between target volume and surrounding tissue. Consequently, increased prescription doses and improved sparing of normal tissue can be achieved. However, the steep dose gradient between tumor and critical structures makes 3D conformal techniques more sensitive to geometric uncertainties [2]. Consequently, accurate setup verification over the course of treatment is very important for an adequate treatment.

Erridge et al. [3] evaluated setup errors during treatment for lung cancer patients by electronic portal image device (EPID) measurements using an off-line correction protocol. Systematic setup errors (1σ) of 1.4, 1.5 and 1.3 mm were observed in the left-right, cranial-caudal and anterior-posterior directions, respectively. Similar data were found by de Boer et al. and Van Sornsens de Koste et al. [4,5]. The accuracy of the measurements of setup errors itself, could however not be evaluated, because a reference procedure (i.e. golden standard) was lacking.

Recently, kilovoltage (kV) conebeam CT scanners (CBCT) integrated with a linear accelerator (linac) became available in many institutions. The scanner is mounted on the gantry of a linac and provides detailed high resolution 3D information of the patient internal anatomy just prior to the treatment [6]. Consequently, the data from the kV CBCT allows accurate measurements of the systematic and random setup errors.

The introduction of the kV CBCT in our department has enabled acquisition of clinical data concerning the setup of lung cancer patients during treatment. First, we measured setup errors with both an electronic portal image device and a kV CBCT scanner during the treatment of 19 patients. Thereafter, the setup errors of subsequently treated patients were measured with the CBCT scanner only. The purpose of this study is to investigate and compare the setup measured with the EPID and with the CBCT. In addition, we will evaluate the clinical setup data using kV CBCT of lung cancer patients during the treatment and the impact of the setup correction protocol.

Material and Methods

Patients and measurements

Both cone beam CT (CBCT) scans and images from the electronic portal-imaging

device (EPID) were acquired for lung cancer patients to compare the setup error as measured by these two techniques. Patients were positioned in an arm support without a body frame. First a CBCT scan was performed immediately followed by the portal images (generally within a time period of less than 5 minutes). For 19 patients, treated between July 2003 and July 2004, a total of 172 scans were made (Table 1). For the first 4 patients the setup verification/correction protocol [7] was based on the EPID images, after March 2004 this protocol was based on the CBCT scans. After the first 19 patients (with both EPID images and CBCT scans), EPID images were only made at the first fraction for quality control purposes. From August 2004 to May 2005 for a total of 43 patients CBCT setup measurements (352 scans) were made for lung cancer patients.

Table 1

	<i>EPID and CBCT</i>	<i>Only CBCT</i>	<i>Total</i>
EPID correction protocol	4 (31)	-	4 (31)
CBCT correction protocol	15 (141)	43 (352)	58 (493)
Total	19 (172)	43 (352)	62 (524)

The number of patients, type of imaging modality and used correction protocol. Number of scans is indicated between brackets. EPID: Electronic Portal Imaging Device. CBCT: Cone Beam Computed Tomography.

EPID images

During radiotherapy, two orthogonal EPID images (anterior-posterior and lateral) were acquired using an a-Si flat panel detector (Elekta iViewGT) using 5 Monitor Units each. These images were acquired using in-house developed software at a resolution of 1 x 1 mm² pixel size at the iso-center plane.

Digital reconstructed radiographs (DRRs) were made from the planning CT using in-house developed software. The planning CT was performed on a single slice CT scanner. The slice distance was set on 5 mm due to the limitation of the planning system (U-Mplan, University of Michigan). A bone template was defined on the DRR (using a simulator film as visual guide). The DRR was matched automatically on the portal field edge, followed by automatic registration and in almost all cases a manual adaptation of the bony anatomy. The vertebra, clavicles and ribs were used for the image registration (Figure 1). Two orthogonal EPID images were used for setup measurements, the registrations of which were subsequently combined to a 3D setup error.

CBCT scanner

The CBCT scanner (Elekta Synergy, Elekta Oncology Systems Ltd., Crawley, West Sussex, UK) consisted of a conventional x-ray tube (kV source) and an a-Si flat panel detector, both mounted on the gantry of the linear accelerator (linac).

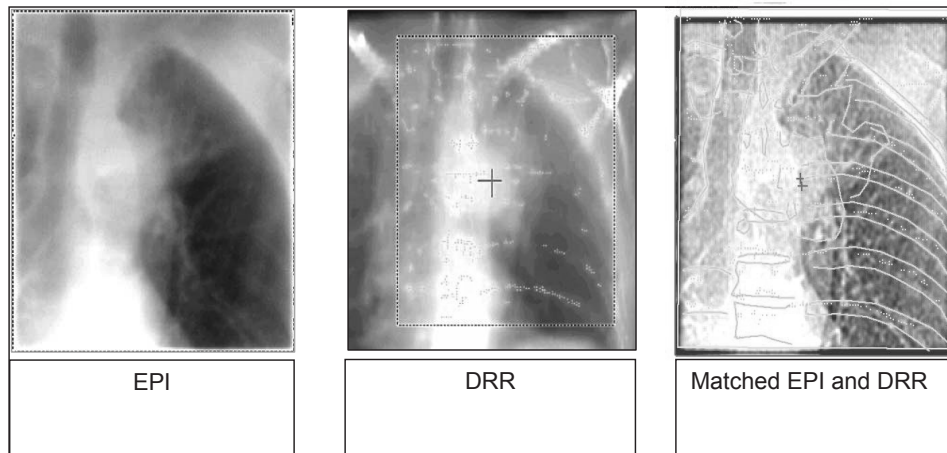


Figure 1. Match of the Electronic Portal Image (EPI) and the Digital Reconstructed Radiograph (DRR). The green dots are the contour tracing dots from the DRR, the green line representing the anatomy structure outline.

The linac (MV source) was an Elekta SL20i medical accelerator.

The lung cancer patients were scanned with a short scan protocol acquiring about 330 or 670 projections (depending of the frame rate of the imager) over an arc of 200° yielding an imaging dose of about 2 cGy at the iso-center. An in-house developed implementation of the filtered back projection algorithm [8] provided a reconstruction of 330 images into a 256^3 volume (1 mm cubic voxel size) in about 21 s on a 2.8 GHz PC. More details were previously described [9]. An object can be relocated within less than 1 mm of the prescribed location using the CBCT scanner, whereby the delivery precision is constant over a duration of at least 3 months [10].

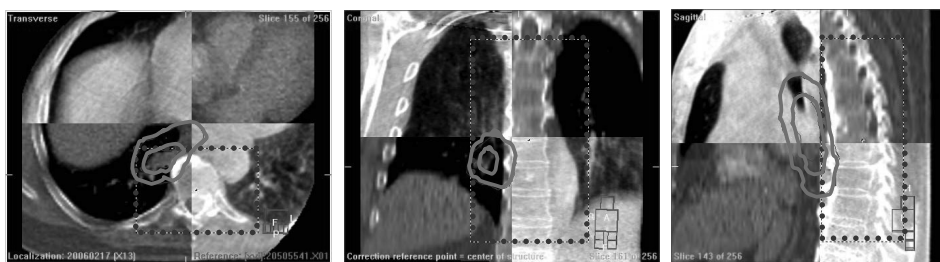


Figure 2. Match of the planning CT and the Cone-Beam CT (CBCT) whereby a user-defined 3-D region of interest (blue dashed line) was positioned around the vertebra. The inner and outer red line represents the gross target volume and clinical target volume, respectively.

Chapter 7

Setup measurements based on CBCT

The planning CT scan and the iso-center position, to be used as reference, was imported from the planning system. The bony anatomy in the CBCT scans was automatically registered to the planning scan using chamfer matching or grey value (cross correlation ratio) matching. The match procedure included a user-defined 3-D rectangular shaped region of interest that was positioned around the vertebrae in the planning CT (Figure 2). The registration was based on a rigid body assumption providing 3 translations and 3 rotations.

Patient setup correction

Setup measurements were performed after completion of the daily treatment to drive an off-line 3D shrinking action level (SAL) protocol [11]. Required corrections had to be applied in the remaining treatments fractions to reduce systematic setup errors. This protocol tests the length of the setup error vector against a shrinking action level: α/\sqrt{N} , with N the number of consecutive measurements and an initial action level (α) of 9 mm. For the first three consecutive fractions setup measurements were performed (i.e. $N_{\max} = 3$). If the mean of vector length (average of the consecutive measurements) was smaller than α/\sqrt{N} , no correction was applied. Subsequently, once a week setup measurements were made. For this weekly check, the average of the last three measurements was tested against an action level of $\alpha = 9/\sqrt{3} = 5.2$ mm. The protocol was restarted (i.e. again 3 consecutive measurements) after a correction was applied. Only setup corrections of 3 mm or larger were applied for the (left-right (LR), cranial-caudal (CC) and anterior-posterior (AP) directions to limit workload.

Differences between EPID and CBCT and statistics

As previously described [12] the setup errors are separated into systematic- and random errors. The random error (σ) is the deviation that occurs between different fractions (i.e. inter-fraction setup variation), while the systematic error (Σ) is the deviation between the simulation patient position and the average patient position (i.e. inter-patient setup variation). The random error for the entire population is the root mean square (RMS) of the individual random errors. The systematic error is the standard deviation of the individual patient errors. The mean, systematic error and the random setup error were calculated for the EPID setup error and CBCT setup error. We evaluated the impact of the corrections if the corrections were derived from the EPID measurements (i.e. theoretical analysis because the clinically used corrections were based on the CBCT). In other words, the corrections based on EPID measurements on the setup accuracy as measured by the CBCT were evaluated. Therefore we first removed the actually performed corrections from the EPID and CBCT data sets (i.e. uncorrected EPID and CBCT dataset). Subsequently, we applied the correction protocol on the uncorrected EPID and

Table 2

Translations (N = 19, n = 170)		Axis	Mean (mm)	S(1 SD, mm)	p*
Difference	EPID – CBCT	LR	0.1	2.2	0.5
		CC	0.7	2.4	< 0.001
		AP	0.3	2.1	0.04

The mean setup error, standard deviation of the translational systematic errors (Σ) and random errors (σ) measured with the EPID and the CBCT, respectively. N and n are the number of patients and the number of measurements, respectively.

CBCT data sets, retrospectively, by calculating couch corrections prescribed by the EPID data (EPID correction) and by the CBCT data (CBCT correction). Hereafter, the EPID correction was added on the uncorrected CBCT data set.

Linear regression analysis of the EPID setup data as a function of the CBCT data was performed. The paired T-test was used to evaluate whether the EPID setup data were significantly different from the CBCT setup data. Correlations between the translational setup differences (i.e. difference between EPID and CBCT) and the rotations measured with the CBCT were tested with the Pearson correlation coefficient. Retrospectively, the corrections applied according to the SAL protocol were removed. The setup errors (vector length) of both uncorrected data and the corrected data (i.e. clinically used data) were analyzed to evaluate the impact of the SAL procedure.

Results

I Setup measurements of EPID and CBCT

Translations; Differences between EPID and CBCT

Setup errors measured with the EPID were plotted against the setup errors of the CBCT (Figure 3). In general the setup errors measured with the CBCT were larger than the EPID setup errors. The regression coefficient (β) for the LR, CC and AP directions were 0.86 (95 % confidence interval (CI) = 0.76 – 0.96), 0.67 (95 % CI = 0.60 – 0.74) and 0.47 (95 % CI = 0.35 – 0.58), respectively.

We calculated the mean of the difference between each pair of measurements (Table 2), i.e. difference between what was measured with the EPID and CBCT for each fraction. For the LR direction the mean difference was 0.1 mm ($p = 0.5$). For the CC and AP directions the mean differences were significantly different from zero (0.7 mm, $p < 0.001$ and 0.3 mm, $p = 0.04$, respectively). If the EPID data were used to determine the required corrections (see material and methods), a mean setup error of 1.8 mm would have been observed in the CC direction (Table 3). However, when evaluating these EPID corrections with the CBCT measurements, an actual mean setup error resulted of -4.5 mm, with a large Σ of 3.8 mm. If the CBCT measurements themselves were used in the correction protocol, a significant smaller

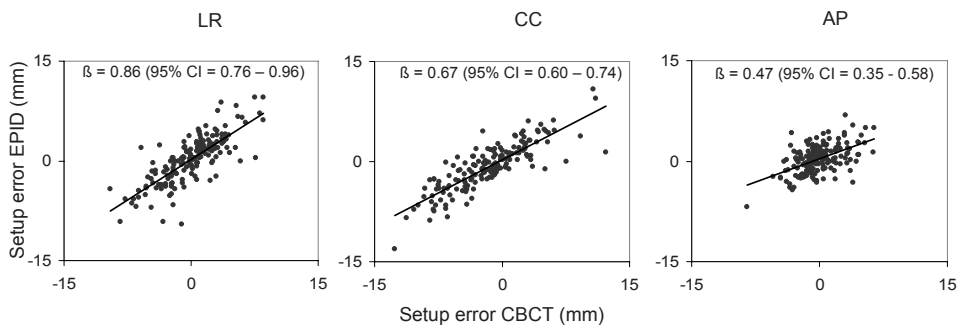


Figure 3. The EPID setup error (vertical axis) as function of the CBCT setup error (horizontal axis) for the Left - Right, Cranial - Caudal and Anterior - Posterior setup errors. CI: Confidence Interval, β : regression coefficient. EPID: Electronic Portal Imaging Device. CBCT: Cone beam Computed Tomography.

mean setup error of -1.3 mm would have resulted with an Σ of 1.9 mm (Table 3).

Rotations; Influence of rotations on difference between EPID and CBCT

Rotational errors (especially out of plane) are difficult to measure using 2D portal image analysis. We therefore evaluated the impact of these rotational setup errors measured with CBCT on the differences observed between EPID and CBCT measured in the translational directions. The correlation coefficient of the rotational setup errors and the vector length in the plane where the largest difference might be expected were calculated (i.e. vector length in the plane perpendicular to the rotation axis). The correlation coefficient of the vector length in the plane perpendicular to the LR axis and the rotations around the LR axis was 0.2 ($p = 0.01$). Similarly, the correlation coefficients of the vector length in the plane perpendicular to the CC and AP axes and the rotations around the CC and AP axis, respectively, were both 0.17 ($p = 0.03$).

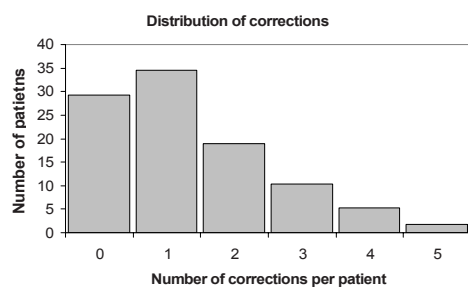


Figure 4. The number of corrections applied per patient during the treatment.

Translations; Setup error of CBCT

Four hundred ninety-three CBCT setup measurements were performed for 58 patients (corrections were based on CBCT). There was quite a variation in the number of corrections applied per patient with a maximum (35%) at 1 correction, for 29 % of the patients no correction was applied and for only 2 % of the patients 5

CBCT setup data; first clinical results and comparison with EPID

Table 3

<i>A: corrections based on EPID (N = 19, n = 170)</i>				
	<i>Axis</i>	<i>Mean (mm)</i>	Σ <i>(1 SD, mm)</i>	σ <i>(1 SD, mm)</i>
EPID	LR	0.0	2.2	4.6
	CC	1.8	2.6	5.2
	AP	0.2	0.9	2.1
CBCT	LR	0.2	3.1	3.2
	CC	-4.5	3.8	3.7
	AP	-0.2	1.6	2.5
<i>B: corrections based on CBCT (N = 19, n = 170)</i>				
CBCT	LR	0.0	1.7	3.1
	CC	-1.3	1.9	4.1
	AP	0.3	1.2	2.6

A. The mean setup error, standard deviation of the systematic errors (Σ) and random errors (σ) using the EPID and CBCT measurements with the corrections based on the EPID data.

B. The mean setup error, standard deviation of the systematic errors (Σ) and random errors (σ) using the CBCT measurements with the corrections based on the CBCT data. N and n are the number of patients and the number of measurements, respectively. EPID: Electronic Portal Imaging Device. CBCT: Cone beam Computed Tomography.

corrections were needed according to the SAL correction protocol (Figure 4). During the treatment of all 58 patients 76 corrections were applied (i.e. 1.3 correction per patient). The total number of corrections (in any direction) was 134. The deviations in the setup were largest in the CC direction for the mean, systematic error as well as the random error (Table 4).

Table 4

<i>A. CBCT (N = 58, n = 491)</i>				
	<i>Axis</i>	<i>Mean (mm)</i>	Σ <i>(1 SD, mm)</i>	σ <i>(1 SD, mm)</i>
	LR	0.2	1.6	2.9
	CC	-0.8	1.7	4.0
	AP	0.0	1.5	2.0
<i>B. CBCT corrections removed</i>				
	LR	0.7	3.1	2.5
	CC	-2.3	4.0	3.4
	AP	-0.1	2.0	2.0

A. The mean and standard deviation of the translational systematic errors (Σ) and random errors (σ) measured with the Cone Beam CT (CBCT), respectively. N and n are the number of patients and the number of measurements, respectively.

B. The mean, Σ and σ if no setup corrections were made.

Setup error of CBCT without corrections

If no corrections were applied to the setup of the patients, the mean of the setup errors in the CC direction was more than 2.0 mm (Table 4). The systematic errors (1 Σ) without corrections were 3.1 mm, 4.0 mm and 2.0 mm for the LR, CC and AP direction, respectively. The random error was 0.6 mm smaller without setup correction in the CC directions, for the LR and AP direction the difference was

smaller (Table 4). Applying the SAL correction protocol, only 2 % of the patients had a mean setup error (vector length) larger than 5 mm. Without this protocol, more than 51 % of the patients would have had a mean set up error larger than 5 mm (Figure 5).

Rotations; Distribution of rotations

The mean rotational setup errors around the LR, CC and AP axis were small (0.1°). For all axes, the standard deviations of both systematic and random errors were of the order of 1 degree.

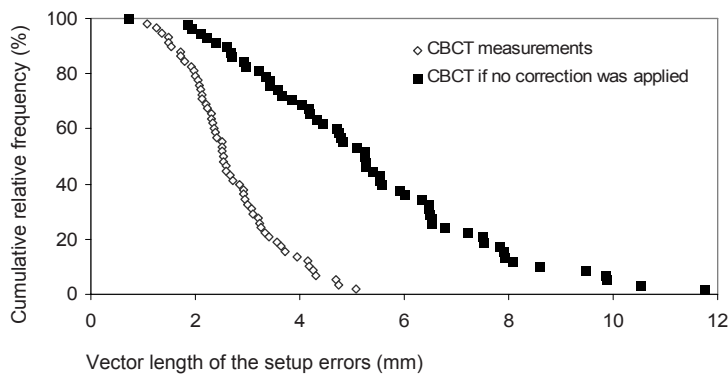


Figure 5. Cumulative relative frequency of the mean of setup error per patient (expressed as the vector length of the 3D setup error) measured with the Cone Beam CT (CBCT) (open squares) and the cumulative frequency of the setup error of the CBCT setup errors if no correction was applied (solid squares).

Discussion

Set up differences of EPID and CBCT

For 19 lung cancer patients, we performed 172 setup measurements with both portal images and CBCT scans. Setup errors measured with CBCT were generally larger than those measured with EPID. The largest difference between the EPID and CBCT measurements were observed in the CC and AP direction whereas the differences in the LR direction were not significant. Assuming that the CBCT system is more accurate [10], one might expect the setup error determined with CBCT to be smaller, since there is less measurement inaccuracy. On the other hand, because portal images were assumed to be less accurate, larger measurement errors might be the result. This study showed that EPID analysis resulted in a smaller estimated setup error in our group of lung cancer patients, and that the discrepancy was statistically significant. If the EPID were used to determine required corrections, a large underestimation of the setup error would have been made. (Table 2 and 3, Figure 3).

There are several potential sources for the discrepancies observed between the EPID and CBCT. *First*, although the time interval between the CBCT and EPID

measurements was small, the observed setup differences between CBCT scans and EPID images might be due to patient and/or respiratory motion. Van Herk et al. [13] investigated this possible explanation of the observed differences. Digital reconstructed radiographs (DRR) were calculated from the CBCT scans and compared with the corresponding EPID images for 4 patients (32 CBCT scans). The difference between the DRR of CBCT data and the EPID image from the same day was generally small (< 1 mm). Consequently, the patient motion between image acquisitions and respiration motion hardly contributed to the observed differences.

Secondly, EPID images measure only the setup errors in the LR, CC, and AP directions. Three-dimensional (3D) CBCT scans provide, in a significant way, accurate information concerning rotations [14]. If rotations were responsible for the observed differences between CBCT and EPID, they were most likely to cause differences in the plane perpendicular to the rotation axis. We did observe a correlation between the rotations and the differences between CBCT and EPID in these planes. Although the correlation was significant, only 20 % or less (correlation coefficient ≤ 0.2) of the observed differences could be explained by rotations. Consequently, the (out-of-plane) rotations, detected by the CBCT, were only partly responsible for the observed differences between CBCT and EPID.

Thirdly, match procedures using CBCT and EPID images do have different regions of interest. The vertebra, clavicles and ribs were used for the EPID image registration whereas the match procedure of the CBCT included only the vertebrae. However, clavicles and ribs are more subject to (respiratory) motion, which should have been resulted in larger setup errors for the EPID (i.e. the opposite of what we observed).

A *fourth* reason might be the poor visibility of anatomical structures in the DRRs (calculated from the planning CT scan) and portal images might be the most important source of setup error differences. Because of this poor visibility it is more difficult to manually shift the portal image to the DRR, which may result in less corrections. CT slice spacing used for treatment planning, which is 5 mm in our study causes most details of the vertebrae to be lost (Fig. 1A).

Setup errors consist of day-to-day variation in patients positioning (i.e. random setup errors) and discrepancies induced during the preparation of the treatments (i.e. systematic errors). In particular, the impact of these systematic setup errors on the dose to the clinical target volume (CTV) was considerably [15]. Previously, Erridge et al. observed similar setup errors as measured in the current study with EPID analysis for 97 lung cancer patients treated in our department. In addition, Van Sornsens de Koste et al and de Boer et al observed similar setup errors in 20 and 40 lung cancer patients, respectively. These studies will probably have had an underestimation of the setup error of lung cancer patients, which may have resulted in an under-dosage to the CTV.

Chapter 7

Setup verification and correction based on CBCT

From the time when the kilo-voltage (kV) CBCT was in clinical use in our department, target positioning was based on the planning CT and 3D kV CBCT images. Consequently, for 58 lung cancer patients accurate setup information was documented during their treatment course.

The setup error measured with the CBCT scan was used to drive a 3D shrinking action-level (SAL) protocol. The goal of the protocol is to reduce the systematic error during the remaining treatment. Our protocol was based on previous results from our institute [16,17] whereby 41 % of the patients had a set-up error with a vector length larger than 5 mm based on portal images. After correction, only 1 % of the patients had a set-up error larger than 5 mm. In our study these numbers were 51 % without correction and 2 % after correction, respectively.

Optimization of the SAL protocol is important to reduce systematic errors with acceptable random errors. A high initial action level (α) might result in fewer corrections but also with larger systematic errors, whereas a low α might result in more corrections with an increase in random errors. We used an α of 9 mm and three subsequent measurements ($N_{\max} = 3$) in the first stage (and after a correction was applied). Using this protocol, 1.3 corrections per patients were needed. Before the use of the CBCT, in our institution 0.9 corrections (data not presented) per patient were applied using the EPID images (using the identical SAL protocol). Van Sornsen de Koste et al. [18] applied 0.8 corrections per patient using a comparable SAL protocol ($\alpha = 8$ mm, $N_{\max} = 3$), and the systematic errors in this study were in the range of our results (1.5 for the LR and CC direction and 1.3 for the AP direction). The estimated setup error equals true setup error plus measurement error. The registration accuracy of the CBCT will reduce the measurement error. Consequently, the measured setup error of the CBCT will be closer to the true setup error. Because the EPID data might have underestimated the errors, fewer corrections were applied during treatment.

Guckenberger et al. [19] evaluated the setup error of the bony anatomy in the stereotactic body frame for 21 patients registered with CBCT. Larger systematic errors (3.2 mm CC, 2.6 mm AP and 1.8 mm LR) were observed whereas the random errors were smaller (2.1 mm CC, 1.1 mm AP and 2.0 mm LR), which is not surprisingly because of the smaller number of scans (fractions). The systematic positioning error of the patients in the stereotactic body frame contributed substantially to the group mean error of the tumor position. Nevertheless, a poor correlation was observed between the position errors of the patients (bony anatomy) and the tumor (soft tissue), which was emphasized for tumors with increased range of breathing motion (which was also observed previously by Wulf et al [20]). This emphasizes the importance of appropriate setup measurements (bony anatomy) and tumor position localization (soft tissue). Respiratory motion (i.e. tumor motion,

CBCT setup data; first clinical results and comparison with EPID

the so called fourth-dimension (4D) in imaging) can be incorporated both in the planning phase (4D-CT)[21,22] and during irradiation (4D-CBCT)[19,23,24]. These image strategies will ensure higher levels of accuracy in treatment delivery. In other words, image guided radiotherapy (IGRT) is the corner stone for current and future irradiation techniques as hypofractionation, dose escalation radiotherapy and gated radiotherapy.

Accurate setup of the patient and corrections for rotational errors will improve the accuracy of the treatment. Optimization of normal tissue complications and tumour control with respect to innovative delivery techniques require accurate imaging techniques. Therefore, the current focus on fractionation schemes and dose adaptation must be accompanied by accurate imaging techniques.

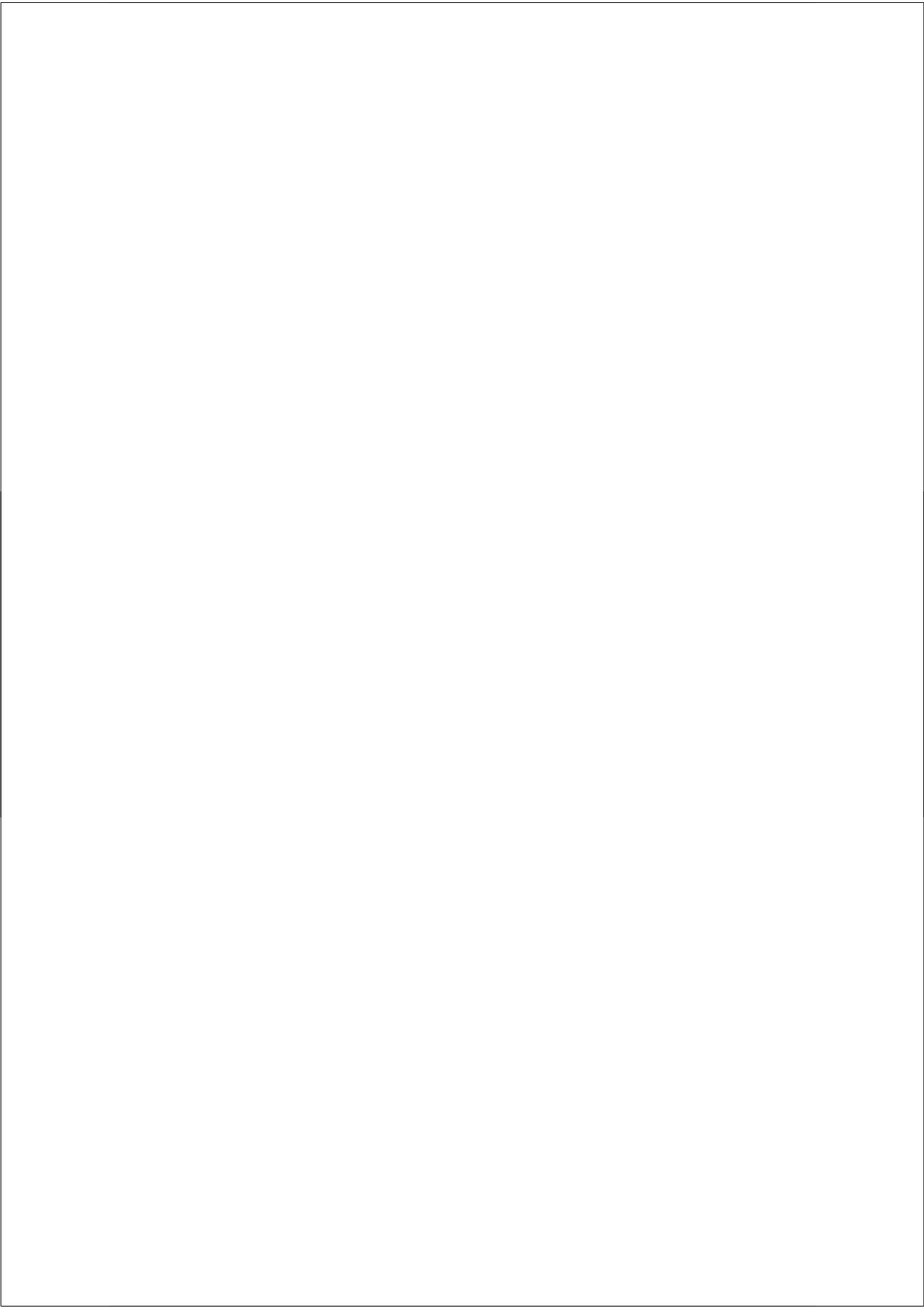
In our study we illustrated, with clinical data, that kV CBCT provides accurate target positioning data for lung cancer patients.

Chapter 7

References

1. Engelsman M, Damen EM, De Jaeger K et al. The effect of breathing and set-up errors on the cumulative dose to a lung tumor. *Radiother Oncol* 2001;60:95-105.
2. Schwarz M, Van der GJ, van Herk M et al. Impact of geometrical uncertainties on 3D CRT and IMRT dose distributions for lung cancer treatment. *Int J Radiat Oncol Biol Phys* 2006;65:1260-1269.
3. Erridge SC, Seppenwoolde Y, Muller SH et al. Portal imaging to assess set-up errors, tumor motion and tumor shrinkage during conformal radiotherapy of non-small cell lung cancer. *Radiother Oncol* 2003;66:75-85.
4. de Boer HC, Van Sornsen de Koste JR, Senan S et al. Analysis and reduction of 3D systematic and random setup errors during the simulation and treatment of lung cancer patients with CT-based external beam radiotherapy dose planning. *Int J Radiat Oncol Biol Phys* 2001;49:857-868.
5. Van Sornsen de Koste JR, de Boer HC, Schuchhard-Schipper RH et al. Procedures for high precision setup verification and correction of lung cancer patients using CT-simulation and digitally reconstructed radiographs (DRR). *Int J Radiat Oncol Biol Phys* 2003;55:804-810.
6. Jaffray DA, Siewerdsen JH, Wong JW et al. Flat-panel cone-beam computed tomography for image-guided radiation therapy. *Int J Radiat Oncol Biol Phys* 2002;53:1337-1349.
7. Bel A, van Herk M, Bartelink H et al. A verification procedure to improve patient set-up accuracy using portal images. *Radiother Oncol* 1993;29:253-260.
8. Feldkamp A, Davis LC, Kres W et al. Practical cone-beam algorithm. *J Opt Soc Am* 1984;A1:612-619.
9. Sonke JJ, Zijp L, Remeijer P et al. Respiratory correlated cone beam CT. *Med Phys* 2005;32:1176-1186.
10. Sharpe MB, Moseley DJ, Purdie TG et al. The stability of mechanical calibration for a kV cone beam computed tomography system integrated with linear accelerator. *Med Phys* 2006;33:136-144.
11. Bel A, van Herk M, Bartelink H et al. A verification procedure to improve patient set-up accuracy using portal images. *Radiother Oncol* 1993;29:253-260.
12. Remeijer P, Geerlof E, Ploeger L et al. 3-D portal image analysis in clinical practice: an evaluation of 2-D and 3-D analysis techniques as applied to 30 prostate cancer patients. *Int J Radiat Oncol Biol Phys* 2000;46:1281-1290.
13. van Herk M, Bentgen A, Remeijer P et al. Comparison of setup error determined with EPID and with cone beam CT for lung cancer patients - how accurate is EPID image analysis in clinical practice for a difficult site? *International Workshop Electronic Portal Imaging, Brighton Abstract* 2004;
14. Remeijer P, Geerlof E, Ploeger L et al. 3-D portal image analysis in clinical practice: an evaluation of 2-D and 3-D analysis techniques as applied to 30 prostate cancer patients. *Int J Radiat Oncol Biol Phys* 2000;46:1281-1290.
15. van Herk M, Remeijer P, Rasch C et al. The probability of correct target dosage: dose-population histograms for deriving treatment margins in radiotherapy. *Int J*

- Radiat Oncol Biol Phys 2000;47:1121-1135.
16. Erridge SC, Seppenwoolde Y, Muller SH et al. Portal imaging to assess set-up errors, tumor motion and tumor shrinkage during conformal radiotherapy of non-small cell lung cancer. *Radiother Oncol* 2003;66:75-85.
 17. Bel A, van Herk M, Bartelink H et al. A verification procedure to improve patient set-up accuracy using portal images. *Radiother Oncol* 1993;29:253-260.
 18. Van Sornsens de Koste JR, de Boer HC, Schuchhard-Schipper RH et al. Procedures for high precision setup verification and correction of lung cancer patients using CT-simulation and digitally reconstructed radiographs (DRR). *Int J Radiat Oncol Biol Phys* 2003;55:804-810.
 19. Guckenberger M, Meyer J, Wilbert J et al. Cone-beam CT based image-guidance for extracranial stereotactic radiotherapy of intrapulmonary tumors. *Acta Oncol* 2006;45:897-906.
 20. Wulf J, Baier K, Mueller G et al. Dose-response in stereotactic irradiation of lung tumors. *Radiother Oncol* 2005;77:83-87.
 21. Vedam SS, Keall PJ, Kini VR et al. Acquiring a four-dimensional computed tomography dataset using an external respiratory signal. *Phys Med Biol* 2003;48:45-62.
 22. Ford EC, Mageras GS, Yorke E et al. Respiration-correlated spiral CT: a method of measuring respiratory-induced anatomic motion for radiation treatment planning. *Med Phys* 2003;30:88-97.
 23. Sonke JJ, Zijp L, Remeijer P et al. Respiratory correlated cone beam CT. *Med Phys* 2005;32:1176-1186.
 24. Kaiser A, Schultheiss TE, Wong JY et al. Pitch, roll, and yaw variations in patient positioning. *Int J Radiat Oncol Biol Phys* 2006;66:949-955.



General Discussion

Discussion

1. Radiotherapy for NSCLC

RT is currently the cornerstone in the treatment of inoperable NSCLC patients. Moreover, it might be possible that in the future early stage operable patients will be irradiated (as an alternative for thoracotomy). It is already known that higher doses of irradiation yield a greater proportion of complete response, higher tumour control and better survival in irradiated lung cancer patients [1,2]. Nevertheless, the possibility to apply higher doses and to add chemotherapy to radiotherapy is limited by the increased probability of treatment related toxicity. Improved patient selection, as well as newly developed high accuracy irradiation techniques and optimizing predictive toxicity models were subject of studies included in this thesis (Chapter 2-7) and will be discussed below.

2. Use of PET scan in the Treatment of Lung Cancer Patients

Tumour stage and performance status are currently the most important prognostic factors for lung cancer patients. Appropriate staging is of major concern and modifications of the Tumour (T) Nodal (N) Metastasis (M) staging system of the IASLC Lung Cancer Staging Project are published in 2007 [3]. This project evaluated data from 46 sources in more than 19 countries (i.e. 67,725 cases of non-small cell lung cancer (NSCLC) treated by all modalities of care between 1990 and 2000) whereby a training subset and a validation subset was used. From these data some changes were proposed (e.g. T2b N0 M0 cases are moved from stage IB to stage IIA, T2a N1 M0 cases from stage IIB to stage IIA, and T4 N0-1 M0 cases from stage IIIB to stage IIIA). These proposed changes might improve the alignment of TNM stage with prognosis and possibly in treatment but are based on data post-dated the period of PET scanning. The introduction of the Positron Emission Tomography (PET) scans in the diagnostic work up has significantly improved the sensitivity of mediastinal nodal staging compared to the sensitivity of the CT scan alone [4,5]. Unforeseen distant metastasis can also be detected by PET scan to differentiate candidates for curative or palliative treatment regimens. Additionally to staging, PET scans can be used to determine the border between tumour tissue and distally located collapsed lung tissue (atelectasis) [6]. As a result, the introduction of the PET scan has influenced the delineation of the target volume [7-11]. Following studies showed that the dose to non-tumour tissue was reduced for many patients if the PET scan information was used additional to the CT scan for tumour delineation [10,12-16]. In addition, better tumour dose coverage might be achieved if tumour definition is based on both CT and PET scans [13,17-19]. Therefore, a pre-RT PET scan is currently a standard procedure in the irradiation treatment of lung cancer patients.

2.1 Prognostic Value of FDG PET Scan and Clinical Implication

The hotspots on PET scans are regions with a high glucose uptake (with high accumulation of the glucose analogue [18F]-fluoro-2-deoxy-D-glucose (FDG)) representing tissues with a high metabolism (e.g. heart musculature, brain tissue and tumours). Aggressive tumours have a higher metabolism (glycolysis) which was already observed by Warburg in the early 19th century [20]. It has been shown that prognostic factors like tumour doubling time, glucose transporter proteins Glut 1 and Glut 3 and proliferation markers Ki-67 [21-23] are correlated with the amount of FDG in the tumour [24-26]. Calculation of the Standardized Uptake Value (SUV) (see paragraph 2.3) is a semi-quantitative method to objectify the amount of FDG in the tumour. The hypothesis that the SUV can be used as a surrogate marker of poor prognostic tumour characteristics was evaluated in lung patients who underwent surgery. Significantly higher pre-operatively measured SUVs were observed in patients with poor outcome compared to patients with favourable outcome [27-33]. The additional value of the SUV for operable patients is however limited because the tumour itself is available for pathology review after surgical resection. For inoperable patients on the other hand, the prognostic value of the SUV (besides performance status and TNM stage) would be of additional value since not all tumour characteristics can be retrieved from biopsies. Moreover, biopsies are not always available (e.g. failed biopsy or because of a contra indication for invasive procedures). As a consequence the prognostic pre-irradiation SUV is of major interest.

For 51 inoperable patients irradiated with a curative intent (stage I-IIIb) the SUV was calculated on the pre-RT PET scan. The SUV proved to be an independent prognostic factor besides performance status and stage for the disease specific survival and overall survival (Chapter 2). The significant different disease specific survival of patients with high SUV tumours and low SUV tumours might be a reflection of the aggressiveness of the tumour. More complex is the observation that lower SUVs were predictive for better tumour response observed at a CT scan after RT (Chapter 2). Higher proliferation rates (of more aggressive tumours) are correlated with higher sensitivity for irradiation [34] (i.e. higher SUVs would have had higher response rates). Nevertheless, higher SUVs were observed for worse response rates (Chapter 2). It might be that these tumours had a (fast) re-growth after irradiation observed at the post-RT CT scan. A correlative study comparing pre and post PET scans as function of the tumour response and survival is interesting to reveal this issue. Mac Manus et al. showed that patients with a complete metabolic response (i.e. PET response) had significantly better outcome [35] but unfortunately no information was given of the pre-treatment SUV. Aerts et al. [36] reported worse survival for patients with residual metabolic active areas. These patients had a significantly higher pre-RT SUV value compared to patients with a complete metabolic response. As

expected, an overlap was observed between the pre-RT high SUV region and the residual metabolic active areas.

In Chapter 2, the important question is raised whether tumours with high SUV values should be treated more aggressively to raise the probability of cure. To solve this issue a study is initiated to boost high SUV areas (i.e. dose escalation to the tumour region with the highest SUV value or the whole tumour, see paragraph 5.5). Hopefully, patients with high SUV will benefit from this new treatment technique/dose escalation resulting in improved outcome comparable to patients with lower SUV values.

2.2 Other PET Tracers

The degree of hypoxia is an important determinant of treatment response, relapse-free survival, and overall prognosis, which is independent of the treatment modality used in cancer patients [37,38]. Although higher glycolysis is observed in hypoxic cells (i.e. Pasteur effect [39,40]) it is known for NSCLC tumours that the FDG uptake is not correlated with hypoxia of the tumour [41,42]. Consequently, FDG PET scans are not appropriate to discriminate oxidized tumour cells from radio resistant hypoxic tumour cells and other tracers visualizing hypoxia are of great interest as potential tumour boost areas [43]. Fluoromisonidazole (FMISO) is a derivative of the nitroimidazole group, which have been investigated as hypoxic cell sensitizer. Other derivatives of nitroimidazole has shown radiosensitizing effects, e.g.[44]. Comparable to the FDG SUV of Chapter 2, also the FMISO SUV is predictive for treatment outcome [45]. Moreover, using FMISO-guided IMRT it was feasible to escalate the dose to radio-resistant hypoxic zones without exceeding the normal tissue tolerance in head and neck cancer patients [46]. Fluoroazomycin arabinoside (FAZA) is another derivative of nitroimidazole and has shown promising results in in-vitro studies [47]. As a result, not only tumour regions with a high FDG uptake are interesting regions for higher doses but also tumour regions with a high uptake of hypoxic tracer should be investigated for this (see paragraph 5.5).

2.3 Methodological Problems of the SUV

A major problem calculating the SUV is the non-standardized calculation method. This problem is not only known for SUV calculated from FDG PET scans but also for the hypoxic tracers as FMISO[45]. Differences in injected tracer, scanning time (i.e. time after injection), reconstruction algorithms, filters, scanner characteristics, sinogram noise and quantification methods might lead to (structural) inter-institutional SUV differences [48]. Even the calculation of a SUV differs between SUV studies; e.g. a SUV_{mean} can be calculated as a mean value within a region of the tumour or a SUV_{max} can be determined within the whole tumour. Because the calculation of the SUV is subject to many uncertainties, comparisons of results

achieved in different institutes should be interpreted with caution. In 2008 the first meta-analysis of studies evaluating the SUV as prognostic parameters was published [49] including our study of Chapter 2. Of the 13 studies in the meta-analysis, 11 studies showed a significant worse outcome for patients with a high SUV. All authors of these studies were asked to provide the individual patient data for a meta-analysis based on individual patient data. Since the PET scans can not be interpreted uniformly, the outcome of this work in progress based on individual patient outcome data might be complicated. More uniform scanning protocols and better (inter- and intra) institutional collaboration between the departments of RT and nuclear medicine is warranted for optimal use of the prognostic value of the PET scan. This should be performed since the PET scan is an important tool in the work-up of lung cancer patients and the SUV information is provided for free and can and should be used to improve the treatment strategy for the individual lung patient.

3. Radiotherapy Induced Lung Toxicity

The introduction of new irradiation techniques (e.g. 3D conformal radiotherapy and Intensity-Modulated Radiotherapy Treatment) facilitates reduction of high dose regions to tumour surrounding tissue. Nevertheless, lung tissue will always be included in the irradiation field and might even receive lower doses to larger volumes. Cellular molecules (e.g. peptides, lipids, and DNA) are damaged directly and indirectly via the interaction with ionizing radiation and will result in an up-regulation of cascades of cytokines mediating pathologic changes (e.g. transforming growth factor beta-1 [50] and IL-6 [51]). For lung, these physiological and pathological responses to irradiation can be divided in an early (i.e. inflammatory) and late (i.e. fibrosis) phase resulting in subsequently related clinical symptoms.

3.1 Radiation Pneumonitis

The early phase, called radiation pneumonitis (RP), can occur weeks to months after thoracic radiotherapy and is a serious complication. Accurately scoring of RP is a tedious work complicated by the possibility of exacerbation of pulmonary comorbidities and/or tumour progression. The diagnosis and treatment of RP should therefore be performed with much caution.

RP is commonly scored according to the National Cancer Institute – Common Toxicity Criteria for Adverse Events (NCI-CTCAE) version 2 or the Southwest Oncology Group (SWOG) toxicity scales. In general, Grade 1 is scored for radiographic changes without symptoms. Grade 2 RP is scored after steroids had been prescribed. Grade 3 RP is scored after oxygen is required and grade 4 for assisted ventilation. Grade 5 is scored after death due to RP. The diagnosis of RP by the clinicians should be performed uniformly, robustly and reproducibly. For example, before grading and scoring RP as an event, the symptoms should relieve after treatment is initiated

and the diagnosis should have been confirmed by radiological changes. Moreover, the adverse events should be scored and graded by physicians experienced in the diagnosis of RP. To date, the NCI-CTCAE version 3 criteria is introduced for RP whereby grade 2 is defined as symptomatic but not interfering with activities daily living (ADL) and grade 3 as symptomatic but interfering with ADL. This grading system may be more influenced by the subjective sensation of both the patient and the physician concerning the ADL.

Scoring radiation induced lung toxicity using the dyspnoea grading system of the NCI-CTCAE version 3 [52] is complicated since dyspnoea can be caused by other reasons than RT induced toxicity. Moreover, to be able to predict radiation induced pulmonary (function) changes as function of patients and/or treatment characteristics, the dyspnoea scores after RT (or other endpoints) should be evaluated relative to the baseline score pre-RT and not as an absolute score [53].

3.2 Predictors for Radiation Pneumonitis

For patients irradiated with conventional fractionated radiotherapy schemes it is known that the lung dose and volume is predictive for RP [54-56]. The dose predicting RP can be expressed as a mean lung dose (MLD) or as a percentage of lung volume receiving more than a threshold dose x (V_x). There is no consensus or consistency between institutes which dose parameter should be used for the prediction of RP. Rodriquez performed a systematic review and concluded that the MLD showed the most consistent results to predict RP [57]. Also after this study including 14 studies, publications proved that Dose Volume Histograms (DVH) derived parameters were predictive for the incidence of RP [58,59]. However, the dose calculation algorithms that were used were inferior to currently used algorithms whereby large differences can be found [60]. Moreover, significant differences can be found between NTCP models calculated as function of dose parameters calculated with different algorithms. Also other factors are contributively for disappointing true positive and false negative predictive values (or in clinical terminology; some patients receiving low lung dose are still developing serious treatment induced complaints after radiotherapy). Retrospectively evaluated characteristics as prior thoracic irradiation, age, smoking history, performance status, lung function, chronic obstructive pulmonary disease (COPD) and sex [61-65] were predictive for RP. However, no study is currently available whereby these factors, which were predictive for RP, were prospectively validated. In the collaborative study of the Duke University with the Netherlands Cancer Institute (NKI) pre-RT criteria were defined which were possibly predictive for the development of RP (Chapter 3). Dosimetric and pulmonary functional parameters (from perfusion SPECT scan and pulmonary function tests) were derived from one cohort of patients (from the Duke University) and validated in the patients treated at the NKI. The prospectively developed model was unable

to accurately segregate patients into high vs. low risk groups. Nevertheless, for both cohorts a correlation was observed between dose parameters and the incidence of RP. Additional work is needed to identify prospectively and validated predictors for RT-induced lung injury. These predictors will be able to select patients who are candidate to receive a more aggressive treatment or patients who are likely to develop serious treatment related toxicity (and should not be treated with an intensified treatment).

3.3 Radiation Pneumonitis after Hypofractionated RT

In contrast to the dose-response evaluations described in conventional fractionated RT, the relation between dose and RP after hypofractionated RT is unknown. Nevertheless, fatal RP toxicities were observed [66] and a possible dose-effect relation is of great interest. Other publications reported a wide range of the incidence of RP (0-29%) [66-71]. The first problem of dose response analysis is the large heterogeneity of treatment techniques, dose parameters and the scoring system of RP. To perform a dose-response analysis, a sufficient number of patients and events are necessary. Until recently only a limited number of institutes performed hypofractionated RT hampering dose-response analysis. Secondly, because only small lung tumours were treated by hypofractionated RT the amount of lung tissue receiving (high) doses is low. This results in a narrow dose range complicating a dose-response analysis. Thirdly, the analysis is complicated because of the uncertainty how to recalculate the physical dose into a biological equivalent lung dose (paragraph 4.1 and 4.2).

Since encouraging tumour control rates are demonstrated, the number of institutes using hypofractionated RT for lung tumours has been increasing in a short period of time (also in the Netherlands). Consequently, the knowledge of a (possibly) dose-response relationship is essential in optimizing hypofractionated RT. To date, it is uncertain whether multiple targets and/or larger tumour volumes can be (re)treated safely. The Hokkaido University in Japan was one of the few departments who applied hypofractionated RT for malignant pulmonary lesions soon after the introduction by Blomgren et al. [72] in 1995. In the following years, this group extended the use of hypofractionated RT since severe toxicities were not observed. Follow up was carefully performed and treatment regimens were adapted on empirical basis; i.e. if no toxicity was observed the dose was increased or larger/multiple lesions were irradiated and if no local recurrence was observed smaller safety margins were used). As a result, a unique data set within a wide dose range was available. For a group of 128 patients a dose-response relation was observed for RP which was comparable with conventional treated patients (Chapter 4). For the higher dose range a steeper increase for the NTCP fit of the hypofractionated treated group of patients was observed. However, for both group of patients, less data was available in the high dose range and the difference in the high dose range was not significant.

The great importance of this study is that also for hypofractionated schedules the

lung dose can be used to estimate the probability to develop RP for larger tumour volumes and/or re-irradiations. In addition, also the time interval between treatment and the incidence of RP was comparable for the two groups. As a result, there is no clinical reason to assume that the physiological process developing RP after hypofractionated RT is different from conventional fractionated RT.

That this dose effect relation can be extended to larger fraction doses can be hypothesized but should be confirmed. In our institute only few (7 %) incidences of RP were observed after 54Gy in 3 fractions. As previously mentioned, the MLD range is limited because only small tumours were irradiated and the incidence is too low for a robust dose-response analysis.

Because the fraction dose is altered from conventional schemes other radiation induced toxicities than RP should be taken into account (paragraph 4.2). For example, recent studies showed an increased risk for brachial plexus toxicity for brachial plexus doses > 26 Gy in 3-4 fractions [73], chest wall pain for chest wall volumes > 30 cm³ receiving 30 Gy in 3-5 fractions [74] and skin toxicity if only 3 beams were used or if only a limited distance between tumour and skin was present [75]. For other reported toxicities the evidence that the clinical complications were caused by the high fraction dose was less strong (e.g. patients treated on centrally located tumour died from centrally located bleeding but for these patients tumour progression was found at this location or patients died due to pneumonitis but the pneumonitis had a bacterial origin) [76].

In conclusion, for fraction doses up to 12 Gy larger volumes and re-irradiation can safely be given concerning RP and other toxicities. For fraction dose of 18 Gy and higher, the incidence of RP is very low due to small volumes but caution should be taken for other (late term) toxicities.

3.4 Long term Pulmonary Toxicity

After the acute phase, long term radiation induced lung tissue damage is characterized by pulmonary fibrosis. This is an irreversible and progressive process of scar tissue in the lungs initiated by collagen deposition by fibroblasts. This results in narrowing of alveolar spaces, thickening of the interstitial layer and a diminished lung volume. Although the pathological processes and the radiological findings are well defined, the clinical implications are uncertain. The long term effect of radiotherapy for lung cancer patients is even more complicated to evaluate than the above described relation between dose and RP. Again, the pulmonary co-morbidity and poor prognosis hampers robust clinical analysis. For lymphoma and breast cancer patients (a patient group with a better prognosis and less pulmonary co-morbidity) a partial recovery from early radiation toxicity was observed between 3 and 18 months after radiotherapy. However, after 18 months, local lung function did not further improve [77]. To evaluate the long term effect of irradiation for lung cancer patients repetitive

pulmonary function tests were performed for 34 patients selected by a long term disease free survival and available pulmonary function tests (Chapter 5). An acute deterioration of pulmonary function after RT without improvement at long term was observed. For the pulmonary compromised patients suffering from COPD a larger decline of the pulmonary function at long term was observed. Likely, the COPD and radiotherapy consolidate the pulmonary impairment induced by the one or the other. Importantly, there was a trend of pulmonary function decline as a function of the lung dose. Consequently, these results are very important since it illustrates that long term surviving patients might have to deal with serious pulmonary side effects which might result in an impaired quality of life.

3.5 Radioprotective Agents

In contrast to radiosensitizing agents, the contribution of agents preventing or reducing radiation induced toxicity is less investigated in clinical trials. The protective value of corticosteroids for RP observed in an animal study [78] could not be confirmed in a clinical study [79]. The use of the immunomodulating and anti-inflammatory agent Pentoxifylline (with effects on hypoxia, inhibition of DNA repair and apoptosis [80]) was protective in a small group (n=40) of breast and lung cancer patients concerning radiation induced lung toxicity [81] although a larger phase III trial could not confirm these results [82]. Another small randomized trial showed a survival benefit in the group patients receiving Pentoxifylline but no toxicity data was given [83]. Angiotensin converting enzyme inhibitor showed anti-fibrotic activity in the lung of irradiated rats [84] but a clinical study could not confirm these results [85]. More promising is a cytoprotective agent Amifostine which is a prodrug that is dephosphorylated by alkaline phosphatase in tissues to a pharmacologically-active free thiol metabolite. The metabolite can act as a scavenger of free radicals generated in tissues exposed to radiation. Amifostine concomitantly given decreased radiation-induced pulmonary injury without diminishing the therapeutic effect of radiation in randomized controlled trials for patients with locally advanced lung cancer [86-88]. Nevertheless, radioprotective agents are not generally used in the clinic. The use of radioprotective agents in future (dose-escalation) trials should be encouraged to evaluate the potential beneficial effect of these agents.

4. Biological Equivalent Dose Calculation after Hypofractionated RT

4.1 Linear Quadratic Model

For conventional fractionated RT the physical dose can be converted into a biological equivalent dose using the linear quadratic (LQ) model [89-91]. The LQ model is a simple mathematical model fitting log cell survival data as function of the dose and additionally enables clinical iso-effect calculations of fractionation schemes with different doses per fraction. Whether the calculation of the biological equivalent lung dose should be performed similarly for conventional fractionated as for hypofractionated schemes is an important question. The clinical applicability of the LQ model at higher fraction doses is uncertain and is questioned/discussed by many investigators [92-96]. Hall and Brenner [96] estimated from the iso-effect data of van der Kogel [97] (i.e. late-responding damage to the rat spinal cord) and Douglas and Fowler [98] (i.e. acute damage to the mouse skin) that the LQ model would be valid for single doses up to 20 Gy. Consequently, no differences would have been expected between different fractionation schemes if the equivalent doses (calculated with the LQ model) are similar. However, no clinical study validated this hypothesis. The fact that RP is the most evaluated toxicity endpoint after lung irradiation (whereby the LQ model with an α/β ratio of 3 Gy is generally accepted [56,99,100]) emphasize not only the clinical relevance but also the scientific importance of these results. Therefore, RP is an appropriate endpoint to evaluate the LQ model and modifications of the LQ model. Using the Normal Tissue Complication Probability (NTCP) model of Lyman [101] the curves of the probability of developing RP as a function of the mean lung dose were similar for hypofractionated RT and conventional fractionated RT if an α/β ratio of 3 Gy was used (Chapter 4). However, it should be questioned whether lung doses corrected according to modified LQ models might improve the predictive value (Chapter 6).

4.2 Modifications of the Linear Quadratic Model

4.2.1 Theoretical background

It is already known for a long time (1954) that for the high dose region the log cell survival is linear and not bending as represented by the definition of the LQ model [102]. To evaluate this issue, modifications of the LQ model were proposed based on cell line and animal iso-effect data [103,104]. These modifications fitted the experimental data better but clinical data was not evaluated. One of the above mentioned modifications of the LQ model was based on the Lethal-Potentially Lethal (LPL) model [105] and was developed by Guerrero et al. [104] (based on cell survival and animal toxicity data). The LPL was superior to the LQ model at higher dose regions fitting the experimental data. Nevertheless, the dose range where the LQ model started to deviate from the LPL model was rather large (cell lines: 0.6 Gy to 37.7 Gy, animal toxicity data: 2.6 Gy to 100 Gy). Carlone et al. [106] showed that

this modification proposed by Guerrero et al. [104] resulted in a LQ model with a linear extension and proposed the nomenclature of the linear-quadratic-linear model (LQL model) of the log cell survival as function of the dose for the high dose range [106]. More recently, Park et al. [103] used a linear extension of the log cell survival as function of the dose for doses higher than a threshold dose (i.e. transition dose d_T).

4.2.2 Clinical applicability

Because the modified LQ model by Guerrero et al. [104] and Park et al. [103] fitted the experimental data better after high single dose RT, this LQL model was evaluated with the clinical data set of Chapter 4. A linear extension of the log cell survival as function of the dose for doses higher than a threshold dose (i.e. transition dose d_T) was used for different values of d_T . The LQL model did not improve the Normal Tissue Complication Probability (NTCP) fits predicting RP for any of the evaluated d_T (Chapter 6).

The first reason for this might be that the evaluated d_T (0, 5, 7 and 9 Gy) were not the appropriate values for lung tissue. However, no higher values could be evaluated because if the d_T approaches the highest fraction dose the dose calculated by the LQL model will approach the dose calculated by the LQ model. As a result, the NTCP fits of the LQL model with d_T 's of 7 and 9 Gy were approaching the NTCP fit of the LQ model because fraction doses from 6 to 12 Gy were examined (only a limited part of the distribution of doses per fraction was larger than these d_T values).

The possibility to evaluate higher transition doses for schemes with higher fraction doses were also investigated (Chapter 6). Also for fraction doses of 18 Gy per fraction the introduction of a higher d_T values (> 10 Gy) would lead to imperceptible differences between the dose calculated with the LQ and the LQL model. Consequently, it might be questioned whether a higher d_T can be clinically evaluated in the future due to limited amount of lung tissue receiving these high doses. Animal studies might elucidate the hypothesis that the lung dose should be calculated according to the LQL model with higher d_T values for lung tissue irradiated with higher ($>> 18$ Gy) fraction doses. On the other hand higher d_T values will apparently not be of additional value in clinical practise.

Another reason that the LQL model did not improve the NTCP fit is that the used dose parameter is not appropriate for this analysis. The mean lung dose is a parameter whereby the high dose and low dose regions are averaged over the whole lung. The percentage lung volume receiving doses higher than a certain threshold dose is another frequently used parameter (see paragraph 3.2). In our analysis it was observed that the MLD and the higher threshold dose parameters were preferable above low threshold dose parameters. In addition, radiographic changes in symptomatic patients are mainly located in high dose lung regions [107,108]. Consequently, parameters

reflecting lung volume receiving high dose might be better suitable for this analysis. Again, to exclude clinical confounding factors, animal studies should be performed to evaluate different dose parameters. Nevertheless, our results indicate that new irradiation techniques with conformal orientated continuous irradiation (with high percentages lung volume receiving low doses, e.g. rapid arc and tomotherapy) will not be correlated with an increased incidence of RP.

[56,94,100].

The complexity of scoring RP (paragraph 3.1) may confound the dose-effect relation. Local dose effect relation derived from follow up SPECT perfusion changes or follow up CT density changes are other (possibly more objective) endpoints and has proven to be of additional value predicting radiation induced lung toxicity after conventional fractionated RT [109,110]. Clinical studies are ongoing to evaluate sequential SPECT scans after hypofractionated RT. Since the differences between the LQL model and LQ model originate from the high dose region, especially dose effect relations in the high dose region are of interest which can be derived from SPECT and CT scans. Another reason to study this is that higher doses per fraction is mainly influencing late term toxicity; late responding tissue is observed to have more bending (i.e. lower α/β ratio,) than early responding tissue. Because late term toxicity is clinically difficult to evaluate (paragraph 3.4), again, SPECT and CT changes are interesting end-points to evaluate the LQL model.

5. Accurate Targeting of the Irradiation

5.1 Setup errors

The introduction of 3D conformal RT and intensity-modulated RT (IMRT) enables conformal delivery of the irradiation to the tumour with the advantage of sparing normal tissue. However, the delivery of dose to the tumour with a conformal treatment plan is more difficult than if large irradiation fields are given since the position of the target is subject to geometric uncertainties due to variability in patient positioning and internal organ motion [111,112]. These geometric uncertainties can be divided in random errors (σ) (i.e. deviations that occurs between different fractions) and systematic errors (Σ) (i.e. deviation between the patient/tumour position of the treatment plan and the average patient/tumour position during treatment).

5.2 Electronic Portal Imaging Device

Setup errors can be verified by electronic portal image device (EPID) measurements performed during the treatment using the megavolt photons of the linear accelerator as source. According to these measurements, corrections can be performed in the remaining number of fractions (i.e. off-line correction protocol). An off-line correction protocol is reducing the systematic errors (random errors can only be corrected by an online correction protocol). Studies evaluating these setup errors

found similar results in the order of about 2 mm in all directions [113-115]. However, the accuracy of the EPID measurements itself could not be evaluated because a reference procedure (i.e. golden standard) was lacking.

5.3 Conebeam CT Scanner

A CBCT scanner consists of a kV source and imager with the central axis perpendicular to the treatment beam verifying the position of anatomical structures and tumour [116]. Consequently, the data from the kV CBCT allows accurate measurements of the systematic and random setup errors. With the introduction of the kV CBCT differences measured by EPID and CBCT according to the patient setup could be evaluated accurately (Chapter 7). The setup errors measured with CBCT were generally larger than those measured with EPID whereby the largest difference was observed in the cranial-caudal and anterior-posterior direction. Because it can be assumed that the CBCT system is the golden standard (confirmed by the highly accurate and precise measurements [117]) it should be questioned what causes the difference between the CBCT and EPID. First, the time interval between the CBCT and EPID measurements might introduce differences. However, Van Herk et al. [118] investigated the time interval between the CBCT registration and the EPID measurements. They observed that differences between the digital reconstructed radiographs (DRR) from the CBCT scans and the corresponding EPID images were smaller than < 1 mm [119]. Rotations (which can be measured by CBCT and not by EPID [120]) were not expected to influence the results significantly since only a weak correlation between the rotations and the differences between CBCT and EPID was observed (Chapter 7). It might be hypothesized that the region of interest (ROI) on the EPID (the vertebra, clavicles and ribs) is more subject to (respiratory) motion than the ROI of the CBCT. This should have resulted in larger setup errors for the EPID compared to the CBCT (region of interest was the vertebra). However, this is the opposite of what was observed (Chapter 7).

Registration of the images of the EPID is more difficult due to the poorer quality compared to CBCT images. As a result, fewer corrections might be applied because they were not considered as necessary. Consequently, an underestimation of the setup error, which was statistically significant, was found (Chapter 7).

5.4 Correction protocols

For conventional fractionated RT treatment schedules mainly off-line correction protocols are used to correct for systematic setup errors. However for hypofractionated regimens only a few fractions with a very high dose are given and high irradiation accuracy is a necessity whereby also random setup errors should be minimized. Also inter-fraction changes of tumour volume, tumour position and pulmonary anatomy and a differential motion between multiple targets can have a major influence on the

delivered dose. Knowledge of the target position(s) and motion is therefore essential before irradiation. Using an online correction protocol whereby not only the patient position is verified but also the target position and motion is determined is possible by the introduction of a 4D-CBCT scan. This scan provides information whether the current treatment plan is covering the target or that the position should be corrected before the irradiation is delivered. In current practice, before all hypofractionated irradiation fractions a 4D-CBCT is performed. For conventional RT treatments a 4D-CBCT is acquired weekly (after a daily acquisition in the first week).

5.5 Dose Escalation and Adaptive Radiotherapy

For higher tumour control probabilities (TCP) dose escalation is needed. For total doses up to 66 Gy, only 17 % one year tumour control is observed (without chemotherapy) [121]. TCP modelling studies estimated that for a TCP of 50% the dose should be escalated to more than 84 Gy in fraction doses of 1.8-2 Gy [122]. Since dose escalation is limited due to toxicity reduction of the normal tissue dose is needed. 4D CT treatment planning [123], the use of specific respiratory position scans (i.e. mid-ventilation scan) [124] and modified IMRT techniques [125,126] can reduce the normal tissue dose as retrospectively observed in dose modelling studies. Limiting the dose escalation to specific tumour regions of interest and not the whole tumour (paragraph 2.1 and 2.2) may also limit the dose to the normal structures. The success rate of these techniques is dependent on the accuracy of the knowledge of the tumour position (and specific tumour regions). Consequently, the introduction of accurate imaging modalities (e.g. CBCT) on the treatment machines whereby adaptive RT can be applied will have a major impact on the prognosis of lung cancer patients in the near future.

References

1. Perez CA, Bauer M, Edelstein S *et al.* Impact of tumor control on survival in carcinoma of the lung treated with irradiation. *Int J Radiat Oncol Biol Phys* 1986;12:539-547.
2. Belderbos JS, De Jaeger K, Heemsbergen WD *et al.* First results of a phase I/II dose escalation trial in non-small cell lung cancer using three-dimensional conformal radiotherapy. *Radiother Oncol* 2003;66:119-126.
3. Goldstraw P, Crowley J, Chansky K *et al.* The IASLC Lung Cancer Staging Project: proposals for the revision of the TNM stage groupings in the forthcoming (seventh) edition of the TNM Classification of malignant tumours. *J Thorac Oncol* 2007;2:706-714.
4. Fischer BM, Mortensen J, Hojgaard L. Positron emission tomography in the diagnosis and staging of lung cancer: a systematic, quantitative review. *Lancet Oncol* 2001;2:659-666.
5. Gould MK, Kuschner WG, Rydzak CE *et al.* Test performance of positron emission tomography and computed tomography for mediastinal staging in patients with non-small-cell lung cancer: a meta-analysis. *Ann Intern Med* 2003;139:879-892.
6. Nestle U, Walter K, Schmidt S *et al.* 18F-deoxyglucose positron emission tomography (FDG-PET) for the planning of radiotherapy in lung cancer: high impact in patients with atelectasis. *Int J Radiat Oncol Biol Phys* 1999;44:593-597.
7. Ashamalla H, Rafla S, Parikh K *et al.* The contribution of integrated PET/CT to the evolving definition of treatment volumes in radiation treatment planning in lung cancer. *Int J Radiat Oncol Biol Phys* 2005;63:1016-1023.
8. Bradley J, Thorstad WL, Mutic S *et al.* Impact of FDG-PET on radiation therapy volume delineation in non-small-cell lung cancer. *Int J Radiat Oncol Biol Phys* 2004;59:78-86.
9. Erdi YE, Rosenzweig K, Erdi AK *et al.* Radiotherapy treatment planning for patients with non-small cell lung cancer using positron emission tomography (PET). *Radiother Oncol* 2002;62:51-60.
10. Mah K, Caldwell CB, Ung YC *et al.* The impact of (18)FDG-PET on target and critical organs in CT-based treatment planning of patients with poorly defined non-small-cell lung carcinoma: a prospective study. *Int J Radiat Oncol Biol Phys* 2002;52:339-350.
11. Steenbakkens R, Duppen J, Fitton I *et al.* A 3D Analysis and Reduction of Observer Variation in Delineation of Lung Cancer for Radiotherapy. *ASTRO 2004 Abstract 2327* 2004.
12. Deniaud-Alexandre E, Touboul E, Lerouge D *et al.* Impact of computed tomography and 18F-deoxyglucose coincidence detection emission tomography image fusion for optimization of conformal radiotherapy in non-small-cell lung cancer. *Int J Radiat Oncol Biol Phys* 2005;63:1432-1441.
13. Der Wel A, Nijsten S, Hochstenbag M *et al.* Increased therapeutic ratio by 18FDG-PET CT planning in patients with clinical CT stage N2-N3M0 non-small-cell lung cancer: a modeling study. *Int J Radiat Oncol Biol Phys* 2005;61:649-655.

Chapter 8

14. Giraud P, Grahek D, Montravers F *et al.* CT and (18)F-deoxyglucose (FDG) image fusion for optimization of conformal radiotherapy of lung cancers. *Int J Radiat Oncol Biol Phys* 2001;49:1249-1257.
15. Grills IS, Yan D, Black QC *et al.* Clinical implications of defining the gross tumor volume with combination of CT and 18FDG-positron emission tomography in non-small-cell lung cancer. *Int J Radiat Oncol Biol Phys* 2007;67:709-719.
16. Vanuytsel LJ, Vansteenkiste JF, Stroobants SG *et al.* The impact of (18)F-fluoro-2-deoxy-D-glucose positron emission tomography (FDG-PET) lymph node staging on the radiation treatment volumes in patients with non-small cell lung cancer. *Radiother Oncol* 2000;55:317-324.
17. De Ruyscher D, Wanders S, Minken A *et al.* Effects of radiotherapy planning with a dedicated combined PET-CT-simulator of patients with non-small cell lung cancer on dose limiting normal tissues and radiation dose-escalation: a planning study. *Radiother Oncol* 2005;77:5-10.
18. Kiffer JD, Berlangieri SU, Scott AM *et al.* The contribution of 18F-fluoro-2-deoxyglucose positron emission tomographic imaging to radiotherapy planning in lung cancer. *Lung Cancer* 1998;19:167-177.
19. MacManus M, D'Costa I, Everitt S *et al.* Comparison of CT and positron emission tomography/CT coregistered images in planning radical radiotherapy in patients with non-small-cell lung cancer. *Australas Radiol* 2007;51:386-393.
20. Warburg O. On respiratory impairment in cancer cells. *Science* 1956;124:269-270.
21. Brundage MD, Davies D, Mackillop WJ. Prognostic factors in non-small cell lung cancer: a decade of progress. *Chest* 2002;122:1037-1057.
22. Harpole DH, Jr., Richards WG, Herndon JE *et al.* Angiogenesis and molecular biologic substaging in patients with stage I non-small cell lung cancer. *Ann Thorac Surg* 1996;61:1470-1476.
23. Younes M, Brown RW, Stephenson M *et al.* Overexpression of Glut1 and Glut3 in stage I nonsmall cell lung carcinoma is associated with poor survival. *Cancer* 1997;80:1046-1051.
24. Duhaylongsod FG, Lowe VJ, Patz EF, Jr. *et al.* Lung tumor growth correlates with glucose metabolism measured by fluoride-18 fluorodeoxyglucose positron emission tomography. *Ann Thorac Surg* 1995;60:1348-1352.
25. Nelson CA, Wang JQ, Leav I *et al.* The interaction among glucose transport, hexokinase, and glucose-6-phosphatase with respect to 3H-2-deoxyglucose retention in murine tumor models. *Nucl Med Biol* 1996;23:533-541.
26. Vesselle H, Schmidt RA, Pugsley JM *et al.* Lung cancer proliferation correlates with [F-18]fluorodeoxyglucose uptake by positron emission tomography. *Clin Cancer Res* 2000;6:3837-3844.
27. Ahuja V, Coleman RE, Herndon J *et al.* The prognostic significance of fluorodeoxyglucose positron emission tomography imaging for patients with nonsmall cell lung carcinoma. *Cancer* 1998;83:918-924.
28. Dhital K, Saunders CA, Seed PT *et al.* [(18)F]Fluorodeoxyglucose positron emission tomography and its prognostic value in lung cancer. *Eur J Cardiothorac Surg* 2000;18:425-428.

29. Downey RJ, Akhurst T, Gonen M *et al.* Preoperative F-18 fluorodeoxyglucose-positron emission tomography maximal standardized uptake value predicts survival after lung cancer resection. *J Clin Oncol* 2004;22:3255-3260.
30. Higashi K, Ueda Y, Arisaka Y *et al.* 18F-FDG uptake as a biologic prognostic factor for recurrence in patients with surgically resected non-small cell lung cancer. *J Nucl Med* 2002;43:39-45.
31. Jeong HJ, Min JJ, Park JM *et al.* Determination of the prognostic value of [(18)F] fluorodeoxyglucose uptake by using positron emission tomography in patients with non-small cell lung cancer. *Nucl Med Commun* 2002;23:865-870.
32. Sasaki R, Komaki R, Macapinlac H *et al.* [18F]Fluorodeoxyglucose Uptake by Positron Emission Tomography Predicts Outcome of Non-Small-Cell Lung Cancer. *J Clin Oncol* 2005;23:1136-1143.
33. Vansteenkiste JF, Stroobants SG, Dupont PJ *et al.* Prognostic importance of the standardized uptake value on (18)F-fluoro-2-deoxy-glucose-positron emission tomography scan in non-small-cell lung cancer: An analysis of 125 cases. Leuven Lung Cancer Group. *J Clin Oncol* 1999;17:3201-3206.
34. Steel GG. Basic Clinical Radiobiology, Text book. 3ed. 1997.
35. Mac Manus MP, Hicks RJ, Matthews JP *et al.* Metabolic (FDG-PET) response after radical radiotherapy/chemoradiotherapy for non-small cell lung cancer correlates with patterns of failure. *Lung Cancer* 2005;49:95-108.
36. Aerts HJ, van Baardwijk AA, Petit SF *et al.* Identification of residual metabolic-active areas within individual NSCLC tumours using a pre-radiotherapy (18) Fluorodeoxyglucose-PET-CT scan. *Radiother Oncol* 2009;91:386-392.
37. Nordmark M, Overgaard M, Overgaard J. Pretreatment oxygenation predicts radiation response in advanced squamous cell carcinoma of the head and neck. *Radiother Oncol* 1996;41:31-39.
38. Overgaard J. Hypoxic radiosensitization: adored and ignored. *J Clin Oncol* 2007;25:4066-4074.
39. Porter JR. Louis PASTEUR; achievements and disappointments, 1861. *Bacteriol Rev* 1961;25:389-403.
40. Porter JR. Louis Pasteur sesquicentennial (1822-1972). *Science* 1972;178:1249-1254.
41. Cherk MH, Foo SS, Poon AM *et al.* Lack of correlation of hypoxic cell fraction and angiogenesis with glucose metabolic rate in non-small cell lung cancer assessed by 18F-Fluoromisonidazole and 18F-FDG PET. *J Nucl Med* 2006;47:1921-1926.
42. Buck AK, Glatting G, Reske SN. Quantification of 18F-FDG uptake in non-small cell lung cancer: a feasible prognostic marker? *J Nucl Med* 2004;45:1274-1276.
43. Tatum JL, Kelloff GJ, Gillies RJ *et al.* Hypoxia: importance in tumor biology, noninvasive measurement by imaging, and value of its measurement in the management of cancer therapy. *Int J Radiat Biol* 2006;82:699-757.
44. Overgaard J, Hansen HS, Overgaard M *et al.* A randomized double-blind phase III study of nimorazole as a hypoxic radiosensitizer of primary radiotherapy in supraglottic larynx and pharynx carcinoma. Results of the Danish Head and Neck Cancer Study (DAHANCA) Protocol 5-85. *Radiother Oncol* 1998;46:135-146.

Chapter 8

45. Eschmann SM, Paulsen F, Reimold M *et al.* Prognostic impact of hypoxia imaging with 18F-misonidazole PET in non-small cell lung cancer and head and neck cancer before radiotherapy. *J Nucl Med* 2005;46:253-260.
46. Lee NY, Mechalakos JG, Nehmeh S *et al.* Fluorine-18-labeled fluoromisonidazole positron emission and computed tomography-guided intensity-modulated radiotherapy for head and neck cancer: a feasibility study. *Int J Radiat Oncol Biol Phys* 2008;70:2-13.
47. Busk M, Horsman MR, Jakobsen S *et al.* Cellular uptake of PET tracers of glucose metabolism and hypoxia and their linkage. *Eur J Nucl Med Mol Imaging* 2008;35:2294-2303.
48. Boellaard R, Krak NC, Hoekstra OS *et al.* Effects of noise, image resolution, and ROI definition on the accuracy of standard uptake values: a simulation study. *J Nucl Med* 2004;45:1519-1527.
49. Berghmans T, Dusart M, Paesmans M *et al.* Primary tumor standardized uptake value (SUVmax) measured on fluorodeoxyglucose positron emission tomography (FDG-PET) is of prognostic value for survival in non-small cell lung cancer (NSCLC): a systematic review and meta-analysis (MA) by the European Lung Cancer Working Party for the IASLC Lung Cancer Staging Project. *J Thorac Oncol* 2008;3:6-12.
50. Anscher MS, Kong FM, Andrews K *et al.* Plasma transforming growth factor beta1 as a predictor of radiation pneumonitis. *Int J Radiat Oncol Biol Phys* 1998;41:1029-1035.
51. Chen Y, Williams J, Ding I *et al.* Radiation pneumonitis and early circulatory cytokine markers. *Semin Radiat Oncol* 2002;12:26-33.
52. De Ruyscher D, Dehing C, Yu S *et al.* Dyspnea evolution after high-dose radiotherapy in patients with non-small cell lung cancer. *Radiother Oncol* 2008;
53. Borst GR, Belderbos J, Burgers S *et al.* In response to: Dyspnea evaluation after high-dose radiotherapy in patients with NSCLC De Ruyscher *et al.* *Radiother Oncol* 2009;
54. Fay M, Tan A, Fisher R *et al.* Dose-volume histogram analysis as predictor of radiation pneumonitis in primary lung cancer patients treated with radiotherapy. *Int J Radiat Oncol Biol Phys* 2005;61:1355-1363.
55. Kim TH, Cho KH, Pyo HR *et al.* Dose-volumetric parameters for predicting severe radiation pneumonitis after three-dimensional conformal radiation therapy for lung cancer. *Radiology* 2005;235:208-215.
56. Kwa SL, Lebesque JV, Theuws JC *et al.* Radiation pneumonitis as a function of mean lung dose: an analysis of pooled data of 540 patients. *Int J Radiat Oncol Biol Phys* 1998;42:1-9.
57. Rodrigues G, Lock M, D'Souza D *et al.* Prediction of radiation pneumonitis by dose - volume histogram parameters in lung cancer--a systematic review. *Radiother Oncol* 2004;71:127-138.
58. Wang S, Liao Z, Wei X *et al.* Analysis of clinical and dosimetric factors associated with treatment-related pneumonitis (TRP) in patients with non-small-cell lung cancer (NSCLC) treated with concurrent chemotherapy and three-

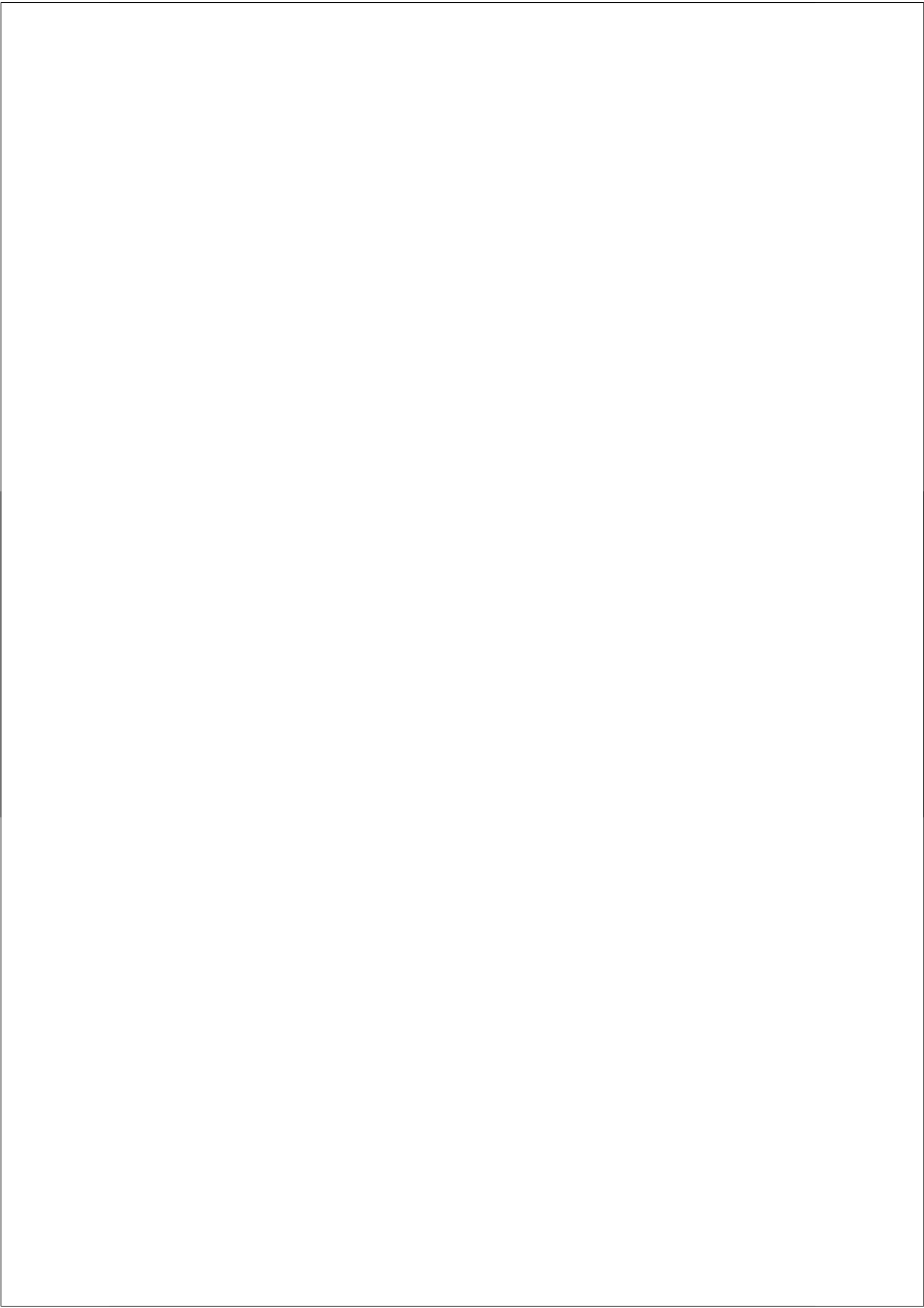
- dimensional conformal radiotherapy (3D-CRT). *Int J Radiat Oncol Biol Phys* 2006;66:1399-1407.
59. Yorke ED, Jackson A, Rosenzweig KE *et al.* Correlation of dosimetric factors and radiation pneumonitis for non-small-cell lung cancer patients in a recently completed dose escalation study. *Int J Radiat Oncol Biol Phys* 2005;63:672-682.
 60. De Jaeger K, Hoogeman MS, Engelsman M *et al.* Incorporating an improved dose-calculation algorithm in conformal radiotherapy of lung cancer: re-evaluation of dose in normal lung tissue. *Radiother Oncol* 2003;69:1-10.
 61. Jin H, Tucker SL, Liu HH *et al.* Dose-volume thresholds and smoking status for the risk of treatment-related pneumonitis in inoperable non-small cell lung cancer treated with definitive radiotherapy. *Radiother Oncol* 2008;
 62. McDonald S, Rubin P, Phillips TL *et al.* Injury to the lung from cancer therapy: clinical syndromes, measurable endpoints, and potential scoring systems. *Int J Radiat Oncol Biol Phys* 1995;31:1187-1203.
 63. Monson JM, Stark P, Reilly JJ *et al.* Clinical radiation pneumonitis and radiographic changes after thoracic radiation therapy for lung carcinoma. *Cancer* 1998;82:842-850.
 64. Rancati T, Ceresoli GL, Gagliardi G *et al.* Factors predicting radiation pneumonitis in lung cancer patients: a retrospective study. *Radiother Oncol* 2003;67:275-283.
 65. Robnett TJ, Machtay M, Vines EF *et al.* Factors predicting severe radiation pneumonitis in patients receiving definitive chemoradiation for lung cancer. *Int J Radiat Oncol Biol Phys* 2000;48:89-94.
 66. Yamashita H, Nakagawa K, Nakamura N *et al.* Exceptionally high incidence of symptomatic grade 2-5 radiation pneumonitis after stereotactic radiation therapy for lung tumors. *Radiat Oncol* 2007;2:1-11.
 67. Aoki T, Nagata Y, Negoro Y *et al.* Evaluation of lung injury after three-dimensional conformal stereotactic radiation therapy for solitary lung tumors: CT appearance. *Radiology* 2004;230:101-108.
 68. Guckenberger M, Heilman K, Wulf J *et al.* Pulmonary injury and tumor response after stereotactic body radiotherapy (SBRT): results of a serial follow-up CT study. *Radiother Oncol* 2007;85:435-442.
 69. McGarry RC, Papiez L, Williams M *et al.* Stereotactic body radiation therapy of early-stage non-small-cell lung carcinoma: phase I study. *Int J Radiat Oncol Biol Phys* 2005;63:1010-1015.
 70. Nagata Y, Takayama K, Matsuo Y *et al.* Clinical outcomes of a phase I/II study of 48 Gy of stereotactic body radiotherapy in 4 fractions for primary lung cancer using a stereotactic body frame. *Int J Radiat Oncol Biol Phys* 2005;63:1427-1431.
 71. Zimmermann FB, Geinitz H, Schill S *et al.* Stereotactic hypofractionated radiotherapy in stage I (T1-2 N0 M0) non-small-cell lung cancer (NSCLC). *Acta Oncol* 2006;45:796-801.
 72. Blomgren H, Lax I, Naslund I *et al.* Stereotactic high dose fraction radiation therapy of extracranial tumors using an accelerator. Clinical experience of the first thirty-one patients. *Acta Oncol* 1995;34:861-870.
 73. Forquer JA, Fakiris AJ, Timmerman RD *et al.* Brachial plexopathy from stereotactic body

- radiotherapy in early-stage NSCLC: Dose-limiting toxicity in apical tumor sites. *Radiother Oncol* 2009;
74. Dunlap NE, Cai J, Biedermann GB *et al.* Chest Wall Volume Receiving >30 Gy Predicts Risk of Severe Pain and/or Rib Fracture After Lung Stereotactic Body Radiotherapy. *Int J Radiat Oncol Biol Phys* 2009;
 75. Hoppe BS, Laser B, Kowalski AV *et al.* Acute skin toxicity following stereotactic body radiation therapy for stage I non-small-cell lung cancer: who's at risk? *Int J Radiat Oncol Biol Phys* 2008;72:1283-1286.
 76. Timmerman R, McGarry R, Yiannoutsos C *et al.* Excessive toxicity when treating central tumors in a phase II study of stereotactic body radiation therapy for medically inoperable early-stage lung cancer. *J Clin Oncol* 2006;24:4833-4839.
 77. Theuvs JC, Kwa SL, Wagenaar AC *et al.* Prediction of overall pulmonary function loss in relation to the 3-D dose distribution for patients with breast cancer and malignant lymphoma. *Radiother Oncol* 1998;49:233-243.
 78. Gross NJ, Narine KR, Wade R. Protective effect of corticosteroids on radiation pneumonitis in mice. *Radiat Res* 1988;113:112-119.
 79. Kwok E, Chan CK. Corticosteroids and azathioprine do not prevent radiation-induced lung injury. *Can Respir J* 1998;5:211-214.
 80. Amano M, Monzen H, Suzuki M *et al.* Increase in tumor oxygenation and potentiation of radiation effects using pentoxifylline, vinpocetine and ticlopidine hydrochloride. *J Radiat Res (Tokyo)* 2005;46:373-378.
 81. Ozturk B, Egehan I, Atavci S *et al.* Pentoxifylline in prevention of radiation-induced lung toxicity in patients with breast and lung cancer: a double-blind randomized trial. *Int J Radiat Oncol Biol Phys* 2004;58:213-219.
 82. Kwon HC, Kim SK, Chung WK *et al.* Effect of pentoxifylline on radiation response of non-small cell lung cancer: a phase III randomized multicenter trial. *Radiother Oncol* 2000;56:175-179.
 83. Misirlioglu CH, Demirkasimoglu T, Kucukplakci B *et al.* Pentoxifylline and alphatocopherol in prevention of radiation-induced lung toxicity in patients with lung cancer. *Med Oncol* 2007;24:308-311.
 84. Ward WF, Molteni A, Ts'ao CH. Radiation-induced endothelial dysfunction and fibrosis in rat lung: modification by the angiotensin converting enzyme inhibitor CL242817. *Radiat Res* 1989;117:342-350.
 85. Wang LW, Fu XL, Clough R *et al.* Can angiotensin-converting enzyme inhibitors protect against symptomatic radiation pneumonitis? *Radiat Res* 2000;153:405-410.
 86. Antonadou D. Radiotherapy or chemotherapy followed by radiotherapy with or without amifostine in locally advanced lung cancer. *Semin Radiat Oncol* 2002;12:50-58.
 87. Antonadou D, Petridis A, Synodinou M *et al.* Amifostine reduces radiochemotherapy-induced toxicities in patients with locally advanced non-small cell lung cancer. *Semin Oncol* 2003;30:2-9.
 88. Mell LK, Malik R, Komaki R *et al.* Effect of amifostine on response rates in locally advanced non-small-cell lung cancer patients treated on randomized controlled trials: a meta-analysis. *Int J Radiat Oncol Biol Phys* 2007;68:111-118.

89. Fowler JF. The first James Kirk memorial lecture. What next in fractionated radiotherapy? *Br J Cancer Suppl* 1984;6:285-300.
90. Tucker SL. Tests for the fit of the linear-quadratic model to radiation isoeffect data. *Int J Radiat Oncol Biol Phys* 1984;10:1933-1939.
91. Thames HD, Jr., Withers HR, Peters LJ *et al.* Changes in early and late radiation responses with altered dose fractionation: implications for dose-survival relationships. *Int J Radiat Oncol Biol Phys* 1982;8:219-226.
92. Barendsen GW. Dose fractionation, dose rate and iso-effect relationships for normal tissue responses. *Int J Radiat Oncol Biol Phys* 1982;8:1981-1997.
93. Denekamp J, Waites T, Fowler JF. Predicting realistic RBE values for clinically relevant radiotherapy schedules. *Int J Radiat Biol* 1997;71:681-694.
94. Fowler JF, Tome WA, Fenwick JD *et al.* A challenge to traditional radiation oncology. *Int J Radiat Oncol Biol Phys* 2004;60:1241-1256.
95. Hall EJ, Brenner DJ. The radiobiology of radiosurgery: rationale for different treatment regimes for AVMs and malignancies. *Int J Radiat Oncol Biol Phys* 1993;25:381-385.
96. Marks LB. Extrapolating hypofractionated radiation schemes from radiosurgery data: regarding Hall *et al.*, *IJROBP* 21:819-824; 1991 and Hall and Brenner, *IJROBP* 25:381-385; 1993. *Int J Radiat Oncol Biol Phys* 1995;32:274-276.
97. van der Kogel AJ. Chronic effects of neutrons and charged particles on spinal cord, lung, and rectum. *Radiat Res Suppl* 1985;8:S208-S216.
98. Douglas BG, Fowler JF. The effect of multiple small doses of x rays on skin reactions in the mouse and a basic interpretation. *Radiat Res* 1976;66:401-426.
99. Fowler JF. The linear-quadratic formula and progress in fractionated radiotherapy. *Br J Radiol* 1989;62:679-694.
100. Thames HD, Ang KK, Stewart FA *et al.* Does incomplete repair explain the apparent failure of the basic LQ model to predict spinal cord and kidney responses to low doses per fraction? *Int J Radiat Biol* 1988;54:13-19.
101. Lyman JT. Complication probability as assessed from dose-volume histograms. *Radiat Res Suppl* 1985;8:S13-S19.
102. Puck T, Marcus P. Action of x-rays on mammalian cells. *J Exp Med* 1956;103:653-666.
103. Park C, Papiez L, Zhang S *et al.* Universal survival curve and single fraction equivalent dose: useful tools in understanding potency of ablative radiotherapy. *Int J Radiat Oncol Biol Phys* 2008;70:847-852.
104. Guerrero M, Li XA. Extending the linear-quadratic model for large fraction doses pertinent to stereotactic radiotherapy. *Phys Med Biol* 2004;49:4825-4835.
105. Curtis SB. Lethal and potentially lethal lesions induced by radiation--a unified repair model. *Radiat Res* 1986;106:252-270.
106. Carlone M, Wilkins D, Raaphorst P. The modified linear-quadratic model of Guerrero and Li can be derived from a mechanistic basis and exhibits linear-quadratic-linear behaviour. *Phys Med Biol* 2005;50:L9-13.
107. Arbetter KR, Prakash UB, Tazelaar HD *et al.* Radiation-induced pneumonitis in the "nonirradiated" lung. *Mayo Clin Proc* 1999;74:27-36.
108. Monson JM, Stark P, Reilly JJ *et al.* Clinical radiation pneumonitis and radiographic

- changes after thoracic radiation therapy for lung carcinoma. *Cancer* 1998;82:842-850.
109. Ma J, Zhang J, Zhou S *et al.* Association between RT-induced changes in lung tissue density and global lung function. *Int J Radiat Oncol Biol Phys* 2009;74:781-789.
110. Zhang J, Ma J, Zhou S *et al.* Radiation-Induced Reductions in Regional Lung Perfusion: 0.1–12 Year Data from a Prospective Clinical Study. *Int J Radiat Oncol Biol Phys* . 2009. In Press.
111. Engelsman M, Damen EM, De Jaeger K *et al.* The effect of breathing and set-up errors on the cumulative dose to a lung tumor. *Radiother Oncol* 2001;60:95-105.
112. Langen KM, Jones DT. Organ motion and its management. *Int J Radiat Oncol Biol Phys* 2001;50:265-278.
113. Erridge SC, Seppenwoolde Y, Muller SH *et al.* Portal imaging to assess set-up errors, tumor motion and tumor shrinkage during conformal radiotherapy of non-small cell lung cancer. *Radiother Oncol* 2003;66:75-85.
114. de Boer HC, Van Sornsens de Koste JR, Senan S *et al.* Analysis and reduction of 3D systematic and random setup errors during the simulation and treatment of lung cancer patients with CT-based external beam radiotherapy dose planning. *Int J Radiat Oncol Biol Phys* 2001;49:857-868.
115. Van Sornsens de Koste JR, de Boer HC, Schuchhard-Schipper RH *et al.* Procedures for high precision setup verification and correction of lung cancer patients using CT-simulation and digitally reconstructed radiographs (DRR). *Int J Radiat Oncol Biol Phys* 2003;55:804-810.
116. Jaffray DA, Siewerdsen JH, Wong JW *et al.* Flat-panel cone-beam computed tomography for image-guided radiation therapy. *Int J Radiat Oncol Biol Phys* 2002;53:1337-1349.
117. Sharpe MB, Moseley DJ, Purdie TG *et al.* The stability of mechanical calibration for a kV cone beam computed tomography system integrated with linear accelerator. *Med Phys* 2006;33:136-144.
118. van Herk M, Bentgen A, Remeijer P *et al.* Comparison of setup error determined with EPID and with cone beam CT for lung cancer patients - how accurate is EPID image analysis in clinical practice for a difficult site? *International Workshop Electronic Portal Imaging, Brighton Abstract* 2004;
119. van Herk M, Bentgen A, Remeijer P *et al.* Comparison of setup error determined with EPID and with cone beam CT for lung cancer patients - how accurate is EPID image analysis in clinical practice for a difficult site? *International Workshop Electronic Portal Imaging, Brighton Abstract* 2004;
120. Remeijer P, Geerlof E, Ploeger L *et al.* 3-D portal image analysis in clinical practice: an evaluation of 2-D and 3-D analysis techniques as applied to 30 prostate cancer patients. *Int J Radiat Oncol Biol Phys* 2000;46:1281-1290.
121. Le CT, Arriagada R, Quoix E *et al.* Radiotherapy alone versus combined chemotherapy and radiotherapy in unresectable non-small cell lung carcinoma. *Lung Cancer* 1994;10 Suppl 1:S239-S244.

122. Martel MK, Ten Haken RK, Hazuka MB *et al.* Estimation of tumor control probability model parameters from 3-D dose distributions of non-small cell lung cancer patients. *Lung Cancer* 1999;24:31-37.
123. Weiss E, Wijesooriya K, Dill SV *et al.* Tumor and normal tissue motion in the thorax during respiration: Analysis of volumetric and positional variations using 4D CT. *Int J Radiat Oncol Biol Phys* 2007;67:296-307.
124. Wolthaus JW, Schneider C, Sonke JJ *et al.* Mid-ventilation CT scan construction from four-dimensional respiration-correlated CT scans for radiotherapy planning of lung cancer patients. *Int J Radiat Oncol Biol Phys* 2006;65:1560-1571.
125. Partridge M, Tree A, Brock J *et al.* Improvement in tumour control probability with active breathing control and dose escalation: a modelling study. *Radiother Oncol* 2009;91:325-329.
126. St-Hilaire J, Sevigny C, Beaulieu F *et al.* Dose escalation in the radiotherapy of non-small-cell lung cancer with aperture-based intensity modulation and photon beam energy optimization for non-preselected patients. *Radiother Oncol* 2009;91:342-348.



Appendices

Summary

Samenvatting

LQ-model modification chapter 6

List of publications

Curriculum Vitae

Acknowledgements

Abbreviations

Summary

Lung cancer is the most common cause of cancer related deaths. Radiotherapy (RT) is an important treatment modality for lung cancer patients since many patients are inoperable. The inoperability is caused by the often advanced stage of lung cancer at presentation but also because the physical performance of many patients is insufficient to undergo surgery (often due to pulmonary comorbidity).

The prognosis of irradiated lung cancer patients is poor due to a high probability of early progression of the tumour and/or metastasis. To improve the prognosis, higher doses should be given to the tumour and the selection of patients benefitting from this higher doses should be improved. Currently, the choice of treatment, which are categorized fractionation schemes, are mainly determined by the tumour stage and the patients' physical performance. Individualized regimens whereby the dose to the tumour is escalated as function of tumour/patient characteristics and normal tissue tolerance is a promising treatment approach. This new principle of treatment requires advanced irradiation techniques, adequate models predicting the normal tissue complication probability and a good patient selection. These topics are evaluated and discussed in the studies included in this thesis.

[¹⁸F]fluorodeoxyglucose (FDG) positron emission tomography (PET) scans is a standard investigation performed during the work up of lung cancer patients for staging and RT delineation purposes. The FDG uptake in the tumour can be determined by the Standardized Uptake Value (SUV). The maximum SUV was of significant prognostic value for the disease specific and overall survival of the patient (Chapter 2). The prognostic value was independent from tumour stage and patients' performance (Chapter 2). As a result, the maximum SUV value can play an important role in the selection of patients and tumour regions benefitting from dose escalation which is investigated in ongoing studies.

Normal tissue complication probability (NTCP) models are important to estimate the risk of adverse events. A dangerous side effect for lung cancer patients is radiation pneumonitis (RP). Previous studies found a relation between dose and RP after conventional fractionated RT. No functional lung parameters were found to have a contributively value to predict RP prospectively and the lung dose remains the most important parameter estimating the probability of RP (Chapter 3). The difficulty to improve predictive models reflects the complexity of this topic and the need for more studies.

Calculating tumour control and normal tissue complication probabilities from dose parameters requires a dose conversion. For conventional fractionated RT the linear

quadratic (LQ) model is extensively validated and generally used for dose conversion to estimate the probabilities of clinical endpoints (i.e. tumour control and normal tissue toxicity). Although the use of hypofractionated RT for lung tumours is increasing, the relation between dose and RP is unknown. Also the applicability of the LQ model is uncertain.

A similar relation between the probability of RP as function of the dose was observed between hypofractionated RT and conventional fractionated RT (Chapter 4). Moreover, the time onset of RP was similar between hypofractionated RT and conventional fractionated RT (Chapter 4).

The LQ model can also be used for the dose conversion after hypofractionated RT to estimate the probability of RP (Chapter 6). Modifications of the LQ model according to cell data, did not improve the predictive value of the lung dose predicting RP (Chapter 6). The dose response relation for RP and the validation of the LQ model after hypofractionated RT is of great interest for current clinical practise (e.g. irradiating larger tumours and re-irradiations) and future trials (e.g. defining dose constraints).

Since lung cancer has a poor prognosis, little is known about the long term consequences of RT on the pulmonary function. The pulmonary function of a group of lung cancer patients fortunate with a long term disease free survival was irreversible deteriorated at longer follow up (Chapter 5). The pulmonary function of patients suffering from pulmonary co-morbidity declined more compared to other patients (Chapter 5). The decline seems to be correlated with the lung dose (Chapter 5). This study is indicative of what can be expected if the prognosis of lung cancer patients is improving. As a result, all possibilities to limit the lung dose should be investigated, explored and applied.

More sophisticated irradiation techniques whereby higher doses to the tumour and lower doses to normal structures can be planned and delivered are dependent of the verification of what is thought to be irradiated and what is truly irradiated. Consequently, appropriate imaging techniques, visualising the regions of interest (tumour and normal structures), before and after irradiation are of great importance. The introduction of linear accelerators equipped with a Cone Beam CT (CBCT) scanner is a major improvement for visualising the tumour and normal structures. Nevertheless, older verification techniques are still in wide spread use.

Comparing the CBCT with the older verification technique showed significant difference (Chapter 7). The patients setup variability is underestimated if the older technique is used (Chapter 7). Knowledge about this difference is important for the irradiation of patients and new treatment protocols should only be implemented with much caution and sufficient quality control.

Appendices

Samenvatting

De meest voorkomende kanker gerelateerde sterfte is long kanker. Radiotherapie (in bepaalde omstandigheden gecombineerd met chemotherapie) is een belangrijke behandeling tegen longkanker. Veel patiënten kunnen niet geopereerd worden doordat de ziekte in een te ver gevorderd stadium is bij de diagnose of omdat de fysieke toestand te slecht is om een operatie te ondergaan (vaak ten gevolge van long ziekten die ook veroorzaakt zijn door roken).

De prognose van veel bestraalde longkanker patiënten is niet goed en de kans is groot dat de tumor terugkomt of uitzaait. Om de prognose te verbeteren na bestraling moet een hoge(re) bestralingsdosis aan de tumor worden gegeven wat een hogere complicatie kans voor het omliggende weefsel met zich meebrengt. Daarom moet er meer inzicht komen in welke patiënten baat hebben bij een hoge dosis en of de risico's van de hoge bestralingsdosis niet te groot zijn. Momenteel wordt het bestralingschema met name bepaald door het tumor stadium en de fysieke conditie van een patiënt. Geïndividualiseerde behandelingsschema's waarbij de dosis voor de tumor verhoogd wordt afhankelijk van specifieke tumor en patiënten factoren en de tolerantie van omliggende normale weefsels is een werkwijze die een verbetering van de prognose kan betekenen. Echter, deze aanpak vergt geavanceerde bestralings technieken, modellen die normale weefsel schade kunnen voorspellen en een goede selectie van patiënten. Deze factoren worden bestudeerd en besproken in dit proefschrift.

Een [¹⁸F]fluorodeoxyglucose (FDG) positron emission tomography (PET) scan is een standaard onderzoek die gemaakt wordt bij long kanker patiënten om de uitgebreidheid van de tumor en mogelijke uitzaaiingen te bepalen (stadiering). Tevens kan een PET helpen om het tumorgebied te bepalen op de CT scan die gebruikt wordt voor de dosis planning van de bestraling. FDG is een met radio-isotoop gemarkeerde glucose analoge die vooral in metabool actieve cellen (o.a. tumor cellen) gaat zitten. Het radio-isotoop zorgt ervoor dat het tumorgebied met de metabool actieve tumor cellen zichtbaar wordt voor de PET scan. De activiteit van de tumor kan worden uitgedrukt met behulp van de Standardized Uptake Value (SUV). De maximale SUV blijkt een significante voorspeller voor de ziekte specifieke overleving, maar ook voor de algemene overleving na bestraling (Hoofdstuk 2). Deze voorspellende waarde is onafhankelijk van het tumor stadium en de fysieke conditie van de patiënt (Hoofdstuk 2). Om deze reden zou de SUV een belangrijke rol kunnen spelen in de selectie van patiënten en die baat hebben bij een hogere dosis. Deze hypothese wordt in lopende studies onderzocht.

Modellen die de kans op bijwerkingen kunnen voorspellen (NTCP modellen) zijn

Appendices

nodig om de risico's van een behandeling in te kunnen schatten. Longontsteking veroorzaakt door bestraling (Radiatie Pneumonitis, RP) is een bijwerking die kan optreden in enkele weken tot maanden na de bestraling. Eerdere studies laten een relatie zien tussen de bestralingsdosis in het long weefsel en het optreden van RP na conventionele bestralingsbehandelingen (waarbij ongeveer 2 Gray per keer gegeven wordt). Longfunctie onderzoeken hebben geen duidelijke bijdrage kunnen leveren om de voorspelling van RP te verbeteren (Hoofdstuk 3). Om hoog risico patiënten op basis van longdosis en longfunctie onderzoeken te kunnen identificeren moeten de resultaten van één groep patiënten in een andere groep patiënten te reproduceren zijn (dit heet het valideren van studies). Echter bij het uitvoeren van de validatie van voorspellende modellen, gebaseerd op longdosis en longfunctie, tussen twee verschillende instituten blijkt de mogelijkheid beperkt (Hoofdstuk 3). De moeilijkheid om het RP voorspellende model te verbeteren laat de complexiteit van dit onderwerp zien. Onderzoek naar een verbetering van de voorspelling naar bijwerkingen is belangrijk en gaande.

Voordat de dosis een voorspellende waarde heeft op de kans van tumor controle en complicatie moet de dosis geconverteerd worden in een zogenaamde biologische dosis. Veel studies hebben laten zien dat dit na conventionele bestralingsschema's gedaan kan worden met het zogenaamde Lineaire Kwadratische model (LQ model). Dit is een model die zijn oorsprong vindt bij cel studies maar die in de klinische praktijk ook toepasbaar is. Dit model is zelfs de basis van bij het berekenen van de te geven dosissen in gezond en tumor weefsel in de hedendaagse radiotherapie. De toepasbaarheid bij gehyprofractioneerde bestralingen is echter onbekend en onderwerp van veel discussies. Bij gehyprofractioneerde bestralingsschema's, (hierbij wordt een veel hogere dosis per fractie gegeven dan bij conventioneel gefractioneerde bestraling), worden goede resultaten gezien met een hogere kans op tumor controle. Om deze reden wordt deze bestralingstechniek in toenemende mate toegepast. Onderzoek naar de relatie tussen dosis en het optreden van bijwerkingen en de toepasbaarheid van het LQ model is daarom van groot belang bij deze vorm van bestraling.

Voor RP is de relatie tussen de dosis en de kans van optreden niet verschillend tussen conventionele bestraling en gehyprofractioneerde bestraling (Hoofdstuk 4). Bovendien was het tijdstip dat RP optreedt niet verschillend tussen deze twee technieken (Hoofdstuk 4).

Het LQ model kan op dezelfde manier toegepast worden voor de berekening van de biologische longdosis na gehyprofractioneerde bestraling als bij conventionele bestralingsschema's (Hoofdstuk 6). Aanpassingen van het LQ model, toegepast naar voorbeeld van celstudies, leverde geen verbetering op (Hoofdstuk 6). De bovenstaande relatie tussen de long dosis en de kans op RP na gehyprofractioneerde

bestraling is van groot belang om de risico's beter te kunnen inschatten. Deze en toekomstige studies moeten leiden tot een betere inschatting van de indicaties voor deze behandeling (b.v. ook grotere tumoren en herbestralingen) en een betere inschatting van limieten waar toekomstige studies/behandelingen aan moeten voldoen. Ook dierstudies zullen hierbij belangrijke (radiobiologische) vragen moeten beantwoorden.

Vanwege de slechte prognose is er weinig bekend over de lange termijn effecten van bestraling op de long functie. Met het verbeteren van de prognose door betere bestralingstechnieken is het van groot belang deze lange termijn effecten te onderzoeken. Uit een groep patiënten die toch een lange ziekte vrije overleving hadden, blijkt dat de long functie irreversibel verslechterd (Hoofdstuk 5). De longfunctie van patiënten met een longziekte verslechterde meer in vergelijking met patiënten zonder long ziekte na bestraling (Hoofdstuk 5). In het algemeen lijkt de verslechtering te zijn gecorreleerd met de long dosis (Hoofdstuk 5).

Deze resultaten zijn van belang om een inschatting te kunnen maken over wat het effect van bestraling is op de lange termijn. Alle mogelijkheden om de long dosis te limiteren zijn van groot belang en zullen geëvalueerd en benut moeten worden om de lange termijn effecten van bestraling te beperken.

Nauwkeurige bestralingstechnieken waarbij een hoge dosis op de tumor en een zo laag mogelijke dosis aan het normale weefsel kan worden gegeven zijn afhankelijk van een betrouwbare controle van de bedoelde en de daadwerkelijke bestraling. Om deze reden is het van groot belang om de locatie van belangrijke structuren (de tumor en het omliggende normale weefsel) goed in te kunnen schatten. De recente introductie van de Cone Beam CT (CBCT) scanner op het bestralingstoestel is een belangrijke stap geweest om de positie van de patiënt en de tumor nauwkeuriger te kunnen instellen tijdens de behandeling. Echter, oudere instel verificatie technieken worden ook nog steeds veel gebruikt. Hierbij wordt een significante onderschatting gemaakt bij het bepalen van de variabiliteit van de patiëntenpositie op het bestralingstoestel (Hoofdstuk 7). Kennis van dit verschil is belangrijk en hiermee moet rekening worden gehouden bij de bestraling, de ontwikkeling en de implementatie van nieuwe protocollen.

Appendices

Appendix of Chapter 6

The LQL model has a linear-quadratic shaped log-survival curve $\alpha d + \beta d^2$ below a threshold dose d_T and a linear shaped log-survival curve $\lambda d + \delta$ above d_T . The LQL model and its derivative are continuous at the threshold dose:

$$\lambda d_T + \delta = \alpha d_T + \beta d_T^2 \quad (1)$$

$$\lambda = \alpha + 2\beta d_T \quad (2)$$

Substituting equation 2 into equation 1 yields:

$$\delta = \alpha d_T + \beta d_T^2 - \alpha d_T - 2\beta d_T^2 = -\beta d_T^2 \quad (3)$$

The effect E_{LQL} of the total dose D given in n fractions of dose per fraction d exceeding d_T is thus given by:

$$E_{LQL} = n(\lambda d + \delta) = n\left(\alpha + 2\beta d_T\right)d - \beta d_T^2 = D \left(\alpha + 2\beta d_T - \frac{\beta d_T^2}{d}\right) \quad (4)$$

With the NTD [15] defined as the total dose given in 2-Gy fractions having an equivalent effect (as determined by the LQ model) as predicted by the LQL model,

i.e., $E_{LQL} = E_{NTD} = NTD(\alpha + 2\beta)$, the NTD can be calculated as:

$$NTD = \frac{E_{LQL}}{\alpha + 2\beta} = D \frac{\alpha + \beta + 2d_T - \frac{d_T^2}{d}}{2 + \alpha / \beta} \quad (5)$$

Appendices

List of publications

Pulmonary function changes after radiotherapy in non-small cell lung cancer patients with a long-term disease-free survival. *Borst GR, De Jaeger K, Belderbos JS, Burgers SA, Lebesque JV.*

Int J Rad Oncol Biol Phys. 2005 Jul 1;62(3):639-44.

FDG standardized uptake value as prognostic factor for inoperable non-small cell lung cancer. *Borst GR, Belderbos JS, Boellaard R, Comans EF, De Jaeger K, Lammertsma AA, Lebesque JV.*

Eur J Cancer. 2005 Jul;41(11):1533-41.

Prospective assessment of dosimetric/physiologic-based models for predicting radiation pneumonitis. *Kocak Z, Borst GR, Zeng J, Zhou S, Hollis DR, Zhang J, Evans ES, Folz RJ, Wong T, Kahn D, Belderbos JS, Lebesque JV, Marks LB.*

Int J Rad Oncol Biol Phys. 2007 Jan 1;67(1):178-86.

Kilo-Voltage Cone-Beam Computed Tomography setup measurements for lung cancer patients; First clinical results and comparison with Electronic Portal-Imaging Device. *Borst GR, Sonke JJ, Betgen A, Reméijer P, van Herk M, Lebesque JV.*

Int J Rad Oncol Biol Phys. 2007 Jun 1;68(2):555-61.

Radiation Pneumonitis for patients treated for malignant pulmonary lesions with stereotactic body radiation therapy. *Borst GR, Ishikawa M, Nijkamp J, Hauptmann M, Shirato H, Onimaru R, van den Heuvel M, Belderbos J, Lebesque JV, Sonke J-J.*

Radiotherapy & Oncology 2009, Jun;91(3):307-13.

Radiation Pneumonitis after Hypofractionated Radiotherapy: Evaluation of the LQ(L) model and different dose parameters. *Borst GR, Ishikawa M, Nijkamp J, Hauptmann M, Shirato H, Bengua G, Onimaru R, Lebesque JV, Sonke.*

Accepted for publication in Int J Rad Oncol Biol Phys.

Appendices

Curriculum Vitae

Gerben Roelof Borst was born in Ermelo, The Netherlands on the 4th of September 1976. In 1996 he obtained his secondary school degree from the Groevenbeek College in Ermelo. In the same year he started medical school at the University of Antwerpen, Belgium. Under the Erasmus Exchange Program he attended the medical school of the Humboldt University in Berlin, Germany, in 2000 for one year. In 2003, after finishing his medical school, he started his training program at the Radiation Oncology department of the Antoni van Leeuwenhoek Hospital-The Netherlands Cancer Institute. This training program consisted of a residency in Radiation Oncology (first under supervision of prof. H. Bartelink and currently under supervision of prof. M. Verheij) and a PhD program (under supervision of prof. H. Bartelink, dr. J.V. Lebesque and dr. ir. J.J. Sonke). For most of the studies included in this thesis he collaborated with other institutes (Duke University Medical Centre, Durham, US; Free University Medical Centre, Amsterdam, The Netherlands; Sapporo University Medical Centre, Hokkaido, Japan). He will finish his Radiation Oncology training in 2011.

Dankwoord

Is dit nou echt het eerste (en enige...) dat echt gelezen wordt? Een belangrijk punt van aandacht is in ieder geval dat het werk in dit boekje er nooit gekomen zou zijn zonder teamwork van velen die zich inzetten voor de behandeling van kankerpatiënten. Dat ik daar bovenop en daarbuiten veel hulp en steun heb gehad om er een proefschrift over te maken is extra fantastisch, daarvoor wil ik velen bedanken van wie ik er enkele speciaal wil benoemen.

Prof. dr. H. Bartelink, promotor. Beste Harry, de vrijheid die je me hebt gegeven binnen mijn AGIKO aanstelling, jouw kennis en enthousiasme zijn de grondslag van het grote plezier dat ik haal uit mijn opleiding en dagelijkse werk. Zelfs nu geef je nog onderwijs, staat je deur open voor allerlei vragen en geef je advies waar mogelijk. Bedankt voor dit alles.

Dr. J.V. Lebesque, co-promotor. Beste Joos, hopelijk is jouw zucht van opluchting na dit proefschrift goed gecorreleerd met het gezucht na één van de vele (vele, vele..) correcties. Ik ben je erg dankbaar dat ik van jouw kritische blik, analytische vermogen en wetenschappelijke interesse gebruik heb mogen maken en ik stel nog steeds je hulp, als je weer bovenduikt, erg op prijs!

Dr. ir. J.J. Sonke, co-promotor. Beste Jan-Jakob, de treshold dose tussen werk en vermaak is dankzij jou uit de formule geschrap; bedankt voor de leerzame, gezellige en inspannende uitstapjes en ik hoop dat je me nog vaak betreft in jouw interessante onderzoekslijnen. Niettemin, geen onderzoek in de toekomst zal de ervaring van de significante resultaten ($p < 0.0001$) van jouw V70 optimalisatie kunnen overtreffen.

Alle betrokkenen van de afdeling nucleaire geneeskunde & PET research van het VUMC, bedankt! Dr. R. Boellaard, Beste Ronald, jouw grote hulpvaardigheid was erg belangrijk bij het analyseren van de PET data, zonder die inzet was de studie niet mogelijk geweest. Het was mijn eerste inter-institutionele samenwerking en in eerste stappen zit het vaakst een misstap, ik heb er veel van geleerd.

Dear Prof. dr. H. Shirato, thank you for the opportunity of our collaboration and the hospitality of you and your department. Dear Dr. M. Ishikawa, dr. G. Bengua and K. Sutherland, dear Masayori, Gerard and Ken, thank you for your great help retrieving the data (a tough job), eating with chopsticks (a tougher job), singing in the Karaoke bar (the toughest job) and finishing the tubes at the Sapporo Summer Festival (乾杯!).

Dankwoord

Prof. M. van Herk en prof. M. Verheij. Beste Marcel en Marcel, bedankt voor jullie enthousiaste en inspirerende bijdrage aan mijn onderzoek en opleiding. Ondanks jullie wat minder unieke voornaam is het wel een uniek voorrecht om op jullie afdeling te mogen werken. Dear prof. dr. L.B. Marks and dr. Z. Kocak, thank you for your knowledge and cooperation in our collaborative study. I really hope new collaborative projects will be started to study and reveal the difficulties in the treatment of lung cancer patients. De overige leden, prof. dr. E.H.D. Bel, prof. dr. A.C. Begg, prof en dr. ir. C.A. Grimbergen wil ik ook graag bedanken voor het lezen en beoordelen van mijn proefschrift.

Alle stafleden van de radiotherapie en de long afdeling wil ik graag bedanken voor de interesse en input van de afgelopen jaren. Beste Jose, het combineren van onderzoek en kliniek is meer dan één plus één in vele positieve opzichten! Bedankt voor je hulp bij het optellen van de twee! Beste Michel en Sjaak, collaboration is the key message, bedankt voor jullie samenwerking, óók de patiëntenzorg profiteert hiervan.

Beste (oud-)assistenten, bedankt voor de fijne samenwerking en gezelligheid. Deze zorgt voor een bijzondere en positieve sfeer binnen onze groep waar ik ook tijdens mijn onderzoeksperiode veel aan heb gehad. De frequentie van onze borrels gaan net als het onderzoek gepaard met ups en downs waarbij de ups veel leuker zijn. Dus de conclusie “meer borrels” is wetenschappelijk verantwoord!

ProjO leden, ook al waren mijn projecten een beetje vreemde eenden binnen onze meetings, jullie input en hulp heb ik zeer gewaardeerd.

Patricia, ik had geen idee wat ik nou wel en niet aan je kon vragen met als gevolg dat ik nu van alles aan je vraag met als resultaat dat het dan wèl goed gaat, bedankt!

Josien, zou je de Japan dataset nog een keer doornemen met $d_T = 10$... Bedankt voor je grote hulp! En Jasper, zou jij dan 4242042 nog kunnen nakijken... Bedankt voor al je hulp voor, tijdens en na “de kelder van Sapporo”.

Helaas konden we maar weinig longfunctie onderzoeken gebruiken door de kleine patiënten groep, maar Marieke, aan jouw inzet heeft het zeker niet gelegen!

Ook voor de statistiek geldt weniger ist mehr, of was het nou mehr ist weniger?!
Michael, Vielen Dank für deine Hilfe!

Appendices

Amai zonne, Stephanie, vanaf onze start moesten we beiden nogal gewoon worden aan dat Amsterdamse gezwam waar we niet altijd goesting hadden. De pintjes uit de frigo en de vele babbels hebben ook 't straffe begin tot een plezante periode gemaakt! Merci zeg!

Jochem, je hebt gewoon net zolang gezocht naar een nieuwe baan totdat je net zo'n bizarre afkorting kreeg als ik; ook dit werk gaat je ongetwijfeld goed af. Veel vermaak en steun heb ik uit onze verbale en non-verbale interacties gehaald (de reportback van onze verplichte OIO retraite heeft de lung-meeting vreemd genoeg nooit gehaald).

Leah, thanks a lot for your help and gezelligheid (en noem je jezelf nu OIFILK of hangt de kaart nu eindelijk niet meer omgekeerd?)

Maddalena, allerhande vragen kon, kan, mocht en mag ik op je af blijven vuren bij een door jou onaflatende inzet van alle mogelijke middelen (met name oude statussen en thesaurus internet programma's) om ze zo goed mogelijk te beantwoorden (hoe zou deze zin in het Engels zijn?). Daarnaast had je ook altijd interesse in mijn werk en privé gerelateerde wel en wee. Bedankt voor dit alles! Jouw inzet is van onschatbare waarde voor het long onderzoek op de afdeling.

Dat ik via mijn werk (of was het nou toch via Sari?) mensen heb ontmoet waarmee ik zelfs erg gezellige trainingsuurtjes kon door brengen geeft een extra dimensie aan dit verhaal! Sparringpartners Sander (McEnroe) Veltkamp en Hans (Zoetemelk) te Poele, bedankt, laten we snel weer wat plannen!

“Focussen, ontregelen en controleren” waren welkome afwisselingen! Jorick, Simon, Bouke en Sil, nu krijg ik de tijd om ook eens naast de baan te laten zien hoe het (niet) moet; cheers!

Jeroen, Jeroen en Klaas. De Veluwe, De Molen, De Gelderblom zijn allemaal niet meer wat het geweest is, gelukkig geldt dit niet voor onze vriendschap. Nu is het eindelijk echt dr. Snuggles!

Bijzonder dat Belgische zaken als Het Paarse en Konijnen kot, de GB, het RUCA, Gala pils, TD's en de Buis aan de basis staan van onze oer-Hollandse degelijke vriendschap (maar dan wel met Bourgondische trekjes). Sander bedankt. Maarten en Garmt, fijn dat jullie ook nu weer naast me staan!

Dankwoord

Waar een “zoldertje met badjas” avontuur in Amsterdam niet toe kan leiden?! Thessa en Ewald, super bedankt voor jullie support! Een zorgzamere zus dan mijn grote zus Marieke bestaat niet. Dankjewel!

Lieve pa en ma. Nooit heb ik hoeven of kunnen twijfelen aan jullie onvoorwaardelijke steun; zonder deze steun was ook dit niet gelukt!

Nou lief (ik zeg alleen maar Sari als er iets mis gaat toch?!), ook dit was weer een bijzonder avontuur, dit keer geen fotoboek maar 2 promotieboekjes. Dat je me zelfs nog bij de lay-out wilde helpen (ahum, jij hebt de hele lay-out gedaan...) is een goed voorbeeld van jouw belangrijke aandeel in onze avonturen. Vol vertrouwen en geluk kijk ik uit naar onze volgende!

Schip ahoy!

A handwritten signature in black ink, consisting of several overlapping loops and a long horizontal stroke extending to the right.

Appendices

Abbreviations

α/β ratio	the ratio of the linear (α) and the quadratic(β) parameters in the LQ model; often used to quantify the fractionation sensitivity
AP	anterior-posterior
CBCT	cone beam CT
CC	cranial caudal
CFRT	conventional fractionated radiotherapy
COPD	chronic obstructive pulmonary disease
CR	complete response
CT	Computer tomography
DE	dose escalation
DSS	disease-specific survival
DLCO	diffusion capacity for carbon monoxide
DFH	dose function histogram
DSS	disease specific survival
DRC	dose response curve
DRR	digital reconstructed radiograph
d_T	threshold dose
DVH	dose volume histogram
EPID	electronic portal image device
FDG	[¹⁸ F]fluorodeoxyglucose
FEV1	forced expiratory volume in 1 second
FVC	forced vital capacity
GTV	gross target volume
Gy	Gray, unit of irradiation
IMRT	Intensity Modulated Radiotherapy
kV	kilovolt
Ln(L)	logarithm of the likelihood function
LR	left-right
LQ	Linear Quadratic
LQ(L)	Linear Quadratic Linear
MLD	mean lung dose
MpLD	mean-perfusion lung dose
MV	megavolt
MBq	Mega Becquerel, unit of radioactivity
CTC	Common Toxicity Criteria
NSCLC	non-small cell lung cancer
NTCP	normal tissue complication probability

Abbreviations

NTD	normalized total dose
OpRP	overall reperfusion weighted response parameter
OS	overall survival
OSEM	ordered subset expectation maximization
PD	progressive disease
PET	positron emission tomography
PFT	pulmonary function test
PORT	postoperative radiotherapy
PR	partial response
RECIST	Response Evaluation Criteria in Solid Tumours
ROC	receiver operating curve
RP	radiation pneumonitis
RT	radiotherapy
σ	random setup error
Σ	systematic setup error
SAL	shrinkage action level
SBRT	stereotactic body radiotherapy
SD	stable disease
SPECT	Single photon emission computed tomography
SUV	Standard Uptake Value
TD ₅₀	dose for a 50% complication probability
TNM	Tumor, Nodes and Metastasis staging system of cancer
VA	alveolar volume
V _x	lung volume receiving doses higher than x
V _{x50}	V _x for a 50% NTCP
V70	VO70
WHO	World Health Organization

